Aspects of Land Surface Modelling: Role of Biodiversity in Ecosystem Resilience to Environmental Change and a Robust Ecosystem Demography Model

Submitted by

Jonathan Richard Moore

to the University of Exeter as a thesis for the degree of Doctor of Philosophy in Mathematics, February 2016.

This thesis is available for Library use on the understanding that it is copyright material and that no quotation from the thesis may be published without proper acknowledgement.

I certify that all material in this thesis which is not my own work has been identified and that no material has previously been submitted and approved for the award of a degree by this or any other University.

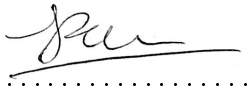

Jonathan Richard Moore

Abstract

Earth's species are disappearing at a rate unprecedented in human history, yet whether this loss will make the ecosystem "services" that support our civilisation more vulnerable to environmental change is poorly understood.

This thesis investigates two different aspects of land surface modelling. It firstly models the role of biodiversity in ecosystem resilience using the Lotka-Volterra and single resource models to model diversity using competition coefficients, stochastic noise and evolution inspired trait diffusion and then examines if higher diversity makes these simple models more resistant to temperature increases.

It secondly develops a theoretical plant demography model, based on the continuity equation, to robustly represent forest size diversity. This avoids both the complexity and maintainability issues seen in Forest Gap models and improves the representation of land use and land cover change and of regrowth time-scales after disturbance, which can be unrealistic in some of the previous generation of Dynamic Global Vegetation Models (DGVMs), such as TRIFFID (Cox et al., 2001).

While the Lotka-Volterra with competition coefficients and the single resource with stochastic noise approaches are found to be impractical, the single resource model with trait diffusion successfully shows that higher diversity requires a faster critical rate of temperature change before system net primary productivity (NPP) collapses.

The continuity equation model of vegetation demography is solved analytically with the size dependence of the growth rate approximated first by a power law and

then with a quadratic. The power law solution can be reduced to a "self-thinning" trajectory, and the quadratic solution gives either a rotated sigmoid or 'U-shape' distribution of plant sizes, depending on the ratio of mortality to maximum growth gradient.

The model is then extended to produce the basis of a new Dynamic Global Vegetation Model (DGVM) called "Robust Ecosystem Demography" (RED), adapting the plant physiology from TRIFFID DGVM to generate a size-dependent growth function. A proportion of the NPP from this growth is used for reproduction and the shading is modelled simply by random overlap. The model is found to better represent regrowth time-scales compared to TRIFFID and is also found to demonstrate an optimum proportion of NPP to reproduction which decreases with plant lifetime.

Acknowledgements

I wish to thank Professor Peter Cox for his supervision, support and advice throughout the PhD, and Dr Chris Huntingford of the Centre of Ecology and Hydrology (CEH) for being my co-supervisor and for his particularly helpful proof reading and comments on the thesis. I also wish to thank CEH for providing the funding for this PhD through the NERC QUERCC project.

I would also like to thank Dr Tim Jupp and Dr Cat Luke for helpful suggestions and advice on the mathematics and to Dr Chris Ferro for helping me in his role as mentor. Thanks also go to Dr Nikos Fyllas, Dr Anna Harper and Professor Karl Niklas and for help with the work on RED.

I would also like to send special thanks to my wife Yumiko and my mother whose love and support were so crucial, particularly in helping me get through a long and severe period of illness that forced me to take a long time out from my research work. I also wish to acknowledge all those both medical and non-medical who helped or supported me in coping with my illness.

Finally, I would like to dedicate this thesis in memory of my Grandmother Beryl Mary Storer passed away a few months before I submitted this thesis.

Contents

List of Figures

List of Tables

Thesis Overview

The Earth's species are disappearing at a rate unprecedented in human history (Chapin III et al., 2000), so much so that some compare the current rates to those of the major prehistoric mass extinction events (McCann, 2000). This loss is thought to be almost completely due to the combined effect of both a rapid increase in the human population, land use change and increasing industrialisation, which is leading to a greater and greater demand for resources (Chapin III et al., 2000). As the natural ecosystems support our civilization any collapse of these ecosystem "services" would be devastating (Dobson et al., 2006; Mooney et al., 2009). So now it is critical we understand how the stability of ecosystems are maintained and whether loss of species and corresponding diversity could lead to the loss of, or fluctuation in, terrestrial ecosystems - which is the subject of this thesis.

Rockström et al. (2009) has suggested that we are operating beyond the safe boundaries of our planet in three key areas of biodiversity loss, climate change and interference of the nitrogen cycle (Figure 1). One of the uncertainties in current knowledge is how two of these, climate change and biodiversity, influence each other.

Of particular importance is understanding the role of biodiversity in "buffering" ecosystems from climate change (Le Quéré et al., 2009; Martin and Watson, 2016). At the global scale, the carbon uptake of the land biosphere is an important factor in reducing the amount of human greenhouse gas emissions that stay in the atmosphere and contribute to climate change (Le Quéré et al., 2009; Le Quéré, 2010; Sitch et al., 2015). So the key question is: can biodiversity protect an ecosystem's

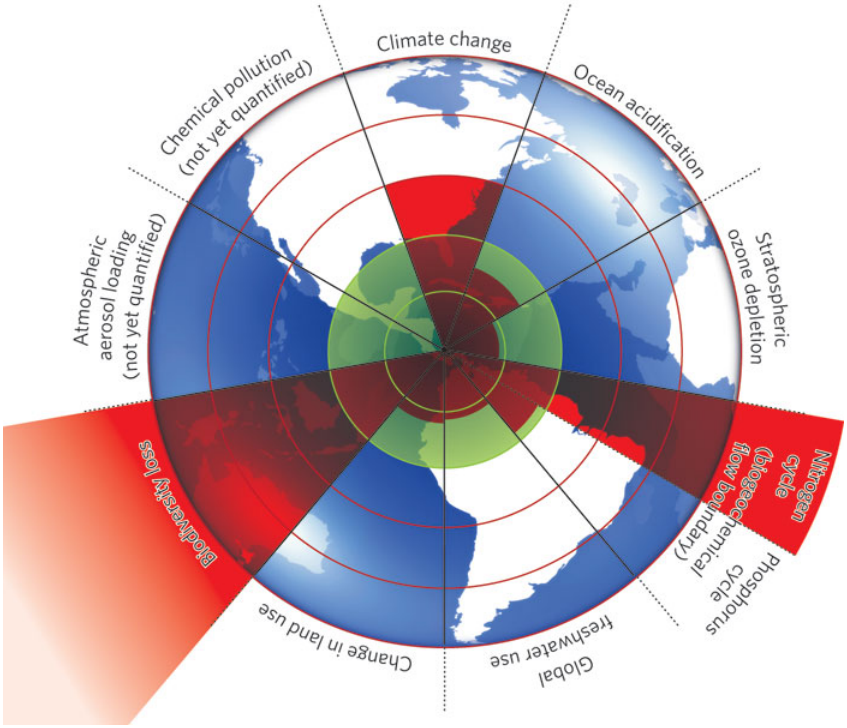

Figure 1: The inner green shading represents the proposed safe operating space for nine planetary systems. The red wedges represent an estimate of the current position for each variable. The boundaries in three systems (rate of biodiversity loss, climate change and human interference with the nitrogen cycle), are argued in this diagram to have already been exceeded. Source: Rockström et al. 2009

ability to absorb greenhouse gases as the climate warms?

This thesis investigates two different aspects of land surface modelling. The first part is concerned with the theoretical analysis of simple ecological models of diversity to see if net primary productivity (net flux of carbon absorbed by vegetation from the atmosphere) is more resilient with higher diversity as the temperature increases. The second part of the thesis develops a theoretical vegetation model to robustly represent forest size diversity and therefore to improve the representation of land use and land cover change in Earth Systems Models.

Chapter 1 reviews the current understanding of diversity and stability in ecological models. The chapter also looks at the historical development of dynamic global vegetation models used in climate prediction and discusses the more recent attempts to improve how these models represent of land use and land cover change.

Chapter 2 uses a Lotka-Volterra based ecological model to model the effect of increasing temperature on the net primary productivity (NPP) of a system which consists of species with a range of temperature optima.

Chapter 3 uses a simple resource model and maintains by diversity by having the environmental temperature varying in time. This is achieved via imposed stochastic temperature "noise", representing weather variations. The noise is used to "tune" the diversity to see if increasing the diversity keeps the NPP more stable.

Chapter 4 adapts the resource model to instead maintain diversity by including micro-evolution via a diffusion process that represents the effect of genetic mutation. The diffusion process acts to increase the number of temperature traits in the system which counteracts the effects of competitive exclusion. This model is then used to compare the effect on the NPP as the model undergoes various rates of temperature increase. By increasing the starting diversity the NPP is shown to be more resilient at higher initial diversities.

The second part of the thesis starts with Chapter 5. This chapter develops the theoretical framework for a new vegetation demography model based on the prin-

ciple of continuity. Analytical solutions are provided for certain simplified cases to allow comparison with numerical solutions.

Chapter 6 couples the demography model to the plant physiology equations used in the TRIFFID dynamic global vegetation (DGVM) to create a forest model based on size classes that compete for light. The model also allocates a proportion of NPP to reproduction, and it is shown that there is a optimum fraction for productivity which depends on the species lifetime.

Finally, chapter 7 summarises the main conclusions gained and outlines research questions that remain outstanding.

Chapter 1

Background

This chapter provides background information relevant to this thesis, based-on literature reviews. In particular it summarises existing research on ecosystem stability and resistance, biodiversity, and large-scale Dynamic Global Vegetation Models (DGVMs).

1.1 Stability

It is important to carefully define what measure of stability is used for an ecosystem, as for example a particular system that is stable according to one definition is not necessarily stable under another definition (Ives and Carpenter, 2007).

Stability definitions (Figure 1.1) can be split into two groups, either based on a system's dynamic stability (in essence its ability to return to the state it had before the perturbation) or how it is affected by a perturbation (resistance and resilience) (McCann, 2000).

The traditional theoretical view of stability is that a system is only stable if it returns to a defined equilibrium state after a perturbation and the faster it returns to that equilibrium the more resilient the system. This view is hard to verify as real ecosystems appear to be stochastic so experimentalists instead use the systems

Table 1 Definitions of stability

Term	Definition
Definitions of dynamic stability	
Equilibrium stability	A discrete measure that considers a system stable if it returns to its equilibrium after a small perturbation away from the equilibrium. A stable system, therefore, has no variability in the absence of perturbations.
General stability	A measure which assumes that stability increases as the lower limit of population density moves further away from zero. Under non-equilibrium dynamics, such limits to population dynamics generally imply a decrease in population variance (see variability definition below).
Variability	The variance in population densities over time, usually measured as the coefficient in variation. Common in experimental tests of stability.
Definitions of resilience and resistance stability	
Equilibrium resilience	A measure of stability that assumes system stability increases as time required to return to equilibrium decreases after a perturbation. A rapid response means that a system recoils rapidly back to its equilibrium state.
General resilience	A measure of stability that assumes system stability increases as return time to the equilibrium/non-equilibrium solution decreases after a perturbation. A rapid response means that a system recoils rapidly back to its equilibrium/non-equilibrium state.
Resistance	A measure of the degree to which a variable changes after a perturbation. Frequently used as a discrete measure that assesses a community's ability to resist invasion (that is, if an invader fails, the community resists invasion).

Figure 1.1: Definitions of Stability. Source: McCann 2000

variability as an indication of stability (McCann, 2000). An alternative definition of stability is that of general stability (Figure 1.1) which is strongly linked to population variance.

This thesis is primarily concerned with the resilience of CO_2 uptake via primary production (photosynthesis) to climate change.

1.2 Ecosystem Diversity

Like stability, there is no universal definition of diversity (Purvis and Hector, 2000).

Diversity is not just restricted to being a measure of the number of species it can also measure traits (e.g. drought resistance etc) or the number of ecosystem functions in a particular system. It can also be defined in terms of "evenness", which is how equally the individuals are divided between the species, traits or functions.

The most common diversity considered is that of species diversity with the number of species known as the species richness. Species evenness also accounts for relative population sizes and can also be considered a measure of the probability of two randomly selected individuals from the system being of the same species (Purvis and Hector, 2000) (see Figure 1.2). For example an ecosystem with 1000 species may still not seem very diverse if 99.9% of individuals are from one species and the other 999 species are very rare, this would be a high richness but low evenness ecosystem. Conversely a high evenness, low richness system of 2 species with equal numbers would also not seem very diverse. Neither richness nor evenness alone can tell the whole story when comparing diversity of ecosystems.

Yet another definition is that of difference, measuring how different two randomly selected species are. This difference can be measured in many different ways, by comparing species traits, functions or genetic makeup.

Most theoretical work has concentrated on how species richness affects ecosystem functioning, the key result being the discovery that rates of ecosystem processes in-

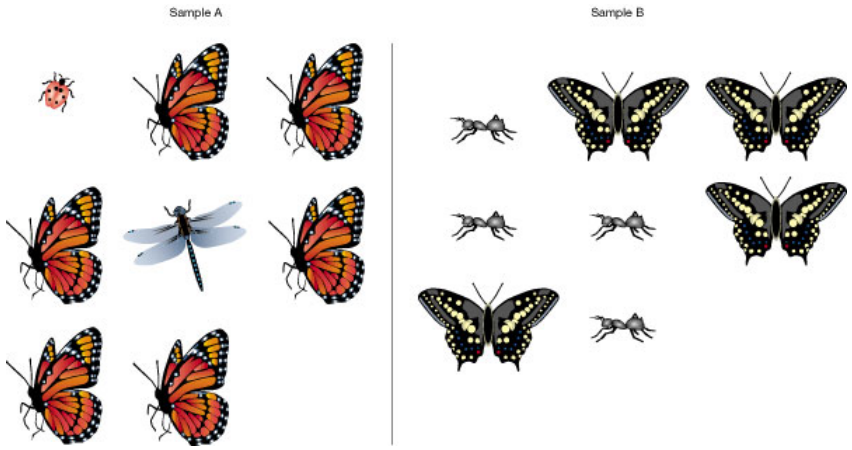

Figure 1.2: Two samples from different locations, illustrating two of the definitions of diversity: species richness and species evenness. Sample A could be described as being the more diverse as it has more species but there is less chance in sample B than in sample A that two randomly chosen individuals will be of the same species. Source: Purvis and Hector 2000

crease strongly with richness at low numbers of species but that this effect saturates at higher species numbers due to overlap in species function (i.e. there appears to be greater redundancy in a species rich environment) (Chapin III et al., 2000; Diaz and Cabido, 2001).

1.2.1 Shannon Diversity Index

The most common measure of diversity that combines both richness and evenness is the Shannon Index H', sometimes known as the Shannon-Wiener Index (Shannon, 1948; Krebs, 1989). This is essentially an entropy measure which measures the complexity of the system. In terms of species, the Shannon Index represents the uncertainty in the species of an individual selected randomly from a sample; if there is only one species then the uncertainty is zero, as more species are added the value of H' increases until it reaches a maximum value for the case of a perfectly even system with all species having the same number of individuals.

A system with S species has a Shannon Index of

$$H' = -\sum_{i=1}^{S} p_i \ln p_i \tag{1.2.1}$$

where the species proportion $p_i = \frac{n_i}{N}$ is the ratio of the number of individuals n_i in that species to the total number N. When the system is even each species has $\frac{N}{S}$ individuals and for each species $p_i = \frac{1}{S}$, as the probability of finding any species is the same. This means the uncertainty and therefore the Shannon Index H' are maximised for any given species richness S.

$$H'_{max} = -\sum_{i=1}^{S} \frac{1}{S} \ln \frac{1}{S} = -\ln \frac{1}{S} = \ln S \tag{1.2.2}$$

Despite being considered by some "as the most profound and useful of all diversity indices" (Jost, 2006) the Shannon Index is also not always easy to estimate accurately in the field as it is only valid for random samples drawn from a large community where the total number of species is known (Krebs, 1989).

1.2.2 Mathematical Definition of Evenness

The evenness, J', can be calculated from the Shannon Index by simply dividing by the maximum value for the number of species in the system.

$$J' = \frac{H'}{H'_{max}} \tag{1.2.3}$$

This means a perfectly even system will have an evenness of 1 and a system with only 1 species will have an evenness of 0, all systems will have an evenness between these two values.

1.2.3 Effective Species

It can be shown (MacArthur, 1965; Krebs, 1989; Jost, 2006) that the Shannon Index can be converted from an Index of diversity (which is not always intuitive)

to an effective number of species, D, using the fact that for any value of the Shannon Index there is an equivalent ecosystem with equally common (i.e. even) species. The number of species in this equally common equivalent system can then be defined as the diversity D of any system with that value of H'.

As $H'_{max} = \ln S$ for an even system then we get an effective number of species, D:

$$D = \exp(H') = \exp\left(-\sum_{i=1}^{S} p_i \ln p_i\right) \tag{1.2.4}$$

1.3 Relationship of Stability to Diversity

1.3.1 Simple Models

Before the 1970s ecologists believed that greater diversity implied increased stability, based-on the observation that simple terrestrial ecosystems tend to have greater fluctuations in population densities than more diverse ones (Odum, 1953; Elton, 1958). MacArthur (1955) showed using a very simple food web model that stability increased with the number of species as long as the nature of the interactions and the structure of the web met certain criteria.

May (1974) challenged this by using linear stability analysis on mathematical models of food webs constructed with random interactions strengths. He showed that such model systems tend to become less stable as the diversity increases, which is in direct opposition to the previous theory and observations.

Yodzis (1981) then discovered that models with food-webs constructed from observed data, including reasonable strengths of interaction between species, were more stable than randomly constructed models. The data used was patchy but the input of real feeding relationships showed that stability was not purely a result of greater species richness but that food web structure and interaction strength were important (McCann, 2000). The exact mechanism or explanation behind this result was not clear though.

1.3.2 Basic Stability Theories

One of the simplest conceptual models of an ecosystem (attributed to Charles Darwin, see Purvis and Hector 2000) is one where each species has its own "niche" - a particular set of optimum conditions unique to itself. This idea of niche differentiation means that the resource use of the system is maximised and so the system is more productive (Naeem, 2002), and therefore it is important in understanding the stability of system productivity. However, if there is only one species per niche the lack of redundancy means that such a system is not able to cope with environmental change - if a species goes extinct, there is no ready replacement to perform its role.

Most ideas on stability through diversity rely on the idea of an "insurance effect" (Naeem, 2002), whereby an ecosystem also has rarer species fulfilling the same function as more dominant ones but which may be better equipped to thrive if the environment changes (Purvis and Hector, 2000). This is a form of negative co-variance (McCann, 2000; Tilman, 2000) which leads to overall stability of the system as a whole or of a particular ecosystem function. The overall effect (known as the averaging effect - McCann 2000) is that the different responses of many species in a system average out in a changing environment. This is analogous to the idea of sampling, where the larger a sample the greater the chance of finding a particular characteristic out of all those available (Naeem, 2002; Loreau et al., 2001).

Most experimental work has been limited to small plots with only a few species, so there has been little verification of stability theories over larger areas and longer time-scales and with full food webs (Purvis and Hector, 2000; McCann, 2000; Worm and Duffy, 2003). There does seem to be an indication of a positive relationship between primary production and species richness in simple synthetic assemblies of plants, but it is difficult to infer anything from these results relevant to real and more complex ecosystems (Diaz and Cabido, 2001). In particular, little work has been done on functional diversity, even though this may have a greater effect on

ecosystem variability than species richness (Diaz and Cabido, 2001).

1.3.3 Interactions and Networks

As suggested by Yodzis (1981) interactions are important in understanding stability. Interactions have two main characteristics - they determine which species in an ecosystem are directly-connected, and they determine the strength of those connections. Interactions can be beneficial (facilitation and mutualism, e.g. pollinators etc) as well as antagonistic (herbivores eating plants and predators eating prey, or direct competition).

Ecological food-webs are networks of interactions but the "rich get richer" nature of network theory used in human social dynamics and internet modelling only partially applies, as competition, abundance, and body size constrain the interactions (Montoya et al., 2006; Gilbert, 2009). Montoya et al. (2006) has suggested the distribution of links in an ecological network may be approximated by: -

$$P(k) \sim k^{-\gamma} e^{-k/\xi} \tag{1.3.5}$$

where $P(k)$ is the probability of a species having k links, and γ and ξ are constants.

Another measure of the structure of food webs is their connectance $C = L/S^2$ (S is number of species and L number of links between them), which for random networks is equivalent to a measure of the clustering of the links (Dunne et al., 2002). Connectance is defined as the proportion of all possible links between species that actually exist in the network (Gilbert, 2009). Densely clustered webs are nearer the norm, as aquatic systems tend to have many life history omnivores (species that feed from more than one trophic level in the food web) and terrestrial systems often have many host-parasitoid interactions (Montoya et al., 2006).

Gilbert (2009) has also shown that connectance can be used as a measure of robustness (integrity of a network) and that the loss of a species causes a change in connectance indicating a loss of robustness. The problem with this study is that it has no clear measure of robustness - so while the study establishes that any change

in connectance, even a positive change, makes the system more vulnerable to further species loss it is not a quantifiable measure. The degree of the distribution (number of species with particular number of links) is shown to be important too, with a more uniform distribution being more stable.

The distance in links between species is quite small with over 80% of species 3 links or less from any other species (Montoya et al., 2006). This suggests any disturbance will spread quickly. However, the effect of a disturbance is also dependent on the strength of the interactive links, as the stronger the interaction the bigger effect a change in one species will have on the other. The more types of prey a species has the weaker each link tends to be. Perhaps slightly less intuitively the more predators preying on a species the lower its predation rate tends to be. McCann (2000) suggests that weak interactions may be a stabilising mechanism and gives an example of two competing herbivore species preyed upon by a common predator. One of the herbivores is both competitively superior compared to the other herbivore, but is also the preferred food type of the predator. This setup is stable as the herbivores negatively co-vary and so a reduction in the stronger herbivore leads to an increase in the other which reduces predation of the former. Also the preference of the predator for the superior herbivore keeps it in check and stops the weaker being out competed to extinction.

Real complex food-webs are observed to have special patterns of interactions. Models show such complex systems have a smaller parameter range of stability compared to simple ones, but that within this small stability zone the ecosystems are more resilient (Montoya et al., 2006). This perhaps goes some way to explain the previous contradiction between observations (suggesting diversity led to stability) and the theoretical results from May (1974) (suggesting the opposite).

1.3.4 Neutral Theory

One very controversial theory is that of neutrality (Hubbell, 2001; Whitfield, 2002). This is a model where all species are treated equal ecologically and differences

between them are ignored with the model only considering random dispersal and the birth and death of individuals and total population (Whitfield, 2002). This means many of the details of species-species interactions are ignored and most of the results are down to chance. Despite appearing to be based on simplistic assumptions the theory produces patterns of species distribution, abundance and co-existence that match those seen in nature.

Neutral theory has limitations as it only applies within one trophic level, fails at scales larger than a few square kilometres, and is more applicable to plants and microbes (Whitfield, 2002). These limitations mean its key use maybe as a simple model to test basic ideas or as a null hypothesis - models including niche differentiation have to be very complex to match the results of neutral theory.

1.4 Sudden Ecological Shifts

Sudden changes in an ecosystem are the most difficult to adapt to (Folke et al., 2004). Such rapid changes can happen when a system is close to a transition point, as then only a small change can trigger a major shift (Scheffer et al., 2001). Systems poised on such a transition point may have a highly non-linear response to perturbations, often associated with multiple stable states and can be hard to predict but a slowing-down of fluctuations may be an early warning signal of a sudden change (Dakos et al., 2008; Scheffer et al., 2009). Stable states are associated with some kind of basin of attraction (very much like potential energy well in a physical system) and it is changes in the environment that alter the depth of this basin and increase the chance that a fluctuation will tip the system from one stable state to another (Scheffer et al., 2001).

Telling if a sudden shift is due to multiple states or if it is just due to a highly non-linear response is not easy. Firstly, a system must show little change as the environment gradually changes until the transition. Secondly, it must have a shift in dominance of species between the two states. It must also be triggered by

stochastic (random) fluctuation and the states must have some form of stabilising feedback whether biological, physical or chemical (Scheffer et al., 2001).

Rietkerk et al. (2004) reviews work extending this idea of sudden shifts to systems which are no longer spatially homogeneous but instead exhibit "patchiness before" a transition. The theory is that there is a short range positive feedback (usually due to a consumer concentrating resources) combined with a longer range negative feedback. The classic example of this is semi-arid regions where water is in short supply and plants tend to concentrate soil moisture by drawing water from soil further away, this produces a patchy landscape of clumps or stripes of vegetation inter-spaced by bare soil (Rietkerk et al., 2004).

There is some debate about whether this patchiness is always indicative of an imminent transition to another state. Pascual and Guichard (2005) suggest the spatial distribution and scale of both the disturbance triggering a shift and recovery processes that occur afterwards are also important. He goes on to propose that a well-mixed disturbance produces a classical phase transition, a distributed disturbance with well-mixed recovery produces self-organised criticality (where internal dynamics move the system to a critical point where large intermittent fluctuations occur). If both the disturbance and recovery are locally distributed then there is no rapid change but instead a broad transition with associated patchiness (known as robust criticality).

1.4.1 Self-Organised Instability

Solé et al. (2002) suggests that increasing diversity drives ecosystems towards instability. He puts forward the idea that immigration and/or speciation due to evolution increases the diversity of an ecosystem but that this increases the interactions within the system and that at a certain level of diversity the increased interactions destabilise the system, leading to extinctions. From this point on the system maintains its diversity through this mechanism (although with a turnover in species).

Solé et al. (2002) suggests that this does not entirely meet the definition of self-organised criticality, as it is not completely internally driven and because the food-web interactions are not homogeneous. Instead he calls this "Self-Organised Instability".

Kauffman (1995) discusses the problem of trying to understand complex, non-linear systems such as ecosystems and suggests that while we may not be able to predict the exact evolution or dynamics of such a system that we can investigate the patterns seen.

1.5 Dynamic Global Vegetation Models and Size Diversity

The Earth's vegetation plays a crucial role in regulating its carbon and hydrological cycles (Bonan, 2008b). For this reason, modelling the response of vegetation across the globe is a critical component of climate change prediction (Fisher et al., 2010).

The land surface has a significant effect on climate as the land and atmosphere exchange energy, carbon and water. The energy exchange depends on both the surface albedo and also latent heat due to water evaporation. A further effect is the momentum exchange due to interaction of the surface roughness with the surface winds (Sellers et al., 1992; Pitman, 2003). All these factors are affected by the amount and type of vegetation on the land surface, so it is important for accurate climate prediction to correctly model both the vegetation atmosphere interactions and the patterns of global vegetation.

1.5.1 Land Surface Model Development

The earliest climate models (which were derived from weather forecast models) had fixed unchanging vegetation which did not respond to changes in temperature, rainfall or wind patterns and purely acted to shield a fraction of ground from solar

radiation and modify moisture transfer. This meant that such models could not predict changes in vegetation and the feedback effects that can have on climate change. An example of this is the albedo difference between desert (albedo 35%) and forest (albedo 10%), so if rain patterns change and a forest either dies off or starts growing on land that was previously desert there can be significant changes in patterns of solar energy absorption (Sellers et al., 1997; Pitman, 2003; Bonan, 2008a).

As computing power has increased climate models have become more sophisticated with more refined spatial resolution (Figure 1.3), and it has also become possible to include more detailed vegetation models. The second generation of models included detailed empirical models of photosynthesis and stomatal conductance - which modulates the loss of water to the atmosphere as transpiration (Sellers et al., 1997; Pitman, 2003). Third generation models further improved the models of photosynthesis allowing the gross (GPP) and net primary productivities (NPP) to be calculated. This allowed explicit modelling of land-atmosphere fluxes of CO_2 and water within Earth System Models (ESMs), which respond to environmental conditions.

NPP represents the carbon assimilated by plants that is available for growth, so the next stage in model development was to represent plants growing by increasing the vegetation carbon density and/or coverage - leading to first generation Dynamic Global Vegetation Models (DGVMs) (Cramer et al., 2001).

Before the development of DGVMs general circulation models (GCMs) excluded the feedback between climate and the biosphere, instead using the results from 'offline' carbon-cycle models that are separate from the climate model. Cox et al. (2000) were the first to correct for this gap in projections, by introducing a fully coupled, three-dimensional carbon-climate model into a GCM. They showed that carbon-cycle feedbacks could significantly accelerate climate change and that under a 'business as usual' scenario, the terrestrial biosphere acts as an overall carbon sink until about 2050, but after that turns into a carbon source. It was also found that

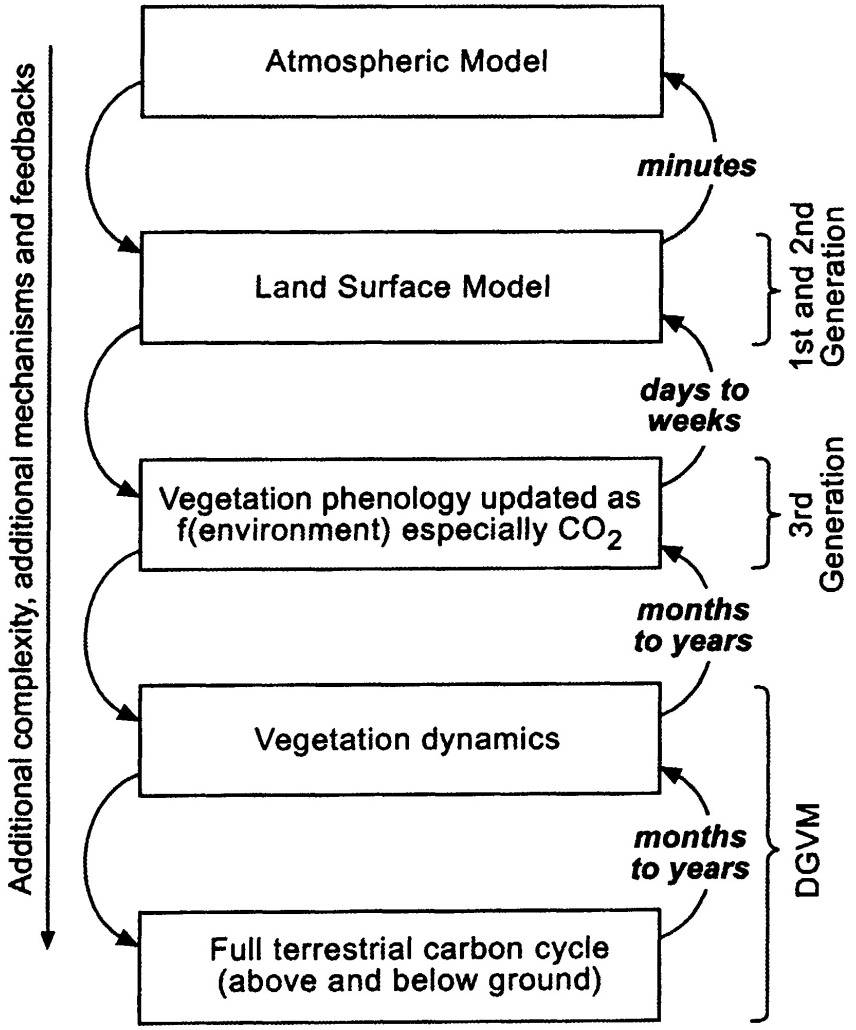

Figure 1.3: Schematic from (Pitman, 2003) that shows the increasing detail in land surface models.

by 2100, the ocean carbon uptake is more than compensated for by the land carbon source, leading to atmospheric CO2 concentrations being 250 p.p.m.v. higher in the coupled model compared to the uncoupled (Figure 1.4).

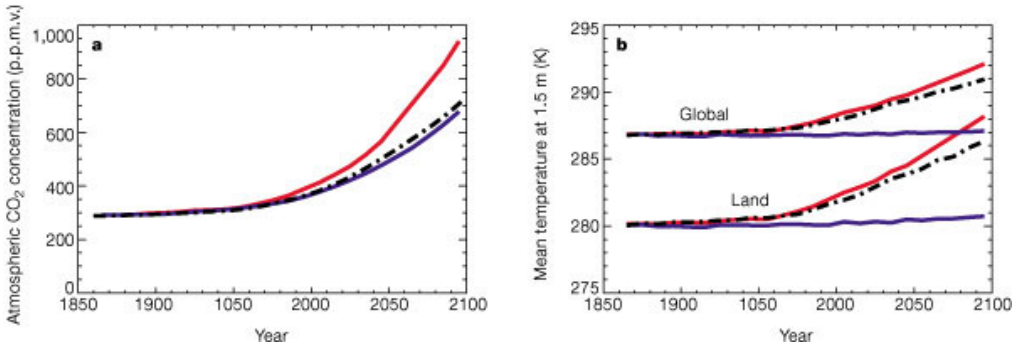

Figure 1.4: From Cox et al. (2000). Effect of climate/carbon-cycle feedbacks on CO_2 increase and global warming. a, Global-mean CO_2 concentration, and b, global-mean and land-mean temperature, versus year. Three simulations are shown; the fully coupled simulation with interactive CO_2 and dynamic vegetation (red lines), a standard GCM climate change simulation with prescribed (IS92a) CO_2 concentration and fixed vegetation (dot-dashed lines), and the simulation which neglects direct CO_2-induced climate change (blue lines). The slight warming in the latter is due to CO_2-induced changes in stomatal conductance and vegetation distribution.

Later studies investigating this effect using a variety of different DGVMs also showed the carbon balance of the terrestrial biosphere to be a key factor in future climate prediction but there was a large difference in the predicted atmospheric CO_2, due primarily to variation between the models in land carbon uptake (Friedlingstein et al., 2006).

Sitch et al. (2008) also studied the response of several DGVMs coupled to a simplified version of the Hadley GCM, known as IMOGEN (Huntingford et al., 2010). While it was found that all the DGVMs consistently accounted for the contemporary land carbon budget the models could diverge significantly in their future predictions under the more extreme emissions scenarios. This was found to be in part due to different responses of the DGVMs' tropical vegetation to drought and to differences in the responses of boreal vegetation to changes in temperature and

moisture.

Scheiter et al. (2013) have suggested current DGVMs have two weaknesses. Firstly most DGVMs classify all vegetation into a small fixed set of PFTs which can hide the real world variation in traits between individuals, species and local environment. This may obscure some of the causes of coexistence and as sometimes PFT traits are used as tuning parameters may not represent maximum-likelihood values. The number of PFTs or functional types needed to represent ecosystem function is also an open question and could be a reason for the variation in the Amazon 'dieback' seen in Huntingford et al. (2008) and Sitch et al. (2008). The suggested solutions are to include more PFTs, and ultimately to model adaptive traits in each PFT.

The second weakness according to Scheiter et al. (2013) is the modelling of competition in DGVMs. The simplest competition models assume the PFT with highest NPP is the only one that can occupy open space; this leads to one PFT dominating. Another approach is to use Lotka-Volterra competition which has the disadvantage of the number of competition parameters increasing with the square of number of PFTs and also of not describing the mechanisms of competition. Arguably a better approach is to explicitly model competition via a resource such as water or light, where the number of competition parameters scale linearly with number of PFTs.

1.5.2 Benefits of Modelling Forest Demography

The early climate DGVMs categorised the vegetation into a number of plant functional types (PFTs) with each type representing an average plant of that group. Many of these models such as TRIFFID (Cox, 2001), LPJ (Sitch et al., 2003), CLM (Bonan et al., 2003), Sheffield DGVM (Woodward and Lomas, 2004) and ORCHIDEE (Krinner et al., 2005) for example do not model size, age or species variation within PFTs. The lack of any differentiation in size (and size variation in growth rate) in these models prevents easy modelling of size dependent processes such as land use change and also makes it more difficult to model PFT light competition, succession and PFT coexistence (Fisher et al., 2010; Huntingford et al.,

2008) and also can contribute to the to poor estimates of time-scales of forest regrowth in TRIFFID. Sitch et al. (2015) discusses there is a need for improved representation of ecological processes in DGVMs, in particular nutrient cycling, demographic dynamics, disturbance (wildfire, windthrow, insects), land use and land cover change in land models, and better representation of the key functional diversity. These processes are needed to help reduce the current uncertainty in the predicting future of the land carbon budget.

To address the lack of any representation of the inherent heterogeneity caused by mortality of large trees and disturbances such as fire and wind throw (Moorcroft et al., 2001; Fisher et al., 2010), models such as HYBRID (Friend et al., 1993, 1997) and SEIB (Sato et al., 2007) have tried to adapt individual based gap models to a global scale. These models can in principle more accurately capture the small scale dynamics, but can be prohibitively expensive computationally to simulate vegetation on a global scale, and thus may have implications for any eventual inclusion as the land surface module of a GCM.

The Ecosystem Demography (ED) model (Moorcroft et al., 2001; Fisher et al., 2010) is one solution to this requirement for a less computationally demanding model which allows the effects of size and gaps to be included. The ED model uses a set of partial differential equations that represent a size and age-structured approximation of a gap model. Unfortunately, so far ED has not yet been found to be practical in climate modelling applications as it needs many dynamically created age classes which need to be constantly merged to avoid an ever increasing number of patches. This has led to problems with complexity and maintainability of the model.

So there is a strong need for a DGVM model that incorporates forest demography, but is robust and easy to maintain within an ESM.

1.6 Discussion

Ecological research has come a long way in understanding the principles of diversity and how competing species coexist, but there is still no definitive theory. Trade-offs, complexity, niches, and neutral theory all seem to have a role to play in creating the diversity we see.

In understanding the resilience of an ecosystem to environmental change this thesis will simplify the question down to how well a system containing a diversity in temperature optima copes with an increasing environmental temperature. The resilience will be measured by comparing the NPP of the system undergoing the temperature change to a system that has a constant temperature.

The later part of the thesis will look to include diversity of plant size, to better model land use and land cover change through forest demography, while avoiding the problems of complexity and maintainability seen in some previous attempted solutions to this problem.

Chapter 2

The Lotka-Volterra Diversity Model

The TRIFFID (Cox, 2001) dynamic global vegetation model (DGVM) (used in the Joint UK Land Environment Simulator (JULES) (Clark et al., 2011)) describes the terrestrial biosphere in terms of the carbon density of the soil and the carbon density and area coverage of five competing plant functional types (PFTs), representing broadleaf trees, needleleaf trees, C3 grass, C4 grass and shrub.

The particular mathematical form of TRIFFID used to model the change in PFT fractional coverage was first used to describe the spread of plants by Carter and Prince (1981) and then later in the Daisyworld (DW) model of (Watson and Lovelock, 1983; Wood et al., 2008). Mathematically it is very similar to the Lotka-Volterra competition Model (LV Model), but only applies competitive effects to its growth term whereas in the standard LV model applies competition effects to the difference of the growth and mortality terms.

The TRIFFID/DW model approach is more applicable to modelling vegetation from the perspective of the carbon cycle, as the specific effect of competition on the growth term is crucial to correctly account for carbon use through photosynthesis and is therefore superior to the LV model approach in this context.

The limited number of PFTs in TRIFFID does not capture the range of temperature traits (such as optimum temperature for growth) available to an ecosystem

undergoing potential environmental change. To study the effect on resilience to an increasing environmental temperature, the LV model used in TRIFFID will be modified to have a large range of species, forming a continuum of temperature traits. For each trait a very simple model with just temperature dependent growth will be used. This a simplifying assumption to limit the number of parameters.

The chapter will first present the model equations and then the dynamical properties of the system before moving onto methods for getting equilibrium coexistence of species. The chapter will also the look at the effect of rate of temperature change on net primary productivity.

2.1 Model Equations

The equation governing the change in the fractional coverage ν_i of each plant species is

$$\frac{d\nu_i}{dt} = \nu_i \left(s\, g_i(T) - \gamma \right) \tag{2.1.1}$$

where $s = 1 - \sum_j \nu_j$ is the bare soil fraction, γ the death rate and g_i the growth rate.

To allow "extinct" species to reappear (simulating species dormant as seeds or from outside the region re-entering when conditions are right) the ν_i on the right hand side is set to a small value ν_{seed} for any extinct species when conditions allow that species to grow and spread.

$$\frac{d\nu_i}{dt} = a_i \left(s\, g_i(T) - \gamma \right) \tag{2.1.2}$$

$$a_i = \begin{cases} \nu_{seed}, & \nu_i < \nu_{seed} \text{ and } \left(s\, g_i(T) - \gamma \right) > 0 \\ \nu_i, & \text{otherwise} \end{cases} \tag{2.1.3}$$

Symbol	Variable / Parameter	Unit
ν_i	Fractional coverage species i	-
a_i	Seed adjusted fractional coverage species i	-
ν_{seed}	Minimum fractional coverage due to seeding	-
s	Fractional coverage of unvegetated space	-
g_i	Temperature dependent coverage growth rate species i	yr^{-1}
g_{max}	Maximum growth rate	yr^{-1}
Γ_i	Non-dimensional temperature dependent coverage growth rate species i	-
γ	Mortality rate	yr^{-1}
τ	Non-dimensional time (per lifetime)	-
T	Environmental temperature	°C
$T_{OPT,i}$	Optimum temperature species i	°C
T_w	Temperature growth curve width	°C
θ	Non-dimensional temperature (per T_w)	-
$\theta_{opt,i}$	Non-dimensional optimum temperature species i	-
C_v	Carbon density of species i	kg C m^{-2}
λ	Fraction of the NPP utilised in increasing the fractional coverage	-
Π	Net Primary Productivity (NPP)	kg C m^{-2} yr^{-1}
Π_N	Normalised gridbox mean NPP	yr^{-1}
α	Rate of temperature increase $\frac{d\theta}{d\tau}$	-
c	Inter-species competition coefficient	-
k	Intra-species competition coefficient	-

Table 2.1: List of variables and parameters for Chapter 2

2.1.1 Temperature Dependent Species Growth Rate

In the model ecosystem we use a very simple model where the growth rate of a species is maximum at its optimum temperature and declines away from this optimum according to the Gaussian function (Figure 2.1). This model is a reasonable approximation of the temperature dependence of the net CO_2 flux as both photosynthesis and respiration are temperature dependent processes (Bonan, 2008a), the net effect of which is a symmetric peak.

$$g_i(T) = g_{max} \exp\left[-\frac{1}{2}\left(\frac{T - T_{OPT,i}}{T_w}\right)^2\right] \tag{2.1.4}$$

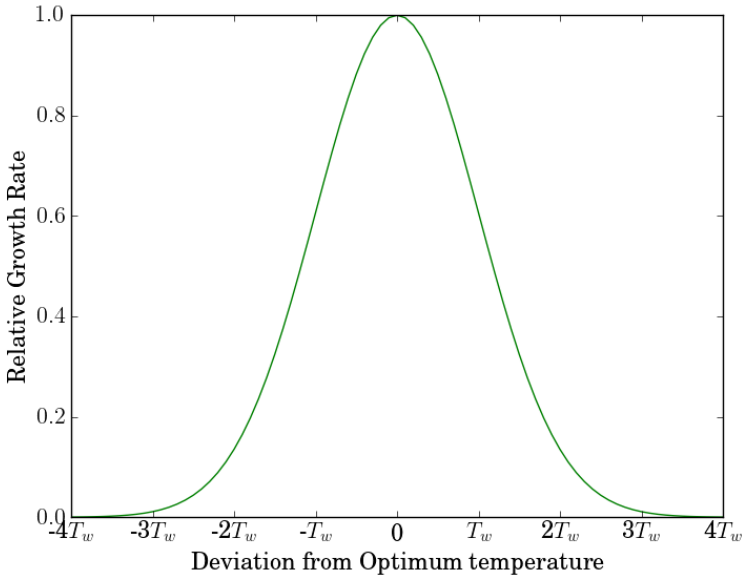

Figure 2.1: Each species has an optimum temperature where its growth rate is at its maximum. This curve shows how the growth rate falls away as the environmental temperature gets further from the plant's optimum temperature. Plot is scaled in terms of the growth curve width T_w in the x-axis, and scaled by g_{max} in the y-axis.

The model has an array of species with optimum temperatures uniformly distributed in temperature. If the number of species is infinite and the difference in optimum temperature between adjacent species infinitely small then we would

have an idealised case, which would be expected to be able to maintain its productivity under any temperature change. To simplify and aid mathematical analysis the model the range of temperature traits is allowed to extend indefinitely. Most plants typically have an optimum temperature in the range 15-30°C, but the temperature range over which plants can photosynthesise is quite large, even as far as below freezing and greater than 40°C for some species in extreme habitats (Bonan, 2008a).

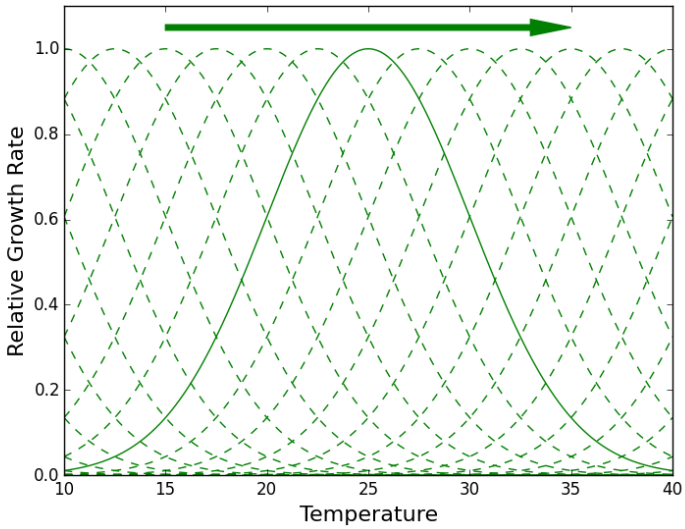

Figure 2.2: Species have uniformly arranged optimum temperatures. Each line is the growth curve of one species; the species with optimum temperature equal to environmental temperature of 25°C is shown as a solid line. If the environmental temperature increases the optimum species will move with it as indicated by the arrow.

2.1.2 Net Primary Productivity

The Net Primary Productivity Π (NPP) is defined in Cox (2001) as the rate of carbon uptake per unit vegetated area due to photosynthesis minus plant respiration for species i: -

$$\Pi = \frac{g_i(T)\, C_{v,i}}{\lambda} \tag{2.1.5}$$

where $C_{v,i}$ is the vegetation carbon density and λ the fraction of the NPP utilised in increasing the fractional coverage.

As each species covers a fractional area ν_i, the mean NPP over the gridbox is: -

$$\Pi = \frac{g_i(T)\,\nu_i\,C_{v,i}}{\lambda} \tag{2.1.6}$$

For the work in this chapter NPP is normalised so NPP of 1 corresponds to the NPP of a species with maximum growth rate (optimum) and fractional coverage of 1 (i.e. entire area of the system).

$$\Pi_N = \frac{g_i(T)}{g_{max}}\,\nu_i \tag{2.1.7}$$

2.1.3 Non-Dimensional Form

For simplicity all species/traits in this chapter are assumed to have the same death rate γ and the same growth curve width T_w. These two variables can then be divided out of the equations and replaced by non-dimensional variables to aid analysis. Using a non-dimensional form is useful as itreduces the number of degrees of freedom to be investigated, and highlights what the important parameter clusters are.

$$\begin{aligned} \tau &= t\gamma \\ \theta &= \tfrac{T}{T_w} \\ \theta_{opt,i} &= \tfrac{T_{OPT,i}}{T_w} \end{aligned} \tag{2.1.8}$$

This has the benefit of not limiting the models to any particular time-scale or temperature scale so the results can apply not just to forests but also to any living system facing a change in its environment.

$$\frac{d\nu_i}{d\tau} = a_i\,(s\,\Gamma_i(\theta) - 1) \tag{2.1.9}$$

$$a_i = \begin{cases} \nu_{seed}, & \nu_i < \nu_{seed} \text{ and } (s\,\Gamma_i(\theta) - 1) > 0 \\ \nu_i, & \text{otherwise} \end{cases} \tag{2.1.10}$$

The new growth rate is then defined as

$$\Gamma_i(\theta) = \frac{g_{max}}{\gamma} \exp\left[-\frac{1}{2}\left(\theta - \theta_{opt,i}\right)^2\right] \tag{2.1.11}$$

The normalised NPP is then

$$\Pi_N = \frac{\Gamma_i(\theta)}{\Gamma_{max}}\,\nu_i \tag{2.1.12}$$

2.2 Equilibrium at Constant Temperature

The system is at steady-state when all fractional coverages are at steady-state. From 2.1.9 it can be seen that any species i is at equilibrium when either:-

$$\begin{aligned} &\nu_i = 0 \\ \textit{or} \\ &\sum_j \nu_j = 1 - \frac{1}{\Gamma_i(\theta)} \end{aligned} \tag{2.2.13}$$

If Γ_i differs between species, only one species can have non-zero coverage when all species are at steady-state. This is because the dominant species will keep growing and reducing the bare soil fraction below the equilibrium threshold for all other species, until only the dominant species remains with a steady-state coverage of: -

$$\nu_j = 1 - \frac{1}{\Gamma_j(\theta)} \tag{2.2.14}$$

If $g_{max} = 0.1$ and $\gamma = 0.01$ then $\Gamma_j = 10$ (assuming the dominant species is at its optimum temperature) we expect the dominant species to have a coverage of 0.9 and all other species zero.

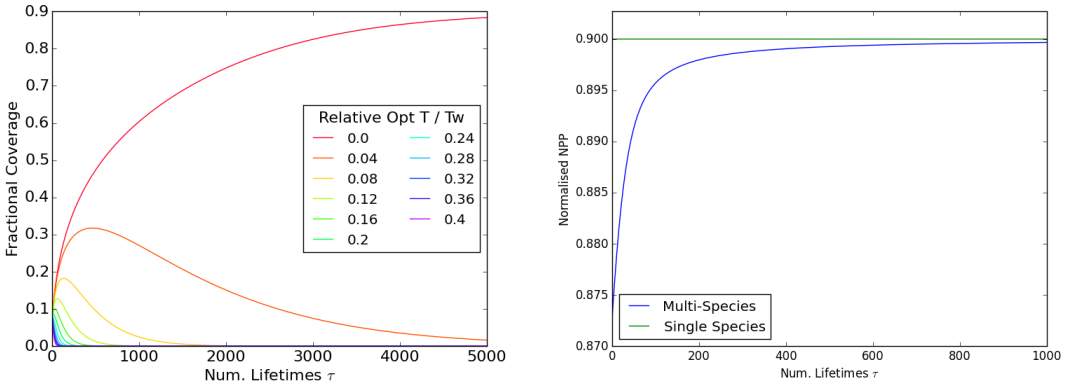

(a) Fractional Coverage **(b)** Productivity (NPP)

Figure 2.3: Evolution of the system for $\Gamma_{max} = 10$, starting from a (non-equilibrium) state where all species have equal coverage to steady-state, where only one dominant species remains. a) Shows the time evolution of species coverage. b) Shows the evolution of the total system NPP. The green productivity curve shows (for comparison) the productivity of single species at steady-state at its optimum temperature.

Figure 2.3 shows the model behaves as expected, this behaviour is also seen for different numbers of species. Interestingly, the NPP appears on visual inspection to reach steady-state faster so it may be useful to investigate the e-folding time-scales of both the dominant species and the total system NPP.

In section 2.3 this constant temperature steady-state solution will be used as an initial condition for changing environmental temperature by assuming the model starts in steady-state with its initial starting temperature.

2.2.1 Effect of Interspecies Competition

The speed at which the system reaches steady-state is determined by the spacing of the species. A larger spacing between the species allows the system to reach steady-state much faster than if they are more closely spaced (Figure 2.4).

The dynamics of this set of equations are that all species will grow and that as they grow the amount of bare soil is reduced which reduces the growth of all species

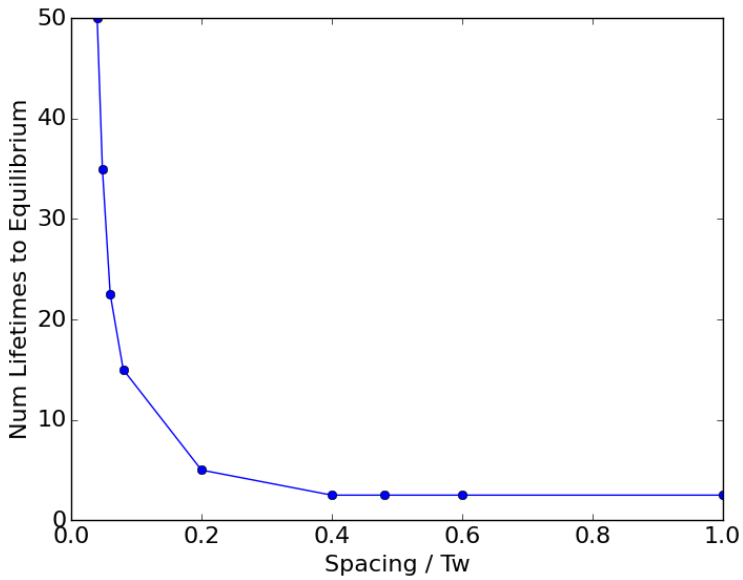

Figure 2.4: Shows the effect of the species spacing on the time-scale of the NPP as the system approaches steady-state. The time-scale is assumed to be time it takes for the NPP to be within 1/e of the final NPP, when $\Gamma_{max} = 10$. The curve shows that the closer the spacing the longer the system takes to reach steady-state.

equally. Once the bare soil is reduced enough the species with the lowest growth rate will start to lose coverage (i.e. when $s < \frac{1}{\gamma_i}$ then $d\nu_i d\tau < 0$), which in turn will increase the bare soil to be used by species with higher growth rates. This process carries on until only the species with the highest growth rate is still growing.

This means that a greater spacing of the species optimum temperatures will cause the species that are further from their optimum temperature to have a lower growth rate. Hence their coverage will therefore decline much sooner than if they are closely spaced.

2.3 Response to Linear Temperature Increase

To investigate the effect of increasing temperature on the model a simple linear increase is used.

$$T(t) = T_{initial} + \left(\frac{dT}{dt}\right) t \tag{2.3.15}$$

Converting to non-dimensional form gives: -

$$\theta(\tau) = \theta_{initial} + \alpha\tau \tag{2.3.16}$$

where α is

$$\alpha = \frac{\left(\frac{dT}{dt}\right)}{\gamma\, T_w} = \frac{d\theta}{d\tau} \tag{2.3.17}$$

The value of α represents the ratio of temperature and biological time-scales, in terms of the number of grow curve widths that the temperature increases by in a species lifetime ($\frac{1}{\gamma}$). So an alpha value of 1 would mean that in time $\frac{1}{\gamma}$ the temperature has increased by T_w.

The system is initialised to the steady-state described by equation 2.2.14 and then the temperature is increased linearly. The increasing temperature changes the dominant species, as this is the species with its optimum temperature closest to the current environmental temperature (as it has the highest growth rate). As soon as the environmental temperature increases to the point where another species has a closer optimum temperature then the dominant species changes. The steady-state of the system is always for the system to evolve towards a state with only the dominant species with coverage given by equation 2.2.14. The increasing temperature means the system never reaches steady-state as this is always moving away from the current system state.

An example of the model response for a particular rate of temperature increase is shown in Figure 2.5. The model has 16 species with relative optimum temperatures arranged linearly from 0 to $0.4T_w$.

The model is initially started with the temperature at that of the optimum temperature of the first species $\theta = \theta_{opt,0}$ and the system in steady-state at that temperature (only optimum species has any coverage). As the temperature starts to increase the growth rate of the first dominant species slowly declines. Once the temperature reaches the half way point between the optimum temperatures of the first and second species then the model transitions to the second species being dominant (i.e. having largest growth rate). At this point the original dominant species starts to decline more rapidly and increase the bare soil allowing the second species to increase.

It takes a long time for the first species to decline due to mortality. The first species will start to decline as soon as its growth rate drops and this will increase the space allowing the second species to start to grow and gain ground on the first species.

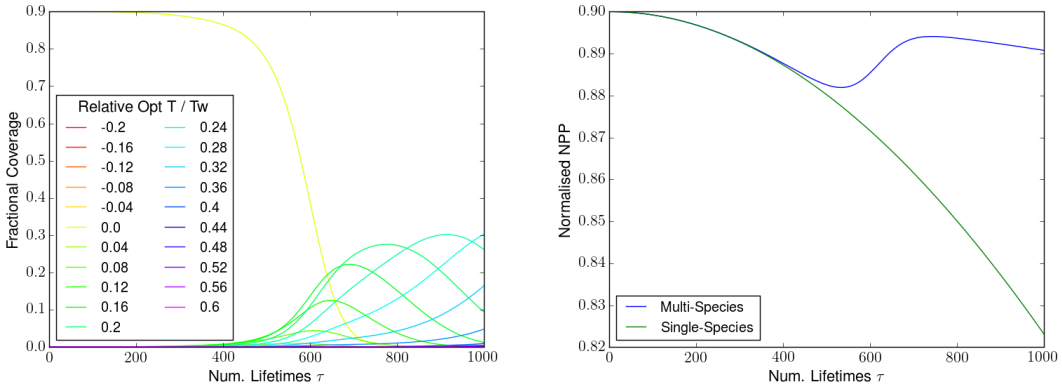

(a) Fractional Coverage

(b) Productivity (NPP)

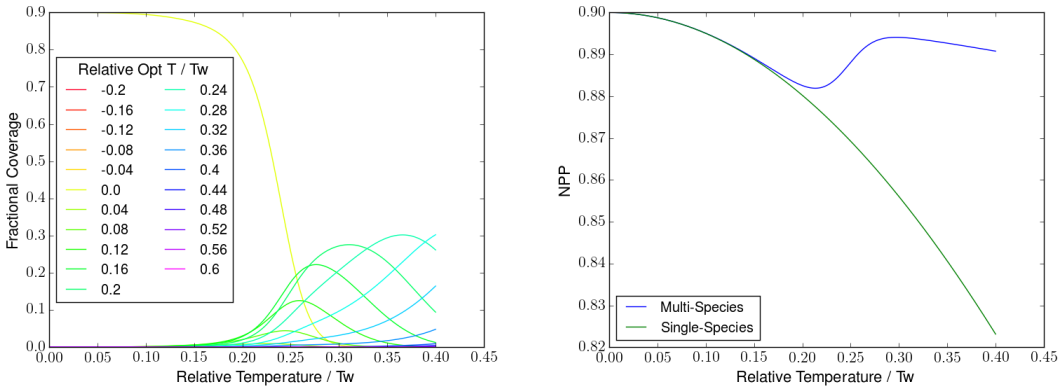

(c) Fractional Coverage

(d) Productivity (NPP)

Figure 2.5: Evolution of the system starting from steady-state when temperature increases linearly by $0.4T_w$ at a rate $\alpha = 0.0004$, with max growth:death ratio $\Gamma_{max} = 10$. a) b) Plotted in terms of time. c) d) Plotted in terms of temperature.

2.3.1 Dynamic Pseudo-Equilibrium

There is a transient phase at the start of the temperature increase as the initially dominant species takes time to decline to the point where other species can get a foothold. This can be seen in Figure 2.5 b) and d) as an overshoot oscillation in NPP with a decaying amplitude. This suggests that the system is in a transient state as it transitions from a steady-state with static temperature to a dynamic pseudo-equilibrium with linearly increasing temperature.

If the temperature is allowed to increase it can be seen more clearly that the NPP oscillation decreases in amplitude and the NPP converges on a fixed level even though the system is still undergoing temperature change (Figure 2.6).

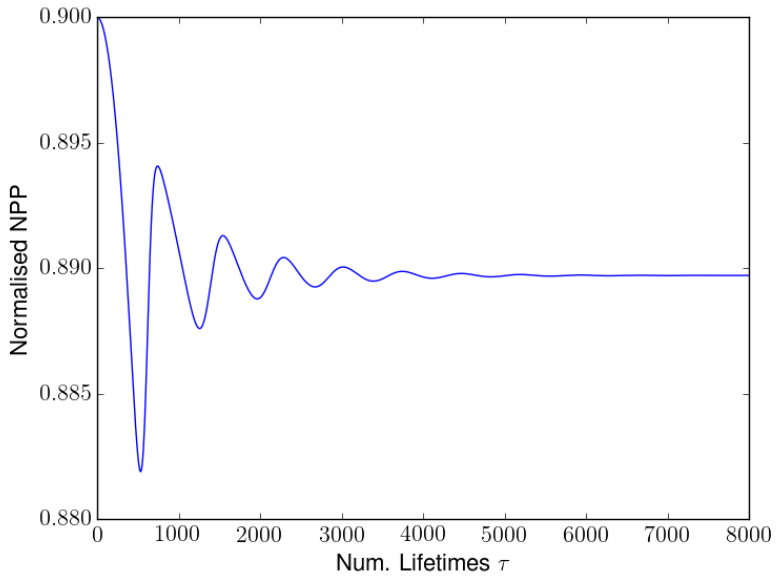

Figure 2.6: Shows the transient oscillation in Normalised total system NPP for rate of temperature increase $\alpha = 0.0004$ (total linear increase in temperature of 3.2 T_w). Species spacing 0.04 T_w and $\Gamma_{max} = 10$.

This pattern is seen for many different rates of temperature increase (Figure 2.7) with faster rates of change giving rise to lower NPP and more heavily damped transient.

The behaviour at this pseudo-equilibrium is that each species' fractional coverage

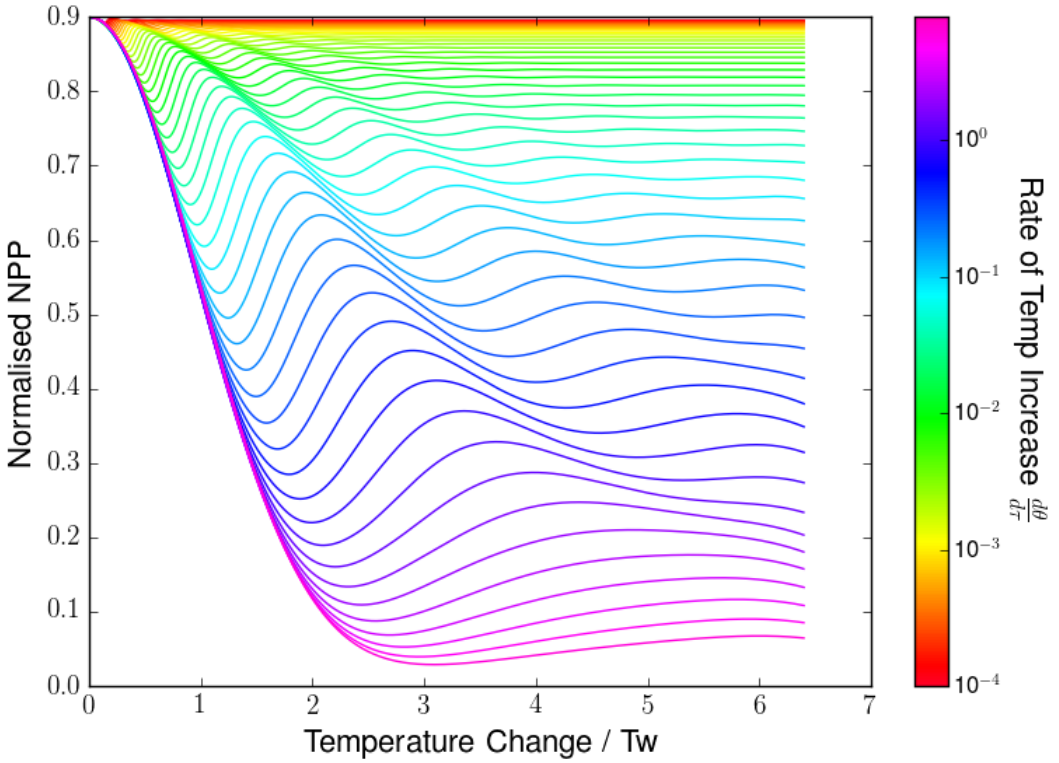

Figure 2.7: Normalised NPP plots for all different temperature increase scenarios. The system in each case has undergone a fixed temperature rise of 6.4 T_w but at different rates. The colour-bar shows the value of α (rate of temperature increase in T_w per lifetime) for each colour curve. Species spacing $0.04T_w$ and $\Gamma_{max} = 10$.

has a Gaussian like shape when plotted against time or environment temperature and the species coverage curves have similar shapes, just translated in time to each other (Figure 2.8). In the early transient phase this behaviour is not seen and while species do have coverages with similar Gaussian like shapes they vary considerably in height and width.

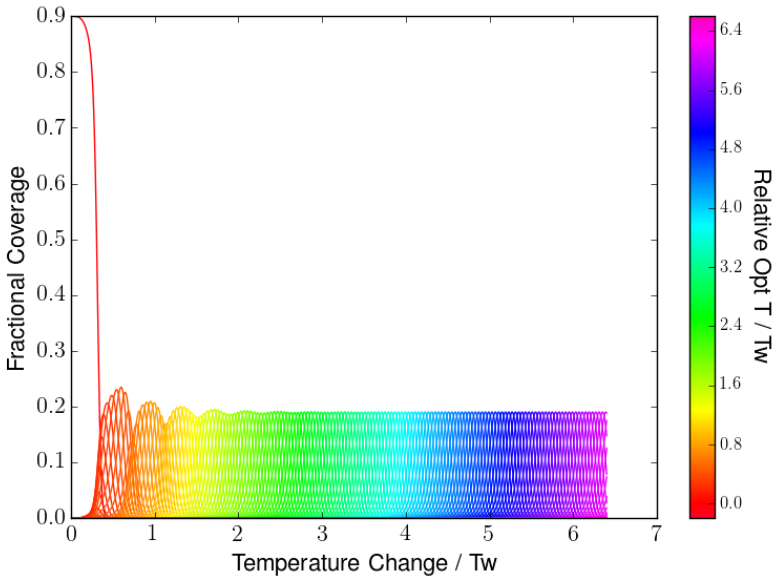

Figure 2.8: Shows the fractional coverage undergoing a temperature rise of rate $\alpha = 0.001$ for 6.4 growth curve widths (6.4 T_w). Each colour curve represents one species with its optimum temperature shown in the colour-bar. Species spacing $0.04T_w$ and $\Gamma_{max} = 10$.

Figure 2.9 shows that the shape of the dynamic pseudo-equilibrium varies with the rate of temperature increase. As the rate of temperature becomes faster the delay between the environment reaching a particular species optimum temperature and the species coverage reaching a peak increases. Also the height tends to decrease (although an initial increase is briefly seen) and the width increases. This is because the previously dominant species have to die first to allow the newly dominant species to take over and as this time-scale is fixed the system lags behind the environmental temperature more and more as the temperature rate increases.

This suggests that there is a rate dependence in the coverage and NPP with both

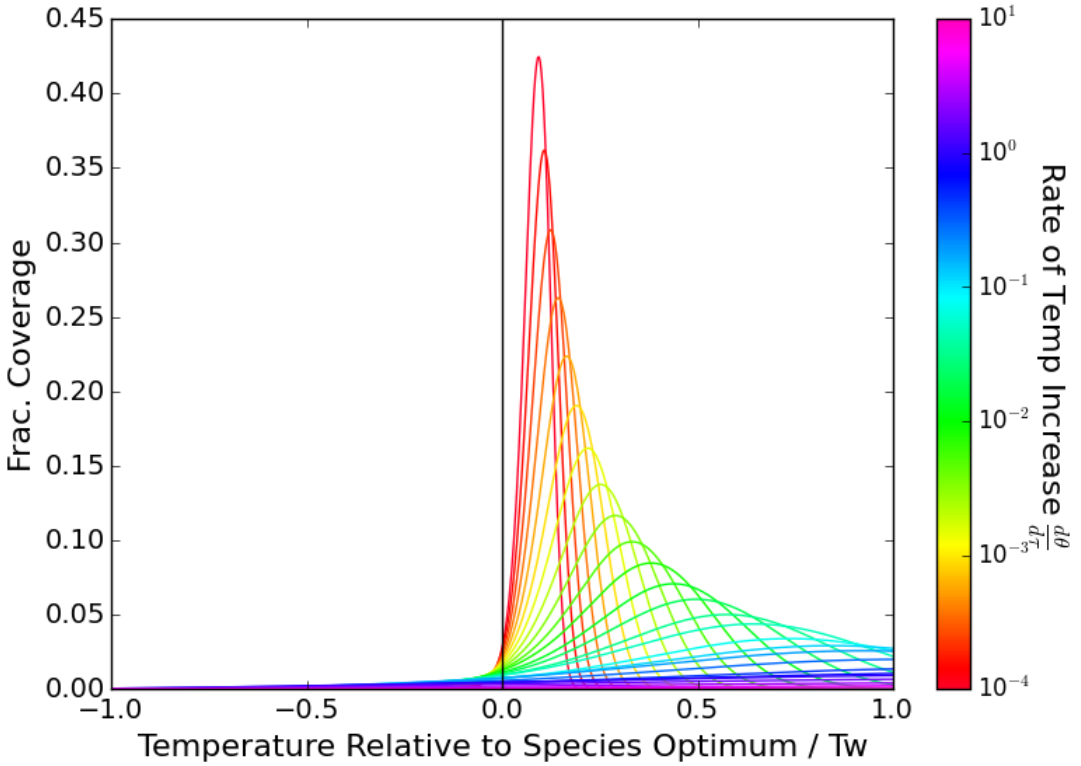

Figure 2.9: Shows how the rate of temperature increase affects the fractional coverage of one species relative to its optimum temperature. The position of the peak moves to higher and higher temperatures as the rate of temperature change is increased. This is because there is a lag in the system created by the time needed for previously dominant species to die off. The colour-bar shows the value of α (rate of temperature increase in T_w per lifetime) for each colour curve. Species spacing $0.04T_w$ and $\Gamma_{max} = 10$.

being suppressed more and more by increasing temperature rates. This can be seen in Figure 2.7 as the pseudo-equilibrium NPP values are reduced as the rate of temperature increase becomes faster.

Figure 2.10 shows this more clearly and shows that there is a critical rate of temperature change where the NPP suddenly falls rapidly. The curves for changes in temperature of less than 8 T_w show different critical rates but these are dependent on the transient phase, so the NPP for any particular rate will initially decrease and then recover somewhat for rates less than the critical rate corresponding to the dynamic pseudo-equilibrium.

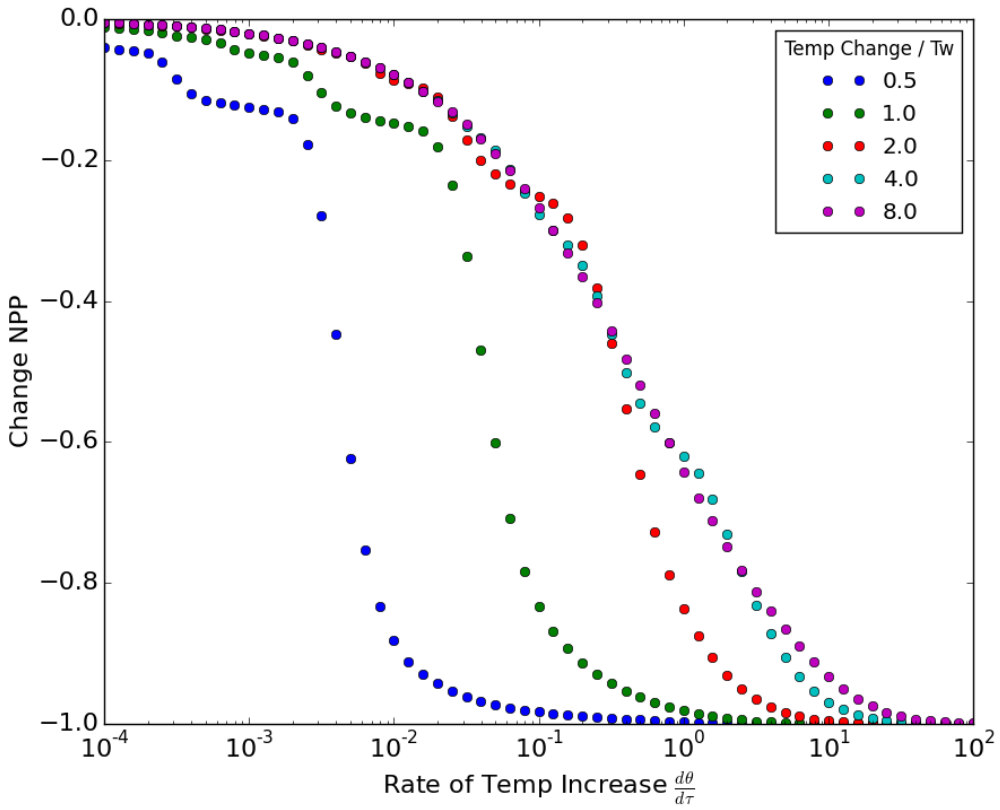

Figure 2.10: Shows the fractional change in normalized NPP for different rates of temperature increase.

2.4 Response to Non-Linear Temperature Increase

The simple linear model switches abruptly from constant temperature steady-state state to a linearly increasing temperature scenario. This creates a temperature gradient discontinuity which may be a cause of the large transient NPP oscillations seen in the model.

To investigate this a new temperature increase model is used based on the simplest possible climate model (Equation 2.4.18). This represents a linearly increasing radiative forcing ΔQ with heat capacity C_p and sensitivity λ. The heat capacity acts to delay any changes and allows the model to more smoothly transition from static to increasing temperature without a discontinuity. This model represents the real world where oceanic diffusion is protecting us at the moment from the real effects of CO_2 at 400ppm.

$$C_p \frac{d\Delta T}{dt} + \lambda \Delta T = \Delta Q = \beta t \tag{2.4.18}$$

If we then non-dimensionalise this and solve we get the solution

$$\theta = \theta_0 + \Delta\theta = \theta_0 + \alpha \left[\tau - \tau_T \left(1 - e^{-\tau/\tau_T} \right) \right] \tag{2.4.19}$$

where

$$\tau_T = \frac{C_p \gamma}{\lambda} \tag{2.4.20}$$

$$\alpha = \frac{\beta \gamma}{\lambda} \tag{2.4.21}$$

In the above α is equivalent to the linear α in section 2.3 and is the rate of increase seen when $\tau >> \tau_T$.

The effect of the non-linear temperature increase can be seen in Figure 2.11. The only effect of having a smoother transition of static to increasing temperature

is to reduce the transient oscillations. The model still converges on the pseudo-equilibrium state seen before but with smaller magnitude oscillations.

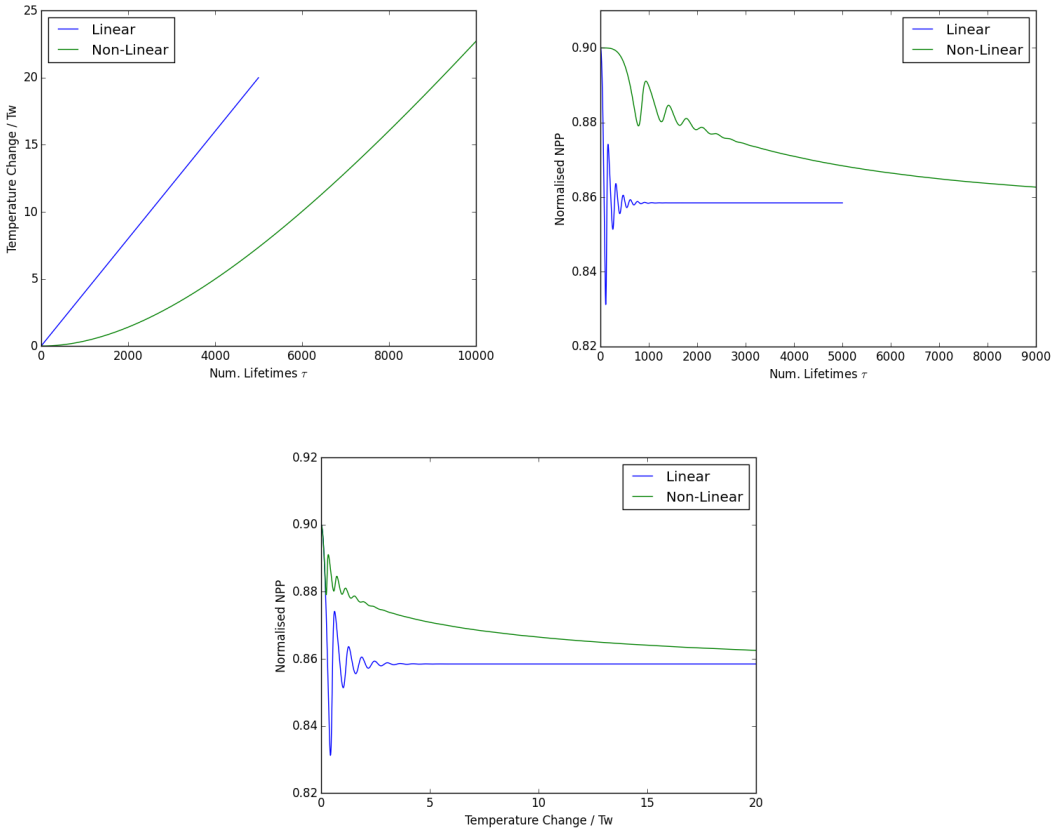

Figure 2.11: Shows the effect of the non-linear model of temperature increase compared to the linear. Both linear and non-linear start with the system in steady-state with the starting temperature. The non-linear model has reduced transient oscillations but still converges on the same pseudo-equilibrium state. Species spacing $0.04T_w$, $\Gamma_{max} = 10$, $\tau_T = 5000$ lifetimes and $\alpha = 0.004$. a) Temperature as function of time b) NPP as a function of time c) NPP as a function of temperature.

Overall this suggests the best comparison of the effect of rate of change on the system is to always compare after any transient effects have died down and to look at the pseudo-equilibrium state.

2.5 Generating Diversity via Competition Coefficients

It is a standard result of Lotka-Volterra competition theory that to get stable coexistence of species, the members of each species must compete more strongly among themselves than with other species (May and McLean, 2007). This is the same idea as that of each species having a 'niche' where it dominates. The advantage of this is that it is easy to achieve but this section shows that this also risks breaking conservation of the coverage.

Details are developed more fully in Appendix A but for an n species system the equations are: -

$$\frac{d\nu_i}{d\tau} = a_i \left[\left(1 - k\nu_i - c \sum_{j \neq i} \nu_j \right) \Gamma_i(\theta) - 1 \right] \tag{2.5.22}$$

where k is the competition coefficient between members of the same species and c the competition coefficient between different species.

This system can be solved to find an equilibrium solution where all species coexist: -

$$\nu_i = \frac{1}{(k + (n-1)c)(k-c)} \left[(k + (n-2)c) \left(1 - \frac{1}{\Gamma_i} \right) - c \sum_{j \neq i} \left(1 - \frac{1}{\Gamma_j} \right) \right] \tag{2.5.23}$$

This requires that $k > c$, which is just the standard result of Lotka-Volterra competition theory but also requires that all species in the system are growing: -

$$\left(1 - k\nu_i - c \sum_{j \neq i} \nu_j \right) \Gamma_i(\theta) - 1 \geq 0 \tag{2.5.24}$$

Any species that does not meet this requirement will be competitively excluded but unless the system is reduced by excluding the uncompetitive species then the above solution will not necessarily hold.

The total coverage is

$$\nu_{tot} = \sum_i \nu_i = \frac{1}{k + (n-1)c} \sum_i \left(1 - \frac{1}{\Gamma_i}\right) \tag{2.5.25}$$

This equation highlights that this type of system has a problem of conserving fractional coverage. The above equation does not naturally constrain either the individual or total coverage between 0 and 1.

As it is difficult to find simple constraints that naturally keep particularly the total coverage below 1 it makes this system difficult to use for simulating the effect of diversity on resilience the environmental change. The conservation issue also highlights the problems in general with the use of competition coefficients, in particular as they do not model any specific mechanism of competition then they cannot be estimated in advance of any instance of competition in the field (Grover, 1997).

2.6 Discussion and Conclusions

The Lotka-Volterra model is an established model of population growth and competition. This chapter has used a form of this model to look at a simple system of plants with different temperature traits.

The simplest version of this model will, for a given temperature, have a steady-state where the species which is most suited to the conditions remains and all others are excluded. The speed of the system reaching steady-state depends on the spacing of species, with more widely spaced species reaching steady-state faster, as the non-optimal species are less competitive and are therefore excluded much quicker.

Once this model undergoes a linear temperature increase the NPP will initially collapse as the previously dominant species dies off. Then, once this species has declined enough, other species which are more suited to the higher temperature can then start to grow. However, further in time as the temperature continues to

increase they too will decline and be replaced by yet another species. The NPP after its initial collapse will follow a transient oscillation before the NPP settles down to a new constant level, albeit lower than the the starting steady-state. This suggests the possibility of a "pseudo-equilibrium", that while the species coverages are constantly changing, the overall NPP is constant in time.

If the system undergoes different rates of temperature increase from 10^{-4} to 100 T_w per lifetime, it can be seen the faster the temperature increases the more the system struggles to maintain its NPP in the “pseudo-equilibrium” state. There seems to be critical range of rates as at 0.1 T_w per lifetime the system is maintaining 80% of its steady-state NPP, by 1 T_w per lifetime it is down to 40% NPP and by 10 T_w per lifetime it is down to 10%.

By changing the temperature increase from linear to one involving a heat capacity, so the system has a lag analogous to the Earth undergoing climate change, it can be seen that the transient oscillations in the NPP are reduced. This suggests the transient is a result of the system being pushed out of its initial steady state when the temperature increase suddenly starts. The system then takes awhile to settle down into the dynamic “pseudo-equilibrium”, once the temperature is increasing.

This study had originally been intended to look at the effect of introducing diversity, to see if having coexisting temperature traits would make the system more resilient to a given rate of temperature increase. The current TRIFFID formulation of the Lotka-Volterra competition model can be adapted, using competition coefficients, to achieve coexistence. Unfortunately it is difficult to keep both the individual species coverages and the total coverage in the range 0 to 1 as the competition coefficients break the conservation of coverage. This suggests the competition coefficients are too abstract and have no mechanism of competition to both conserve coverage and allow coexistence.

In TRIFFID itself competitive coexistence (i.e. coefficients other than 1 or 0) only occurs for competition between the two tree PFTs and the two grass PFTs and the sum of coefficients of each competing pair is always equal to 1. While it is

theoretically possible for the PFT fractional coverages in TRIFFID to drop below 0 or become greater than 1, the limitations just mentioned restrict this to values of the growth and competition coefficients that are never reached in practice. It would still be worthwhile adding guard clauses to the code to make sure PFT coverages always remain in the range 0 to 1, to prevent future changes to TRIFFID possibly causing the coverages to no longer always being in the desired range.

The next chapter will avoid these issues by using a resource based model rather than Lotka-Volterra and to use temperature stochasticity instead of competition coefficients as a means to maintaining coexistence of species with different temperature traits.

Chapter 3

Stochastic Resource Model

The Lotka-Volterra model (hereafter the LV model), initially applied to predator-prey mammal populations was amongst the first mathematical models of species competition and coexistence (May, 1974; May and McLean, 2007). In the LV model competition takes place through competition coefficients which are chosen empirically to reproduce observed features of the ecosystem, such as its species-mix. However, there is typically no mechanism that can be used to determine the competition coefficients, which introduces an arbitrary element to the LV model that makes prediction difficult (Grover, 1997). Arguably, a better alternative is to model competition mechanistically in terms of the competition for limiting resources, such as nutrients or light. A process basis is also always more appropriate for prediction, as this allows the effects of any driver changes on competition parameterisation to be explicitly modelled, and in a way not possible with fitted competition co-efficients.

Tilman and co-workers have extensively studied resource competition both for species competing for a single resource and for multiple resources (Tilman, 1982; Grover, 1997). Resource competition models are based on the assumption that competition happens purely via the limiting resource and not through direct competition (Grover, 1997; May and McLean, 2007). Resources are typically modelled as a scalar without spatial dimension or environmental heterogeneity. With these

simplifying assumptions, the multiple resource case allows coexistence, but competition for a single resource always results in a single dominant species (Tilman, 1982; Grover, 1997).

Lehman and Tilman (2000) also studied a single resource model with a varying environmental temperature and growth rates for each species that are temperature dependent, with each species having a unique optimum temperature for growth. All species are otherwise identical except for their optimum temperature. Growth rate is modelled as a Gaussian function of temperature with the peak corresponding to the species optimum temperature. Whichever species is closest to its optimum temperature will have superior growth and if the temperature is constant that species will exclude all others.

However, by including temperature variability Lehman and Tilman (2000) found that coexistence could be achieved as the species with the growth advantage was constantly changing as the temperature varied. As long as the temperature change is fast enough and over a big enough range, several species can be maintained in coexistence. This is an intriguing result that hints at one possible mechanism (i.e. environmental temporal variability) to maintain species diversity.

This chapter extends the mathematical analysis of the Lehman and Tilman (2000) model to examine the sensitivity of its diversity and productivity to the stochastic nature of the temperature variability. To address the key question of whether a more diverse ecosystem is likely to be more resilient to climate change the model is also further extended by including a linearly increasing trend on the varying temperature.

3.1 Model Equations

The equations of the resource model system (Lehman and Tilman, 2000) are: -

$$\begin{aligned} \frac{dR}{dt} &= a(S-R) - Q\frac{R}{R+K}\sum_j g_j(T)\,B_j \\ \frac{dB_i}{dt} &= \left[g_i(T)\,\frac{R}{R+K} - \gamma\right] B_i \\ g_i(T) &= g_{max}\,\exp\left[-\frac{1}{2}\left(\frac{T-T_{OPT,i}}{T_w}\right)^2\right] \end{aligned} \tag{3.1.1}$$

Symbol	Variable / Parameter	Unit
B_i	Biomass species i	t ha^{-1}
g_i	Temperature dependent biomass growth rate species i	year^{-1}
g_{max}	Maximum growth rate	year^{-1}
γ	Species i mortality	year^{-1}
T	Environmental temperature	°C
$T_{OPT,i}$	Optimum temperature species i	°C
T_w	Temperature growth curve width	°C
R	Resource availability	t ha^{-1}
S	Resource supply	t ha^{-1}
Q	Unit biomass resource cost	-
K	Resource half saturation constant	t ha^{-1}
a	Conversion rate unavailable to available resource	year^{-1}
R^*	Equilibrium resource level	t ha^{-1}
B_i^*	Equilibrium biomass level of dominant species	t ha^{-1}

Table 3.1: List variables and parameters for Chapter 3

The term $\frac{R}{R+K_i}$ is known as the Monod formulation (see Figure 3.1). This model gives a saturation in growth as R increases, which is known to be a simplistic yet

good approximation for microbial and plankton growth but is also reasonable for higher plants (Grover, 1997; Tilman, 1982).

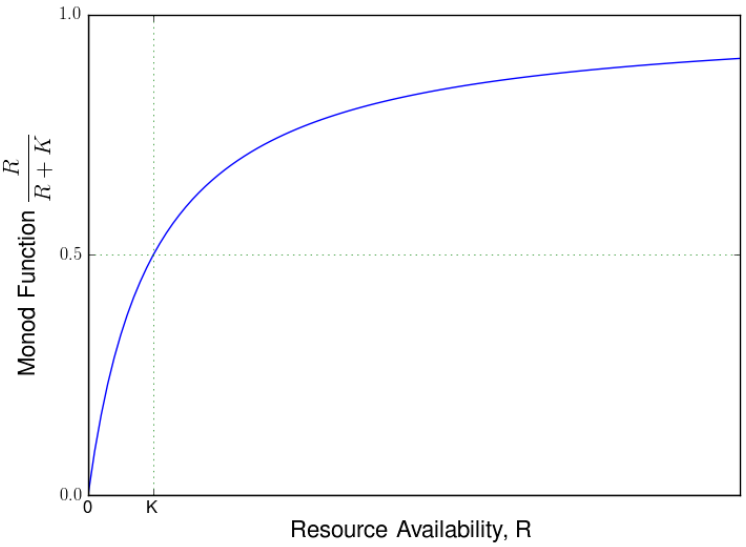

Figure 3.1: The Monod Growth Function

The variation of $\frac{1}{dB_i}\frac{dB_i}{dt}$ with R and g is shown in Figure 3.2 (note the plot uses $r = \frac{R}{S}$).

From equation 3.1.1 it can be seen that there is a unique resource level R^* (Tilman, 1982; Grover, 1997) that gives zero growth $\frac{dB_i}{dt} = 0$ for each species.

$$R^* = \frac{K\gamma}{g_i(T) - \gamma} \tag{3.1.2}$$

As $\frac{R}{R+K}$ is a continuously increasing function of R (see Figure 3.1), any resource level below R* will give $\frac{dB_i}{dt} < 0$ and any resource level above R* will give $\frac{dB_i}{dt} > 0$. This means the species with the lowest R^* will dominate and will displace all others in time. This is because as species' populations grow they reduce the resource availability R (see Equations 3.1.1) and so a species with a low R^* will still be growing when species with higher R^* have stopped growing.

Once all other species go extinct the dominant species has an equilibrium biomass level of: -

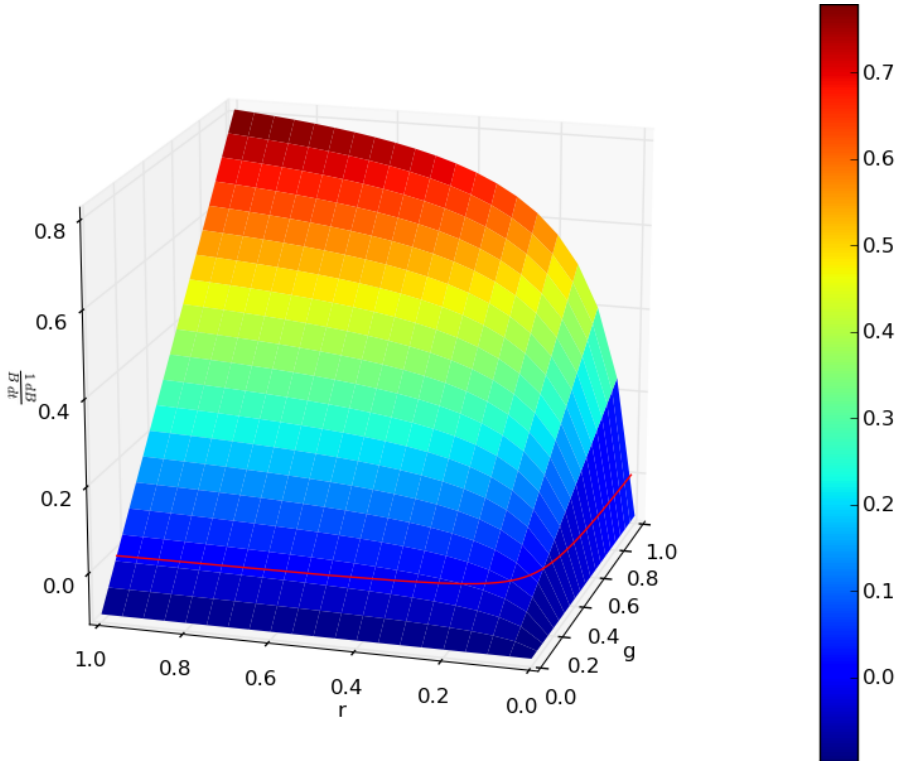

Figure 3.2: Variation of $\frac{1}{dB_i}\frac{dB_i}{dt}$ with growth rate g(T) and $r = \frac{R}{S}$. The red line indicates where $\frac{1}{dB_i}\frac{dB_i}{dt} = 0$.

$$B_i^* = \frac{a(S - R_i^*)(R_i^* + K)}{gQR_i^*} = \frac{a\,(S - R_i^*)}{Q\,\gamma} \tag{3.1.3}$$

3.2 Non-Dimensionalised System

To aid analysis and identification of timescales then the system can be non-dimensionalised. All quantities in equation 3.1.1 can be dimensionalised in terms of dimensions of time $[t]$, resource $[R]$, temperature $[T]$ or species biomass $[B]$.

$$\begin{aligned} &B = [B] \\ &a,\ g_i(T),\ \gamma = [t^{-1}] \\ &R,\ S,\ K = [R] \\ &Q = [RB^{-1}] \\ &T,\ T_w,\ T_{OPT,i} = [T] \end{aligned} \tag{3.2.1}$$

This allows to refine our variables in terms of a new dimensionless set:-

$$\begin{aligned} k &= \frac{K}{S} \qquad r = \frac{R}{S} \qquad b_i = \frac{Q\,B_i}{S} \\ \theta &= \frac{T}{T_w} \quad \theta_{OPT,i} = \frac{T_{OPT,i}}{T_w} \quad \tau = t\gamma \\ \mu &= \frac{a}{\gamma} \qquad \Gamma_i = \frac{g}{\gamma} \end{aligned} \tag{3.2.2}$$

Giving us a new set of equations: -

$$\begin{aligned} \frac{dr}{d\tau} &= \mu(1 - r) - \frac{r}{r + k} \sum_j \Gamma_j(\theta)\, b_j \\ \frac{db_i}{d\tau} &= b_i \left[\Gamma_i(\theta)\, \frac{r}{r + k} - 1 \right] \\ \Gamma_i(\theta) &= \Gamma_{max}\ exp\left[-\frac{1}{2}\,(\theta - \theta_{OPT,i})^2 \right] \end{aligned} \tag{3.2.3}$$

3.3 Dynamics of One Species with One Resource

The simplest system is one species growing with one limiting resource and having a fixed growth rate (corresponding to a fixed temperature).

$$\begin{aligned} \frac{dr}{d\tau} &= \mu(1-r) - \frac{r}{r+k}\Gamma\, b \\ \frac{db}{d\tau} &= b\left[\Gamma\,\frac{r}{r+k} - 1\right] \end{aligned} \tag{3.3.1}$$

This system has 2 equilibria: -

$$\begin{aligned} (r,b) &= (1,0) \\ (r,b) &= (r^*, b^*) \end{aligned} \tag{3.3.2}$$

where $r^* = \dfrac{k}{\Gamma - 1}$ and $b^* = \mu(1-r^*)$.

There are three regimes which depend on the value of Γ (See Appendix B.1). These are shown in Table 3.2.

Table 3.2: Dynamical regimes

Regime	$(r,b) = (1,0)$	$(r,b) = (r^*, b^*)$	r^*
$\Gamma > (k+1)$	Unstable	Stable	$r^* < 1$
$1 < \Gamma \leq (k+1)$	Stable	Doesn't Exist	$r^* > 1$
$\Gamma \leq 1$	Stable	Doesn't Exist	$r^* < 0$

To understand the model behaviour under the three regimes then it is necessary to look at the nullclines and model trajectories on phase plot for each case. The nullclines for resource is given by equation (3.3.3) and for biomass by equation (3.3.4) below.

$$b = \frac{\mu(1-r)(r+k)}{\Gamma r} \tag{3.3.3}$$

$$r = r^* = \frac{k}{\Gamma - 1} \tag{3.3.4}$$

3.3.1 Stable regime $\Gamma > (k+1)$

This regime is the only one where a population can be maintained as it has both enough resource supply and high enough growth rate.

The phase plot with nullclines for $\Gamma > (k+1)$ can be seen in Figure 3.3(a). Where the nullclines cross there is a stable equilibrium with the unstable equilibrium at $(r, b) = (1, 0)$. The green line on Figure 3.3(a) shows the variation of the position of the stable equilibrium with changing growth rate g, this will be discussed in section 3.3.4.

The dynamics can be seen in Figure 3.3(b). The system always heads towards the resource nullcline and from there then follows that nullcine to the stable equilibrium.

The same dynamics can be seen in terms of the biomass and resource levels as a function of time in Figure 3.4.

3.3.2 Insufficient Resource Regime $1 < \Gamma \leq (k+1)$

In this regime while the single species has an intrinsic growth rate that is higher than its mortality the resource supply is not high enough to maintain growth and reduces the intrinsic growth rate below mortality even when the available resource is at its maximum.

The direction fields and nullclines for $1 < \Gamma \leq (k+1)$ are shown in Figure 3.5. Again the system heads first to the resource nullcline and then to the equilibrium, this time to $(r, b) = (1, 0)$ which the only equilibrium and is stable. The $(r, b) = (r^*, b^*)$ equilibrium doesn't exist as $r^* > 1$, meaning the resource supply S is smaller than the equilibrium resource level and hence cannot supply enough resource for growth to balance mortality.

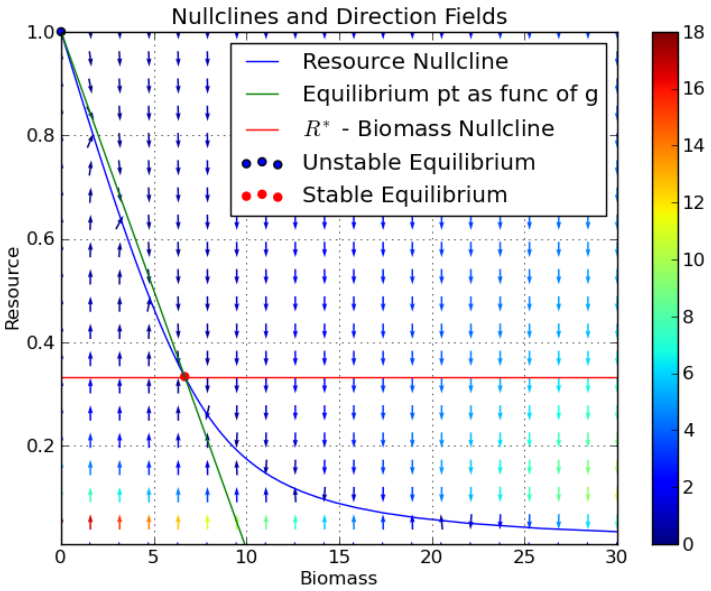

(a) Nullclines

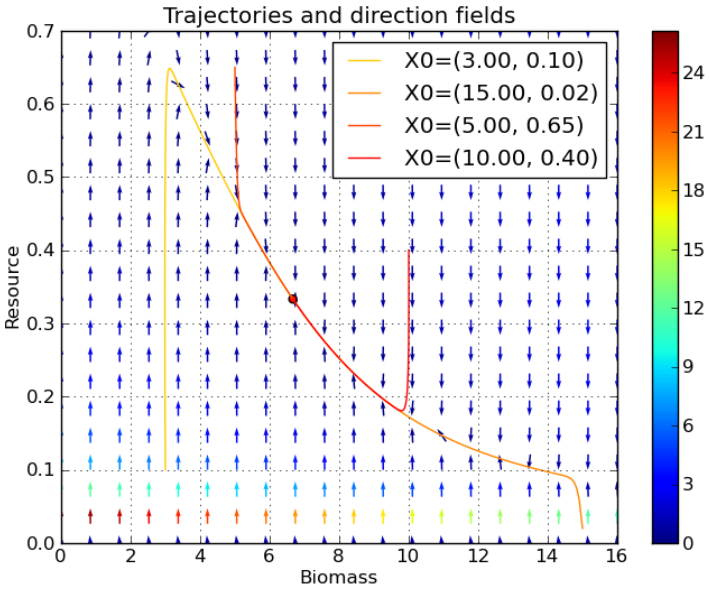

(b) Typical trajectories

Figure 3.3: Phase plot including direction fields of the system for $\Gamma > (k+1)$. In a) where the nullclines cross is the stable equilibrium and the green lie shows how stable point changes with growth rate g. b) Shows typical trajectories starting from different initial points, all head towards the nullcline and then follow it to the stable equilibrium point.

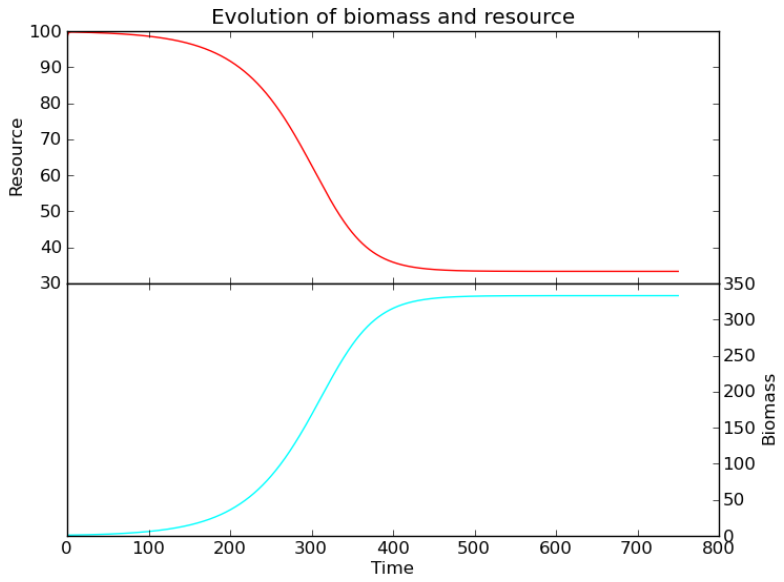

Figure 3.4: Plot of resource and species biomass with time. Show the system achieving equilibrium state from initial state of low biomass and high resource availability.

3.3.3 Mortality Dominated Regime $\Gamma \leq 1$

In this regime the intrinsic growth rate is below the mortality, so none of the species can survive regardless of how much resource supply the ecosystem can provide. Hence in Figure 3.6, all trajectories travel to the stable equilibrium (red dot), corresponding to zero biomass.

For $\Gamma \leq 1$ (Figure 3.6) the system again heads to $(r, b) = (1, 0)$. As $\Gamma \leq 1$ and $\frac{r}{r+k} < 1$ so $\frac{1}{b}\frac{db}{dt} < 0$ always.

3.3.4 Effect of Varying Γ

As we are interested in studying the effects of temperature on coexistence, it is useful to understand how the simple one species system responds to a change in the growth:death ratio term Γ, as this typically is a function of temperature. The most logical place to start is to understand how a change in Γ changes the equilibrium of the system.

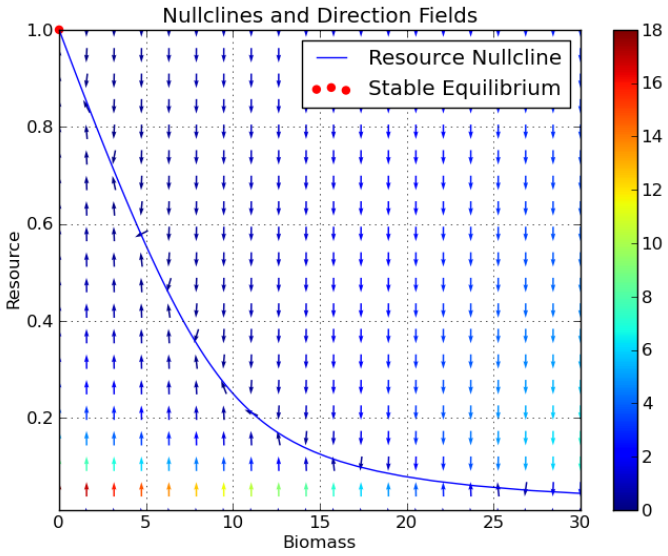

(a) Nullclines

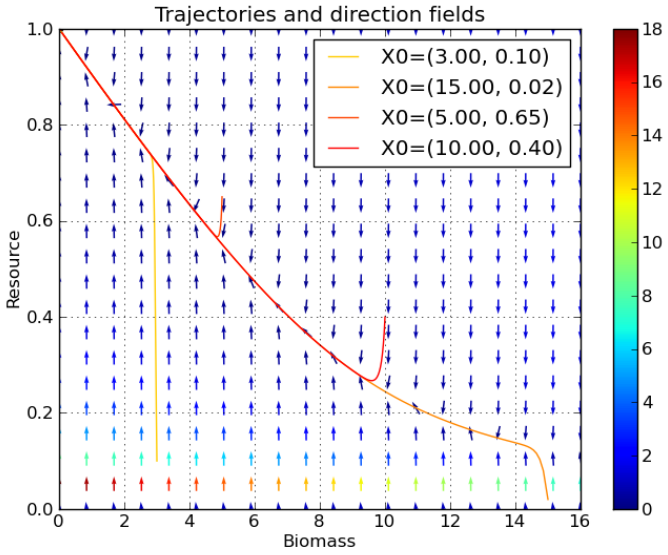

(b) Typical trajectories

Figure 3.5: Showing the direction fields of the system for $1 < \Gamma \leq (k+1)$. In a) only the resource nullcline can be seen as the biomass nullcline is now higher than r=1 and so can no longer cross the resource nullcline. The equilibrium at $(r, b) = (1, 0)$ is stable. b) Shows typical trajectories starting from different initial points, all head towards the nullcline and then follow it to the stable equilibrium point at $(r, b) = (1, 0)$.

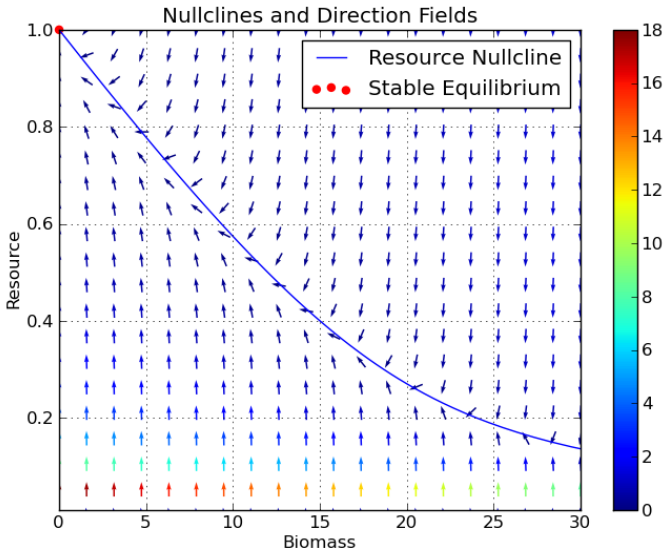

(a) Nullclines

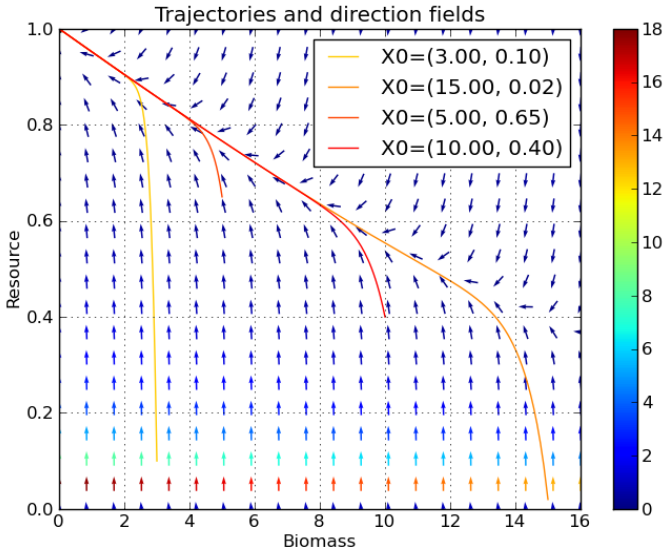

(b) Typical trajectories

Figure 3.6: Showing the direction fields of the system for $\Gamma \leq 1$. In a) only the resource nullcline can be seen as the biomass nullcline is now negative and so cannot cross the resource nullcline. b) Shows typical trajectories starting from different initial points, all head towards the nullcline and then follow it to the stable equilibrium point at $(r, b) = (1, 0)$.

The equations for the equilibrium resource and biomass levels are: -

$$r^* = \frac{k}{\Gamma - 1} \tag{3.3.5}$$

$$b^* = \frac{\mu(1-r^*)(r^*+k)}{\Gamma r^*} = \mu(1-r^*) = \frac{\mu(\Gamma-(1+k))}{(\Gamma-1)} \tag{3.3.6}$$

Figure 3.7 shows these equations graphically.

The values of equilibrium resource and biomass are only meaningful when positive and also the equations governing the system do not allow negative values to be reached. So this shows again that $\Gamma > (k+1)$ must be true for the non-trivial equilibrium $(r, b) = (r^*, b^*)$ to exist. When $\Gamma \leq (k+1)$ then system goes to $(r, b) = (1, 0)$. A corrected version taking this into account can be seen in Figure 3.8.

For $\Gamma > (k+1)$ as Γ changes the position of the equilibrium changes and this is a straight line from $(r, b) = (1, 0)$ to $(r, b) = (0, \mu)$ as is seen in Figure 3.9.

So any change in Γ will move the equilibrium along this line, with the magnitude depending non-linearly on Γ. From this we can more easily understand any dynamics changing Γ, such as $\Gamma(\theta)$ with θ varying in time.

3.4 Dynamics of Two Species with One Resource

This system has three equilibria: -

$$\begin{aligned} (r, b1, b2) &= (1, 0, 0) \\ (r, b1, b2) &= (r_1^*, b_1^*, 0) \\ (r, b1, b2) &= (r_2^*, 0, b_2^*) \end{aligned} \tag{3.4.1}$$

where $r_i^* = \dfrac{k}{\Gamma_i - 1}$ and $b_i^* = \mu(1 - r_i^*)$ (See Appendix B.2).

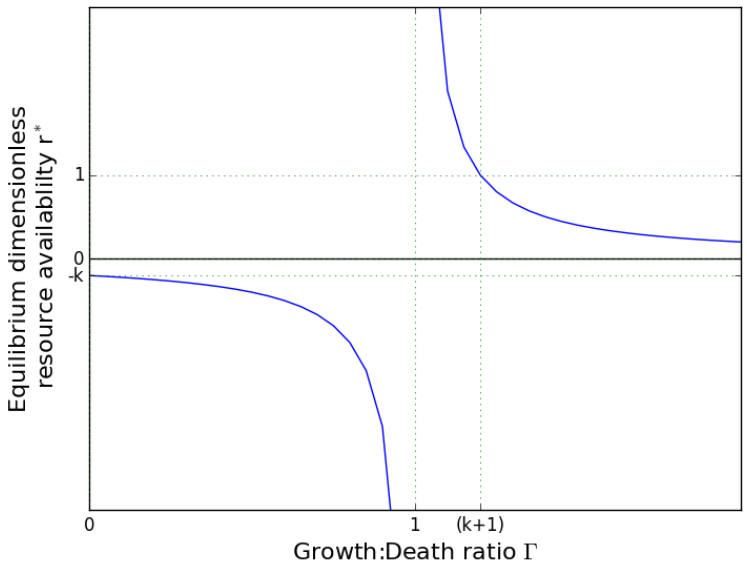

(a)

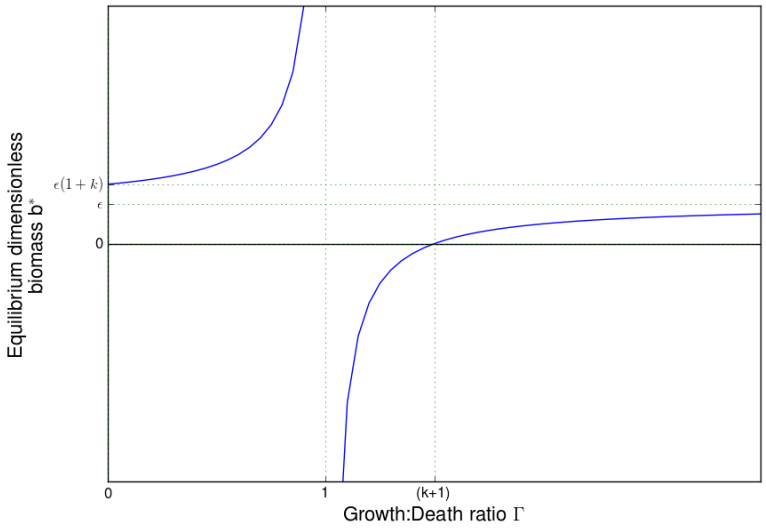

(b)

Figure 3.7: Shows a) The variation of equilibrium resource availability r^* with Γ, and b) the variation of the equilibrium species biomass b^* with Γ.

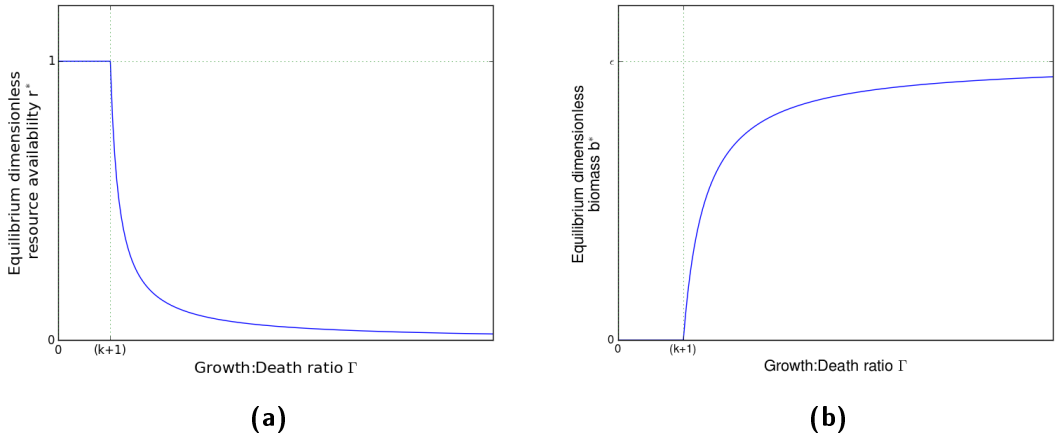

Figure 3.8: This is a adjusted version of Figure 3.7, showing the equilibrium values of a) r and b) b. For $\Gamma > (k+1)$ this is identical to Figure 3.7, but for $\Gamma \leq (k+1)$ the system goes to $(r, b) = (1, 0)$.

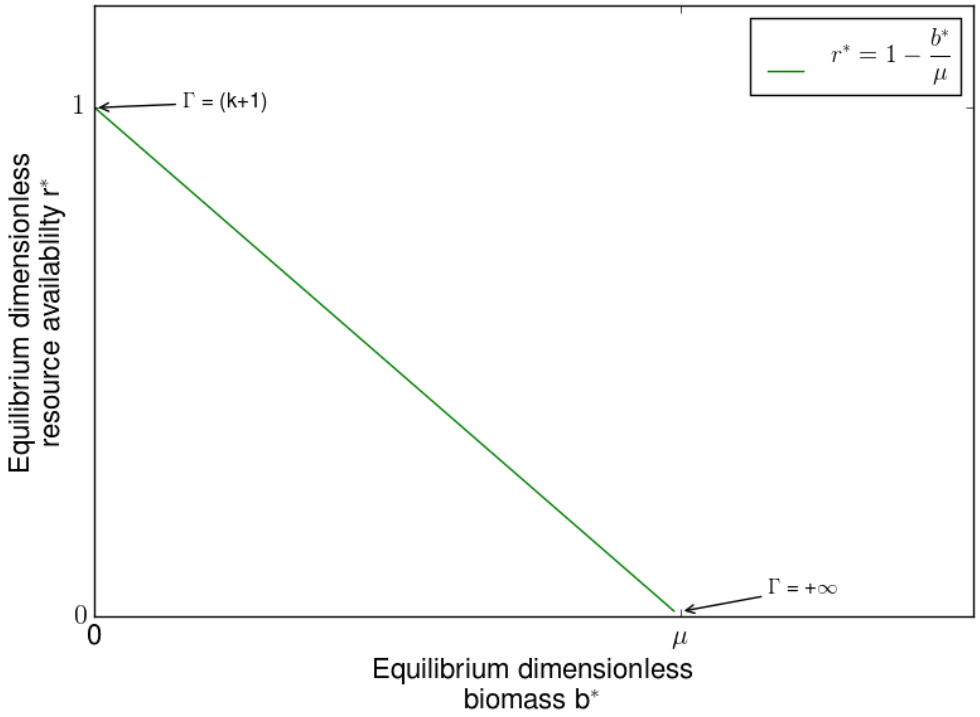

Figure 3.9: The equilibrium resource availability is linearly related to the equilibrium biomass. The position on this line is determined by the value of the growth:death ratio Γ.

Only one equilibrium is ever stable. If $\Gamma \leq (k+1)$ for all species then (r,b1,b2) = (1,0,0) is stable and the system will evolve towards this one and all species go extinct. If $\Gamma > (k+1)$ then which ever species has the higher growth rate will exclude the other species and remain as the sole dominant species with biomass $b_i^* = \dfrac{\mu(\Gamma_i - (k+1))}{(\Gamma_i - 1}$.

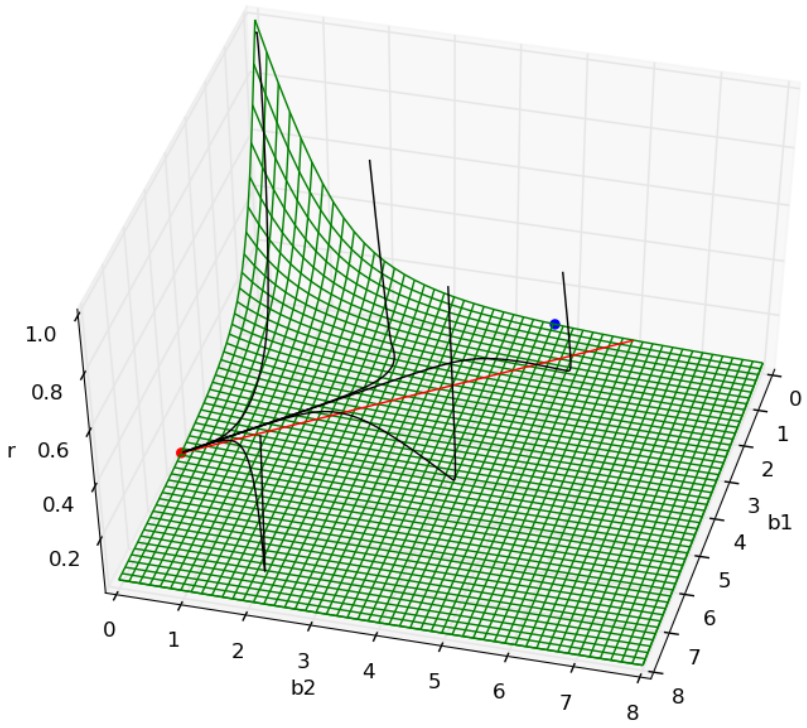

Figure 3.10: Shows the evolution of this system from different initial conditions. The red spot represents the stable equilibrium of the dominant species, the blue dot the unstable equilibrium of the other species. The green surface represents the surface where the $\dfrac{dr}{d\tau} = 0$, while the red line shows where r_1^* (the plane of $\dfrac{db_1}{d\tau} = 0$) crosses the surface. The black lines show the different paths towards the stable equilibrium.

Figure 3.10, shows that when $\Gamma > (k+1)$ and $\Gamma_1 > \Gamma_2$ the system evolves to the equilibrium of species 1 as expected. The general evolution is that first the resource changes rapidly towards the resource null-surface (i.e. $\dfrac{dr}{d\tau} = 0$) and then heads towards the line connecting the two equilibria of the two species and from this line heads towards the dominant equilibrium.

3.5 Resource Model with Varying Temperature

3.5.1 Maintaining Diversity with Temperature Noise

There is a comprehensive literature surrounding why we can observe extensive biodiversity in many land regions of the world. Currently proposed explanations can be grouped in to four main hypotheses. These are: -

1. Heterogeneity (either spatial or temporal) in the environmental forcing (May and McLean, 2007; Tilman, 2000, 2004). The extreme case of this is Neutral Theory (Hubbell, 2001), where all species in a trophic level have identical properties and it is purely random fluctuations that determine the abundance of species.

2. Trade-offs such as competition (long term superiority) vs colonization ability (ability to colonize an area after disturbance to the ecosystem) or trade-offs in acquiring different resources.

3. Interactions between trophic levels, eg predators tending to prey on more numerous species and allowing otherwise inferior competitors to coexist.

4. Niches, where each species is adapted to particular conditions. This would correspond to any imposed spatial variability in imposed meteorological conditions; for example one species may thrive in cool conditions another in warm.

The model of Lehman and Tilman (2000) uses temporal heterogeneity as species are only differentiated by their temperature properties and as the environmental temperature fluctuates due to temperature "noise". If the noise properties are such that the temperature will change fast enough that species do not experience temperatures they are not suited to long enough to die out, then species will co-exist and trait diversity will be maintained.

Lehman and Tilman (2000) and the work in this chapter ignore other interactions such as trade-offs or spatial variability. We also do not model directly allelopathy

(suppression of competitors by release of biochemicals) nor directly model space or light competition.

3.5.2 Comparison with Previous Work

Lehman and Tilman (2000) used a resource system of several species competing for one resource to study ecosystem stability. They used a system where the temperature changed at the beginning of every simulation year to a new random value chosen from a uniform distribution on the interval [20, 30]°C. The equations used were: -

$$\begin{aligned} \frac{dR}{dt} &= a(S-R) - Q\frac{R}{R+K}\sum_j g_j(T)\,B_j \\ \frac{dB_i}{dt} &= \left[g_i(T)\,\frac{R}{R+K} - \gamma\right] B_i \\ g_i(T) &= g_{max}\,\exp\left[-\frac{1}{2}\left(\frac{T-T_{OPT,i}}{T_w}\right)^2\right] \end{aligned} \tag{3.5.1}$$

A typical result from (Lehman and Tilman, 2000) is shown in Figure 3.11.

$a = 1.0$	$g_{max} = 1.0$	$T_w = 1.0$
$S = 100.0$	$K = 10.0$	$T_{mean} = 25.0°C$
$\gamma = 0.1$	$Q = 2.0$	

Table 3.3: Tilman's Model Parameters

This system shows clear coexistence as the system never reaches equilibrium before the temperature changes. This result was easily replicated using the Euler method for solving differential equations numerically (Figure 3.12).

The problem with this model is that the temperature variation is crude with the temperature held constant for a fixed period of time (every simulation "year") and then a new temperature taken from a uniform temperature distribution on the

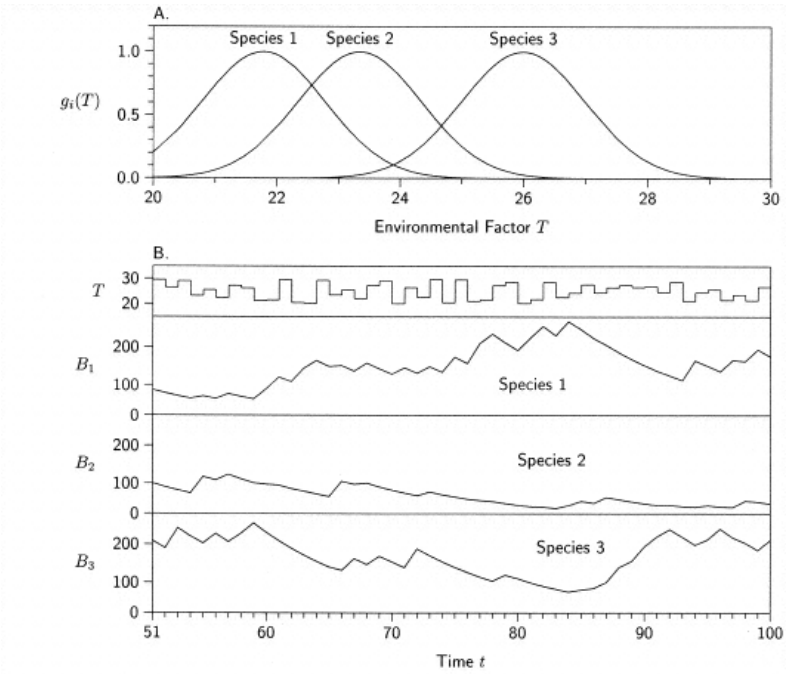

Figure 3.11: Simulations of the resource model from Lehman and Tilman (2000). The system is that of equation (3.5.1) using parameters of Table 3.3. **A**, Maximal growth rates of three species as a function of the environmental factor T. Here the points of maximal growth are approximately $T_{OPT,1}$ = 21.78°C, $T_{OPT,2}$=23.35°C, and $T_{OPT,3}$=26.00°C **B**, Sample trajectory for the above three species competing. The top curve shows the environmental factor as a function of time (a driving variable); the lower three curves show biomass of individual species (response variables). The first 50 time units in all the resource simulations allowed the system to settle but did not take part in further calculations.

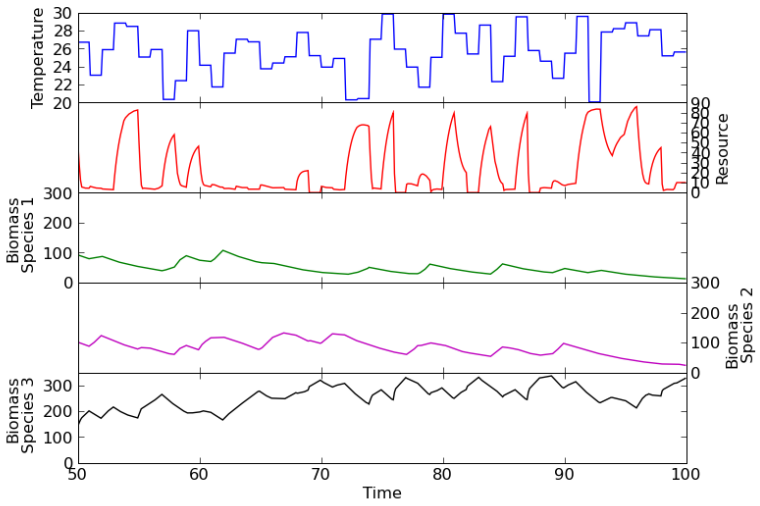

Figure 3.12: Shows replication of the result from Lehman and Tilman (2000)

interval [20, 30]°C for the next time period. This creates a series of temperature "steps" with the value of each step randomly taken from the distribution.

This is crude and not a true stochastic simulation, which hinders analysis and is less representative of real world systems.

3.5.3 Stochastic Model

This model uses the system from the previous section but exchanges the "stepped" temperature noise of that system for one with a constant mean temperature with "red" noise. The noise is generated using the Orstein-Uhlenbeck process often seen in financial analysis (Uhlenbeck and Ornstein, 1930; Onalan, 2009; Sura and Gille, 2003). This process is a modified continuous time random walk (Wiener process), where there is now a term that tends to return the process back towards the centre with a greater attraction the further the system is from the centre.

This allows the whole system to be represented as a stochastic differential equation and more easily be analysed.

The equation for the temperature with "red" noise and having mean T_o is: -

$$dT = \alpha(T_o - T)dt + \sigma dW \tag{3.5.2}$$

where α is the relaxation parameter, that governs how quickly the temperature returns to the mean T_o, and σ the noise magnitude and W denotes the Wiener process (dW effectively being Gaussian noise).

Simulations (example in Figure 3.13) were run using equations (3.5.1) and (3.5.2), for a variety of values of the parameters α, T_w and σ. Each simulation used four species having optimum temperatures of 22.5, 24.5, 26.5 and 28.5 °C and a mean environmental temperature $T_0 = 25$ °C. The resulting diversity was plotted on two dimensional pseudo-colour plots with each block of colour representing the diversity at those particular parameter values. As there were three parameters then several "slices" through the three dimensional parameter space were plotted for each of the three available orientations (see Figures 3.14, 3.15, 3.16).

The diversity was measured using the Shannon Index (which is a measure of information entropy, see Equation 1.2.1) and then converted to effective species (see Equation 1.2.4) (Jost, 2006; Dewar and Porté, 2008). The effective species shows the equivalent number of evenly (i.e. same number of each species) coexisting species needed for the same Shannon Index. As the Shannon Index is maximised for a given number of species, when all species have equal abundance (i.e. the system is even) then the effective species will be less than the number of actual species unless the system being measured is actually even.

Clear patterns of diversity can be seen as the properties of the noise change. The diversity follows an arrowhead shape in $\sigma - T_w$ space (Figure 3.14) with medium levels of diversity in the middle of the arrow and high diversity at the edge and low levels outside.

Analysing this system though, to explain the patterns is not trivial because of the coupled nature of the biomass and resource equations. The resource level is the same for all species and the resource level is influenced by all species, this

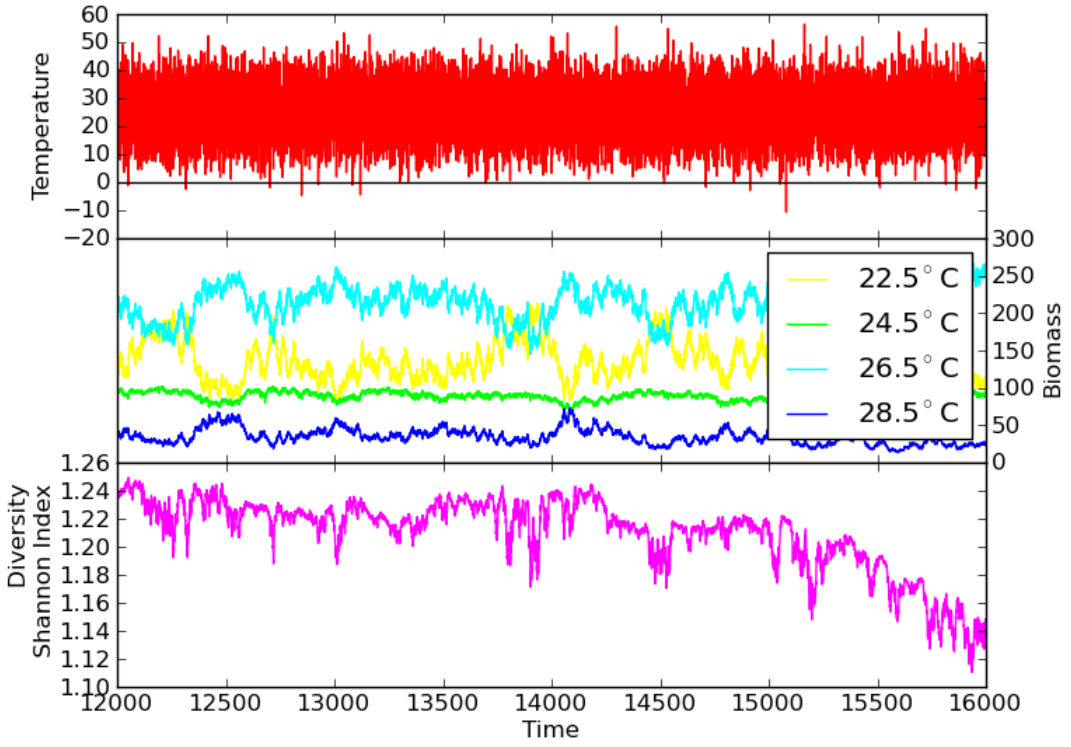

Figure 3.13: For each combination of noise parameters, the system was run for a long enough time for the diversity to settle down. The final quarter of the Shannon diversity index (Equation 1.2.1) time series was then averaged to obtain a measure of diversity corresponding to the noise parameters. This plot shows an example of the final quarter of the time series for $\alpha = 3.0$, $\sigma = 17.5°\text{C}$, $T_w = 5.0°\text{C}$.

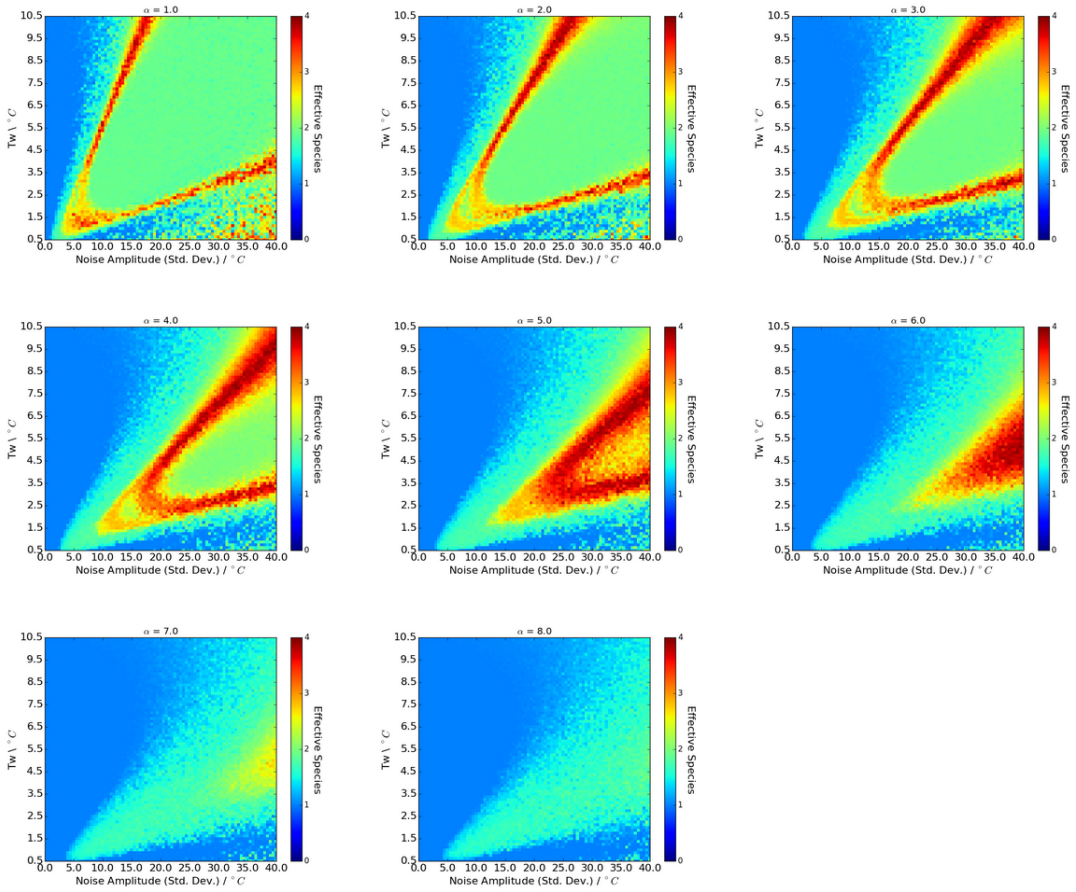

Figure 3.14: Each plot is a "slice" of constant α and shows how the diversity in effective species varies with the parameters T_w and σ. The ecosystem has four species identical apart from their optimum temperatures (22.5, 24.5, 26.5 and 28.5 °C) and has mean temperature of 25°C. (See Appendix C for larger versions)

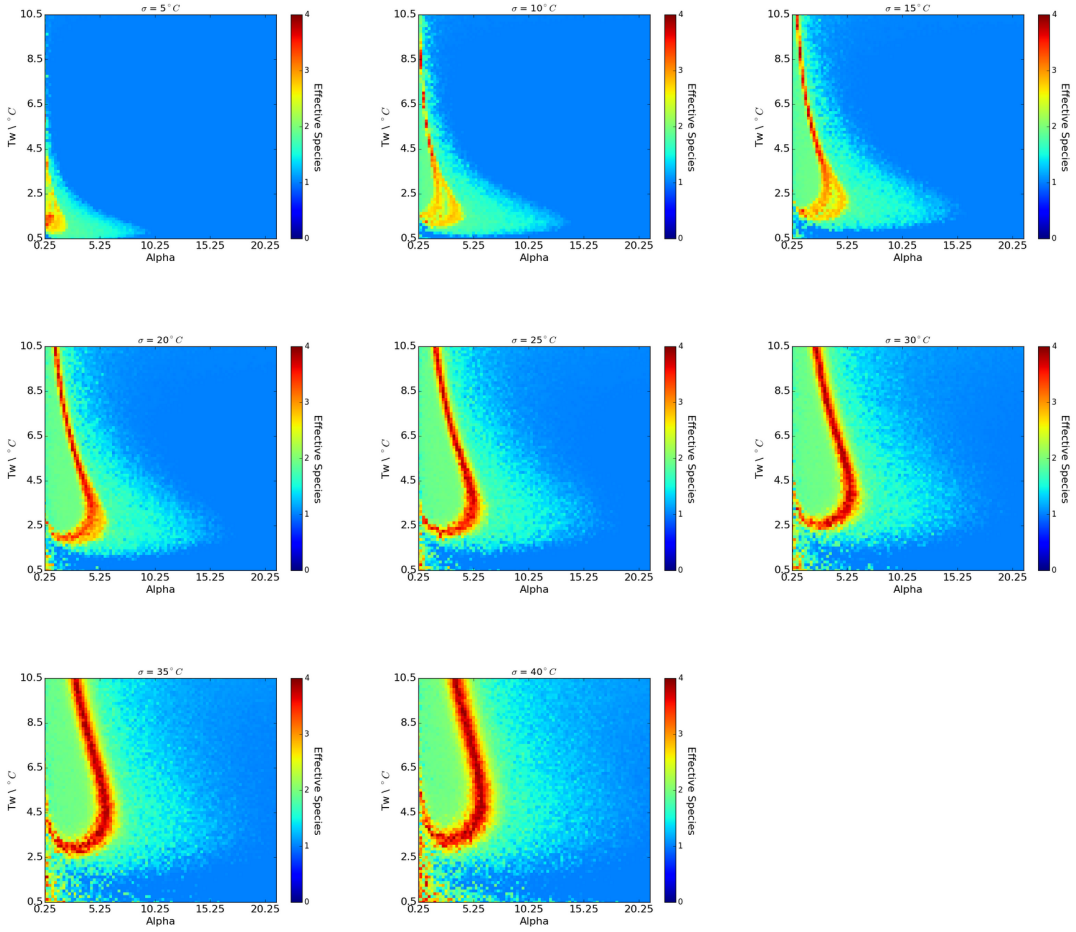

Figure 3.15: Each plot is a "slice" of constant σ and shows how the diversity in effective species varies with the parameters T_w and α. The ecosystem has four species identical apart from their optimum temperatures (22.5, 24.5, 26.5 and 28.5 °C) and has mean temperature of 25°C. (See Appendix C for larger versions)

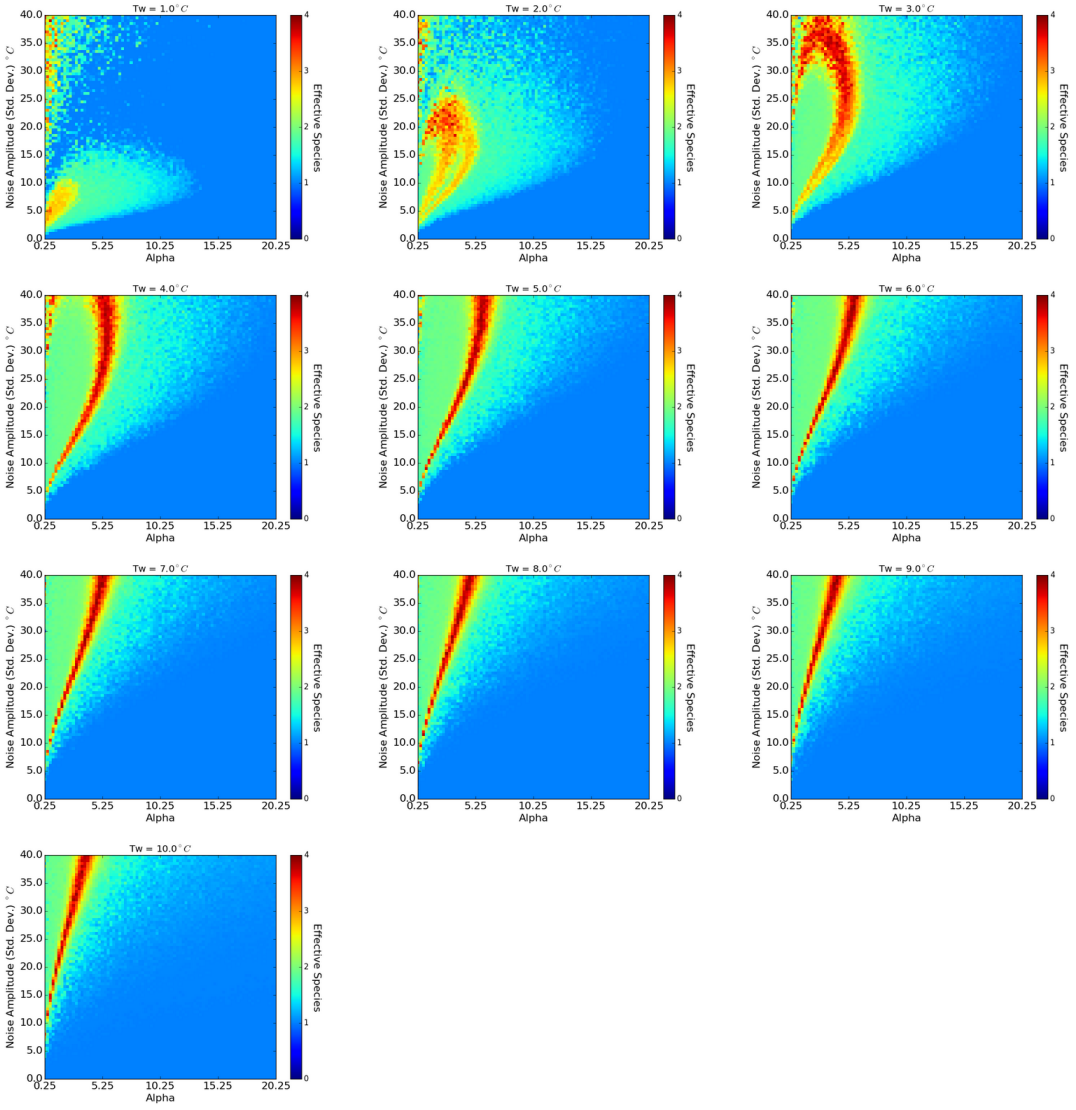

Figure 3.16: Each plot is a "slice" of constant T_w and shows how the diversity in effective species varies with the parameters σ and α. The ecosystem has four species identical apart from their optimum temperatures (22.5, 24.5, 26.5 and 28.5 °C) and has mean temperature of 25°C. (See Appendix C for larger versions)

creates complex dynamics as the temperature dependent growth rates vary with the fluctuating temperature.

3.5.4 Diversity Patterns in Terms of Resonant Frequency

As stated explaining the patterns directly is difficult due to the complex coupling of resource and biomass differential equations, making analytic assessment difficult. Instead we adopt a numerical approach, and see if the system can be forced in to resonant modes. To see if the system has resonant frequencies the temperature can be varied sinusoidally with no noise. If the frequency and amplitude are then changed then any resonance will be seen and hopefully the frequencies can be related to time-scales in the system.

An initial study was done using the 4 species used in the study of noise on diversity (optimum temperatures of 22.5, 24.5, 26.5 and 28.5 °C). This showed a clear resonance at frequencies 2.4 and 3.6 (arbitary time units)$^{-1}$. These correspond to time periods of approximately 0.42 time units and 0.278 time units respectively (see Figure 3.17). The time-scales of the biomass equations are $\frac{1}{g_m}$ and $\frac{1}{\gamma}$ which are 1.11 time units and 10 time units respectively. So the resonances are of the right order to be related to these timescales.

Time series of both the low (off peak) and high (on peak) evenness cases (see Figures 3.18 and 3.19), show a complex pattern of species dynamics which cannot be easily explained.

If instead we choose optimum temperatures for 7 species symmetric around the mean temperature (optimum temperatures of 22, 23, 24, 25, 26, 27 and 28 °C), we instead one resonance peak at frequency of 2.9 (see Figure 3.20). This peak occurs at a position that is exactly between the two peaks in figure 3.17.

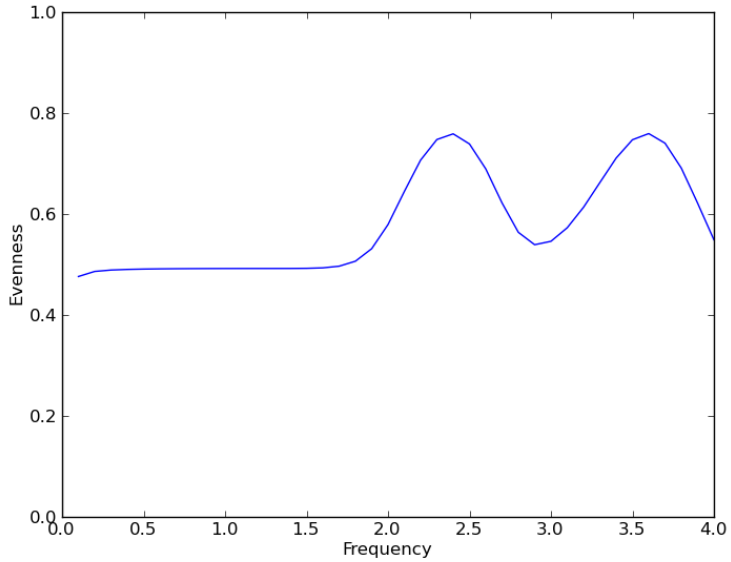

Figure 3.17: Evenness versus frequency of sinusoidal temperate variation for $T_w = 5.0$°C and amplitude = 8.0°C. The evenness is simply the Shannon Index divided by the natural logarithm of the number of species present. Two clear resonances are seen at frequencies 2.4 and 3.6.

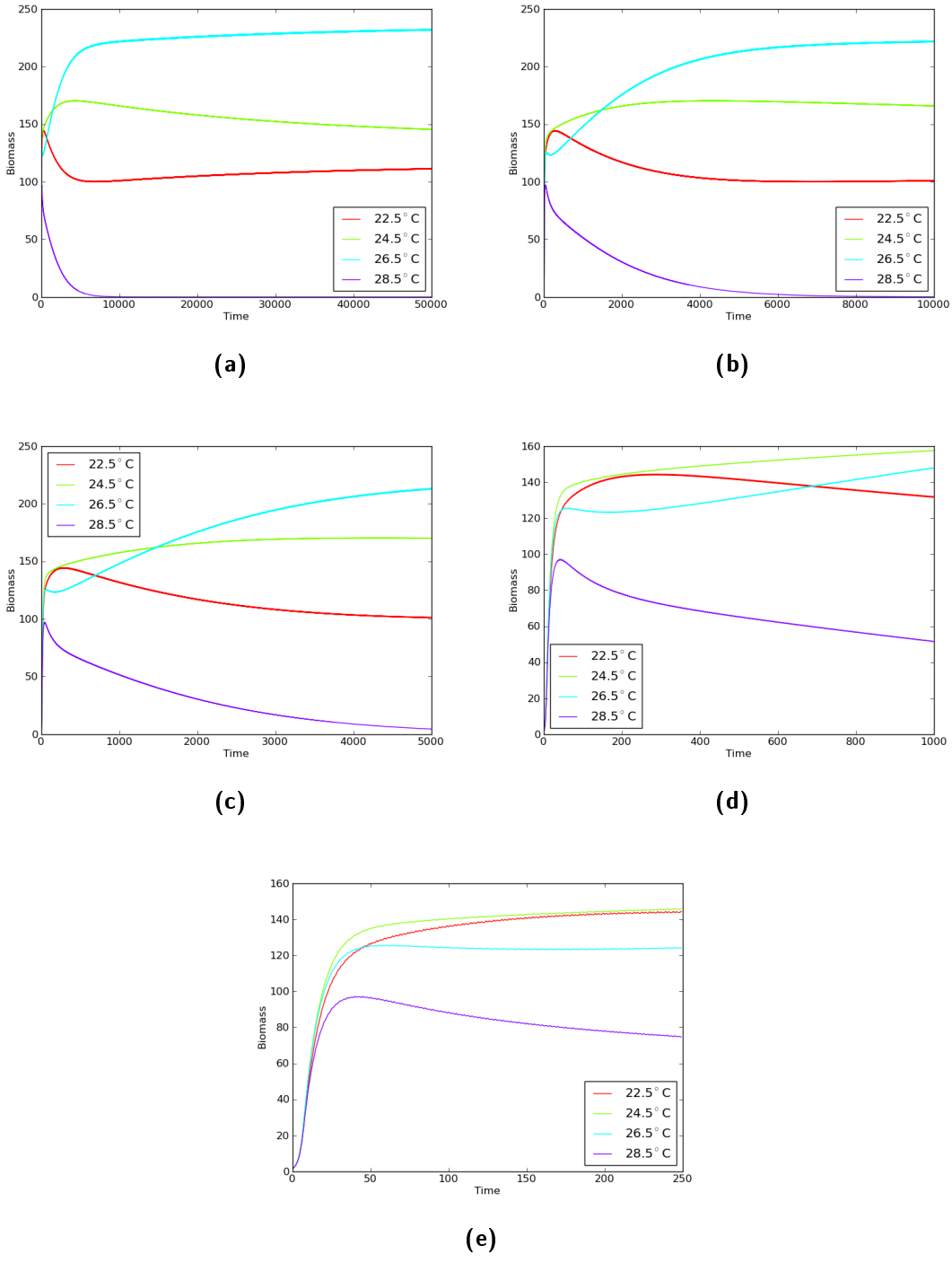

Figure 3.18: Shows the time series for freq 3.6 (high diversity), amplitude 8°C and $T_w = 5$°C. In each panel, the same simulation is shown, but covering decreasing time intervals from 0 to a) 50000 b) 10000 c) 5000 d) 1000 e) 250. Shows the complex pattern of different minima and maxima of the different species and how they coexist.

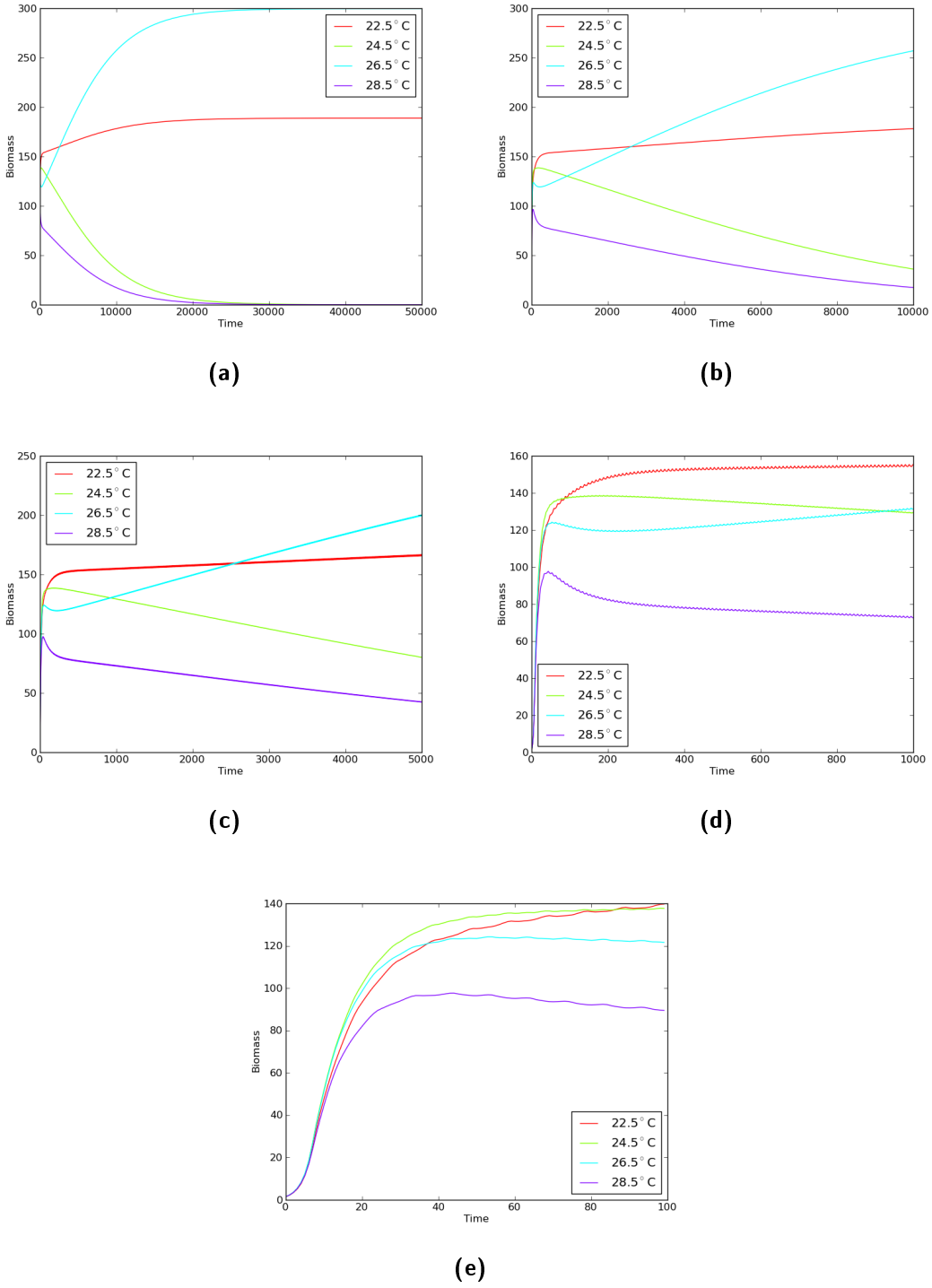

Figure 3.19: Shows the time series for freq 2.9 (low diversity), amplitude 8°C and $T_w = 5$°C. In each panel, the same simulation is shown, but covering decreasing time intervals from 0 to a) 50000 b) 10000 c) 5000 d) 1000 e) 100. Shows the complex pattern of different minima and maxima of the different species and how they coexist.

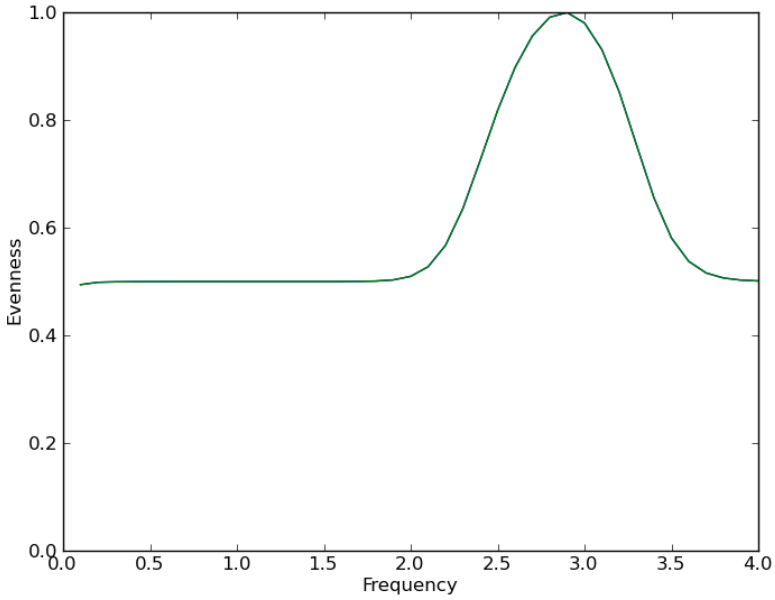

Figure 3.20: Evenness versus frequency of sinusoidal temperate variation. Resonance when species optimum temperatures symmetrically arranged around the mean temperature.

Simple Two Species Case

As the previous examples are complex and have multiple species it seems sensible to now instead consider the simplest case of two species, one whose optimum temperature matches the mean of (25°C) and one whose optimum temperature is displaced from the mean temperature (26°C). Then we can study how the dynamics change as we change the amplitude and frequency of the temperature oscillation and the separation of the two species optimum temperatures.

This system doesn't have the sharp resonance (Figure 3.21) seen in the previous more complex example, but as it still exhibits coexistence it is still useful to understand the mechanism of how the temperature oscillation allows this.

A phase plot (Figure 3.22) shows how the evolution of the system changes from the constant temperature to oscillating temperature case. The system broadly follows the same pattern as the constant temperature case but with species 2 having non-

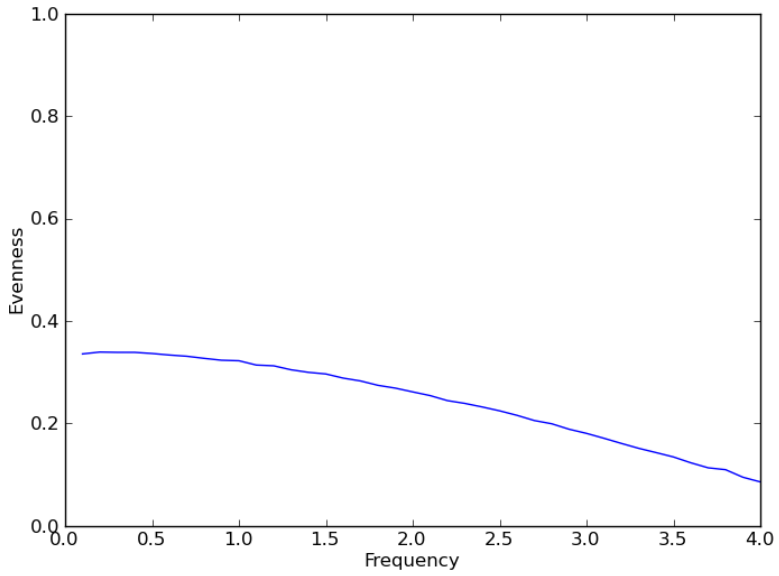

Figure 3.21: Shows there is no sharp resonance for a simple 2 species system (optimum temperatures 25°C and 26°C) but there is still coexistence.

zero biomass and higher resource levels, whereas the constant temperature case leads to species 1 excluding species 2.

The growth rate oscillates (Figure 3.23) as the temperature oscillates. As this is purely a function of temperature, the shape of the growth rate oscillation for each species is unchanging in time.

The time series (Figure 3.24) clearly shows that the trend of the sub-dominant species (26°C) goes through several clear stages. Firstly, it is growing then it levels off and then decreases strongly with the decrease tailing off until it just oscillates around a static mean. Meanwhile the dominant species is always increasing but with the rate of increase declining.

To understand this more fully, we consider the system in terms of its behaviour over one temperature oscillation at different stages of its evolution (Figure 3.25). The key effect on a species is the resource level and the shape of the factor $\frac{r}{r+k}$ over a cycle. Only this and the growth rate effect the species biomass in this model, as the death rate γ is the same for all species and the growth rate oscillation is

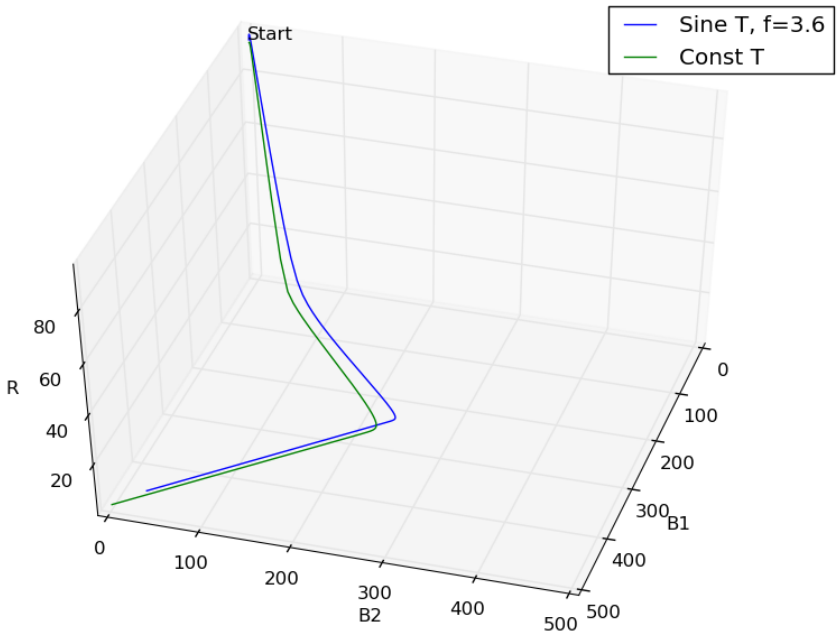

Figure 3.22: Phase plot of two species with temperature oscillation compared to same species with constant temperature. The oscillation amplitude is 8°C, the optimum temperatures are 25 and 26°C and $T_w = 8.0$°C.

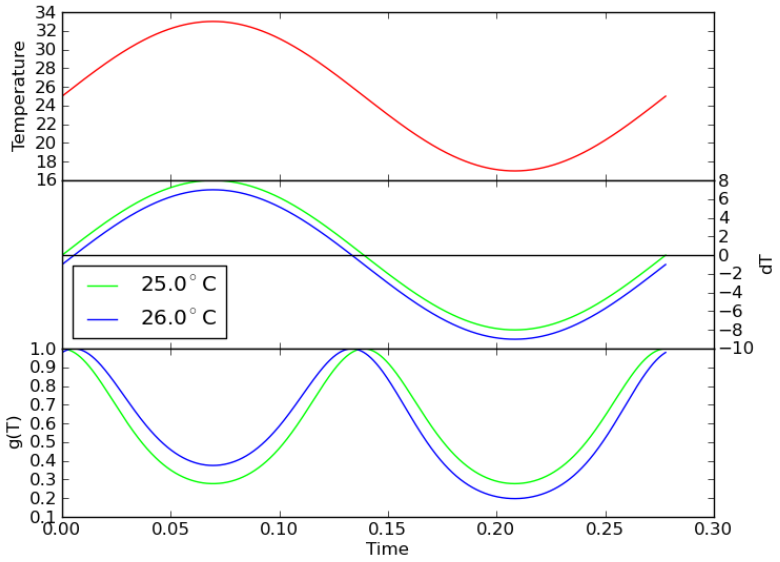

Figure 3.23: Shows how the growth rate varies during one temperature oscillation.

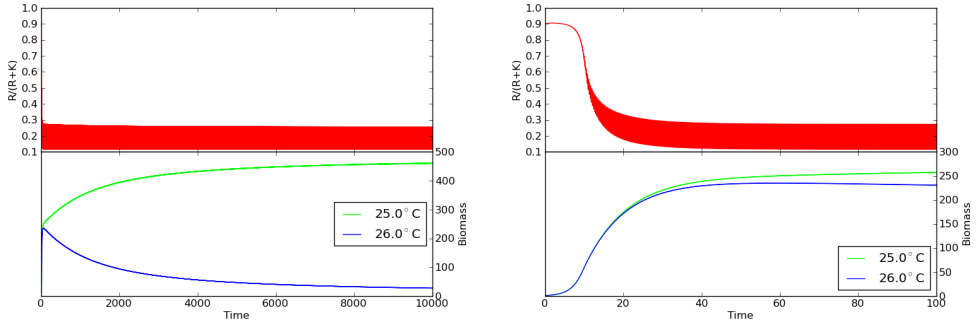

Figure 3.24: Time series for case where Frequency 3.6, amplitude of 8 and T_w=5 as shown in Figure 3.22. a) Shows the system to its 'pseudo equilibrium' with 26°C species still coexisting with dominant one. b) Close up of early part of time-series showing the turning point in the 26°C species. The top $\frac{R}{R+K}$ curve has very high frequency at the scale shown, so the individual cycles cannot be seen.

unchanging as it depends only on temperature.

This means all the dynamics we see are purely due to the multiplication of its growth rate oscillation with the oscillation in $\frac{R}{R+K}$. Figure 3.25 shows that change in shape of the $\frac{R}{R+K}$ oscillation produces the stages we see in the sub-dominant species 26°C.

Initially the resource level is dropping strongly and the oscillation in R is relatively small compared to the background trend, and the net effect when multiplied by the growth rate curves (see Figure 3.23) is of both species increasing.

At t=60 the background resource level has stopped dropping so strongly and we get an oscillation with a smaller peak followed by a larger peak. As we progress to t=100 and t=9000 the first peak grows bigger so that by t=9000 they are of similar size.

The increase in size of the first peak will mean the rate of change of the dominant species 25°C will diminish, as is seen, as it has a lower growth rate in this region. Conversely the rate of change of the sub-dominant species 26°C is boosted by this

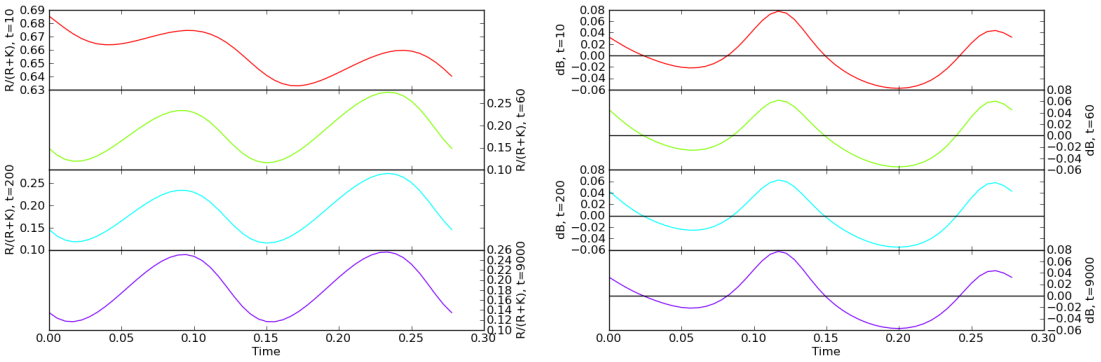

(a) **(b)**

Figure 3.25: Shows a) The the shape of factor $\frac{R}{R+K}$ over one cycle at different points in the evolution of the system. b) Shows $\frac{dB}{dt}$ for the 26°C species. The four time points chosen are t=10 where both species are increasing, t=60 where 26°C species has stopped growing, t=100 where 26°C species is decreasing and t=9000 where that species has almost stopped decreasing again. Frequency 3.6, amplitude of 8 and T_w=5.

and both species reach a pseudo equilibrium, oscillating around constant mean biomass.

This behaviour may well be due to the fact that as each species grows it reduces the resource level. Over one cycle the sub-dominant species will reduce the resource rate the least in the early part of its cycle. When the level of this species increases this effect is more pronounced and as it decreases less so. This explains the increase in the first peak as the sub-dominant species declines.

Frequency Limits

There are two limits to frequency, firstly the limit where the frequency approaches infinity and secondly the limit where it approaches zero. In either case the equilibrium biomass B* would be reached at each point in the temperature cycle. If we then multiply this function by the probability distribution function of a sine wave we can in theory calculate the expected value of each species biomass in this case.

The growth rate varies with temperature:-

$$g(T) = g_m exp\left(-\frac{1}{2}\left(\frac{T - T_{OPT,i}}{T_w}\right)^2\right) \tag{3.5.3}$$

The equilibrium species biomass is:-

$$b^*(g) = \frac{a(g - \gamma(k+1))}{d(g-\gamma)} \tag{3.5.4}$$

PDF of a sine wave

$$p(T) = \frac{1}{\pi\sqrt{A^2 - (T - T_{mean})^2}} \tag{3.5.5}$$

So expectation of biomass undergoing a sine oscillation in T is :-

$$\mathbb{E}\{b^*\} = \int b^*(g(T))\, p(T)\, dT \tag{3.5.6}$$

This integral cannot be easily solved directly so the only way to solve it would be to take a Taylor series of b and integrate this to get an approximation of the expected value of b.

If the integral is simplified by assuming a continuous range of species with all possible optimum temperatures then at each point on the sine oscillation the species with an optimum temperature equal to the the temperature at that point will be dominant. The expectation value of the biomass will then be: -

$$b_o^* = \frac{a(g_{max} - \gamma(k+1))}{\gamma(g_{max} - \gamma)} \tag{3.5.7}$$

3.6 Effect of Temperature Trend on Noise Maintained Diversity

We now return to considering the situation where temperature contains noise. The single resource model so far has a static mean temperature, but in a climate change scenario this mean temperature trend would increase. The simplest possible trend is a linear increase in temperature.

$$T(t) = T_0 + \frac{dT}{dt}t \tag{3.6.8}$$

The rate $\frac{dT}{dt}$ is determined by the required change in temperature $\Delta T = T(t_{final}) - T_0$ from t_0 to $t = t_{final}$.

$$\frac{dT}{dt} = \frac{\Delta T}{t_{final} - t_0} \tag{3.6.9}$$

Species ranged uniformly in their optimum temperatures from $14°C$ to $81°C$, with a spacing of 1° C between species. Noise parameters were chosen as ones that seem "reasonable" and give high starting diversity ($\alpha = 5.25$, $\sigma = 30.0$°C, $T_w = 5.0$°C). The biomass of all species is not allowed to fall below the seed value of 0.001 to represent re-population from dormant seeds or from outside the model "area" when conditions are favourable for re-population.

If the model is only run once then the noise hides some of the effect (figure 3.26).

Instead multiple runs can be averaged (Figure 3.27) and this averages out the single run deviations and show the expected dynamics in much the same way that many tosses of a dice will converge on the expected probability distribution.

The diversity varies in an oscillating pattern while the NPP and total ecosystem biomass is fairly constant. This suggests that such a system with noise maintained diversity is stable under the temperature change scenario used. The oscillation of

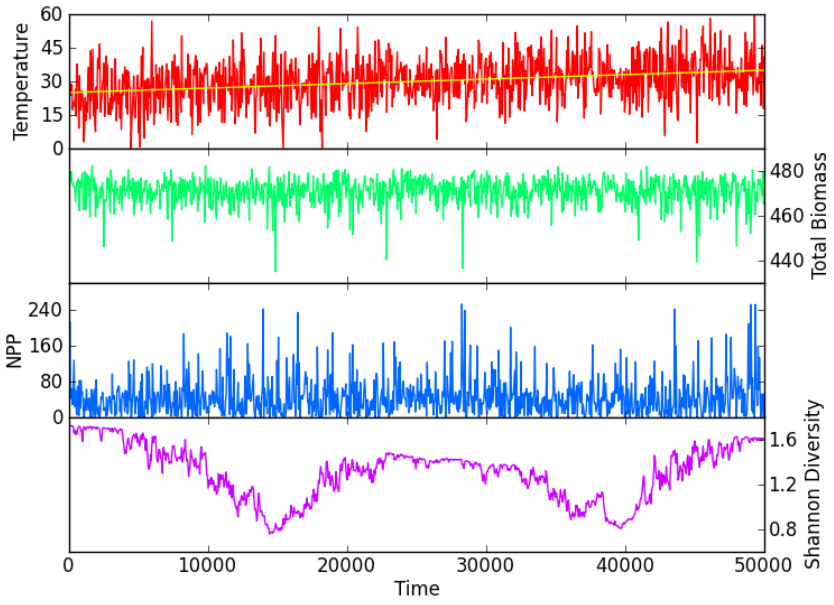

Figure 3.26: Shows the result of 1 run of the model with a temperature trend, with 10° C increase in mean temperature. Model has been run with 67 species spaced by 1°C with $\alpha = 5.25$, $\sigma = 30.0$°C, $T_W = 5.0$°C.

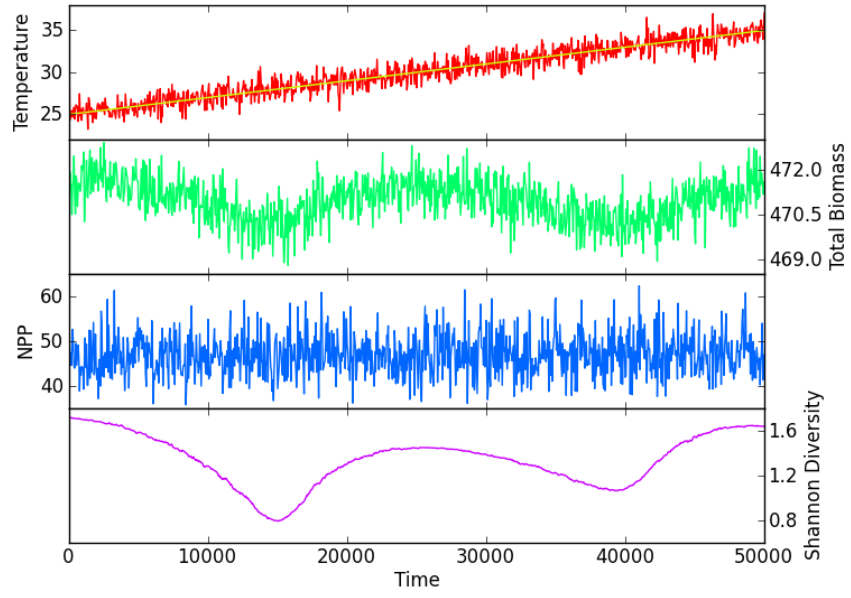

Figure 3.27: Averaged results of 100 runs of the model, with 10° C increase in mean temperature using same parameters as Figure 3.26.

the diversity can be seen to arise from the pattern of individual species biomasses as the system undergoes the temperature change (Figure 3.28).

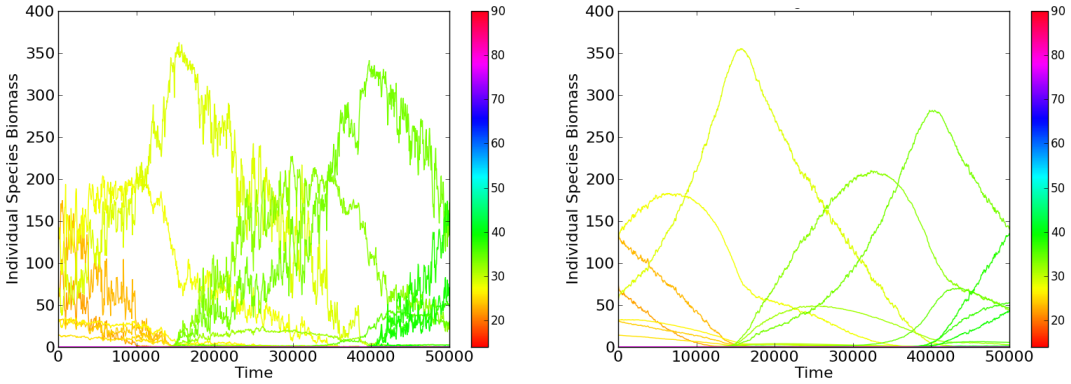

Figure 3.28: Shows a) The variation of species biomass during 1 run of the model and b) the average of 100 runs. The colour corresponds to the optimum temperature of the species.

3.6.1 Effect of Seed value and Optimum Temperature spacing

To check how much effect the seed parameter and the optimum species temperature spacing have on the results of the temperature trend a range of simulations were run using a different parameter values.

The effect of the seed parameter (figure 3.29) is quite significant on the diversity but unless the parameter is increased to 0.1 it has little effect on the biomass and the NPP appears unchanged for all values of the seed parameter.

The optimum species temperature spacing (figure 3.30) again has a profound effect on diversity magnitude, although the curve shapes are similar. Meanwhile there is no effect on NPP and although it does have some slight effect on the total biomass, in that the phase of the oscillation is shifted in time, the mean and amplitude appear to be very similar.

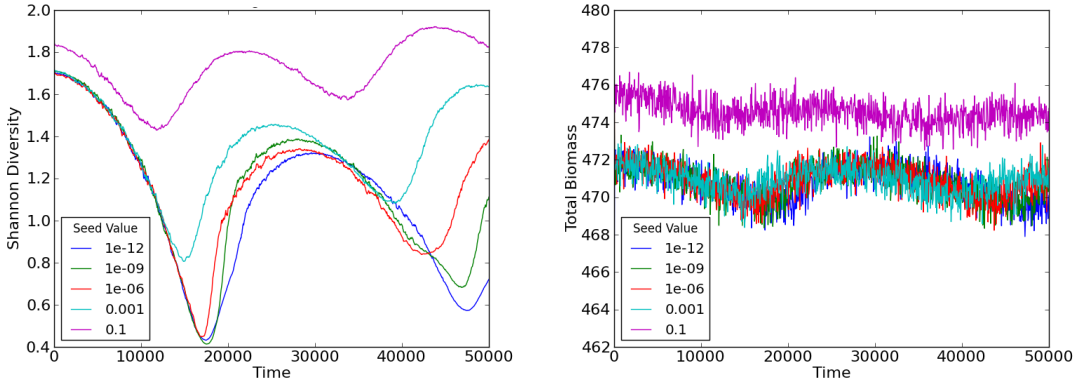

(a) Diversity

(b) Total biomass

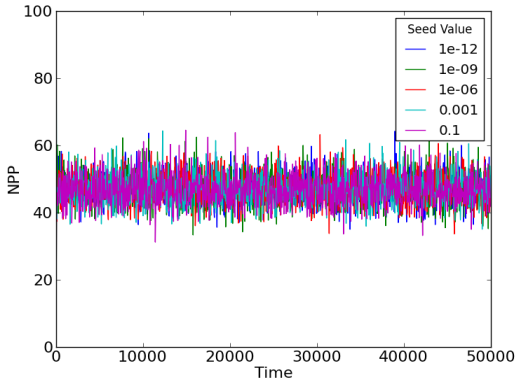

(c) NPP

Figure 3.29: Variation in response with different seed parameters (other parameters same as Figure 3.26).

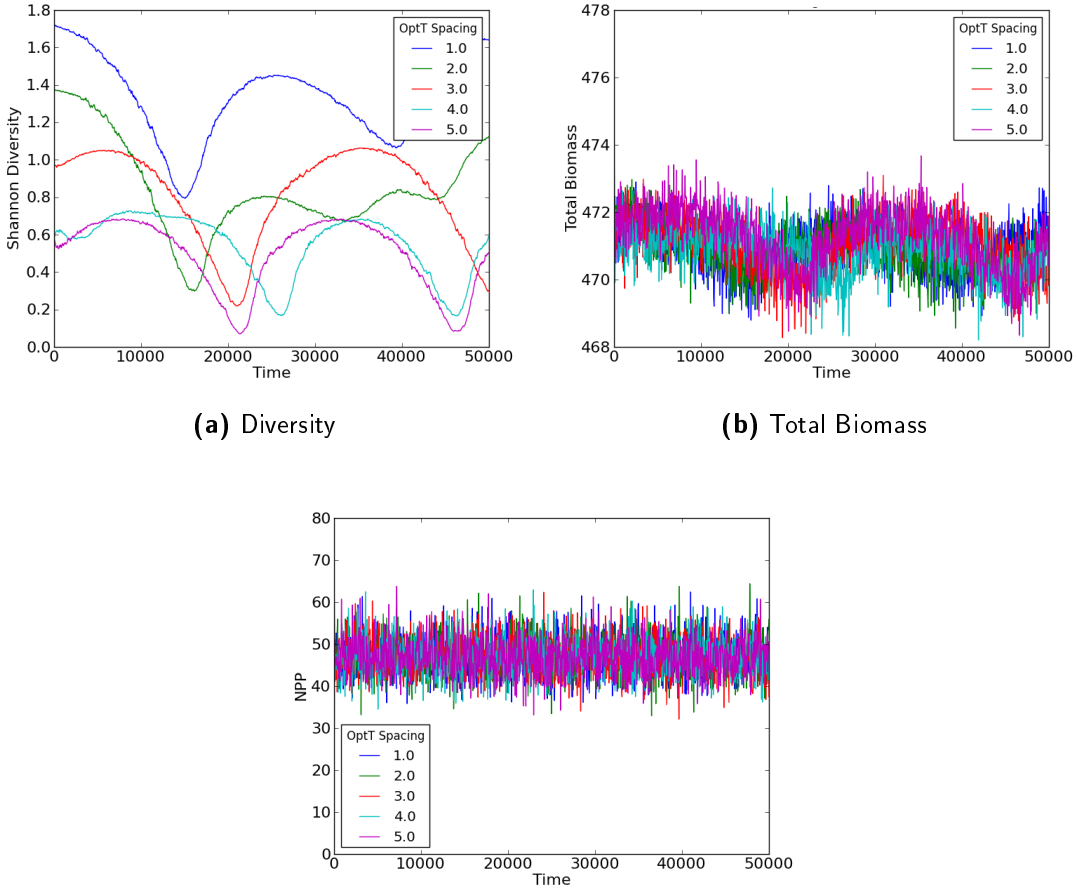

(a) Diversity

(b) Total Biomass

(c) NPP

Figure 3.30: Variation in response with different optimum temperature spacing of 14 species (other parameters same as Figure 3.26).

3.6.2 Effect of Rate of Temperature Change

The rate of climate change has shown to be critical factor in whether an ecosystem is resilient or if it will reach a "tipping point" and collapse (Lenton et al., 2008). To test the resilience of this particular system the model was run with different temperature changes over the same period of time (50000 time units). The seed value of 0.001 and species spacing of 1°C were used for each simulation.

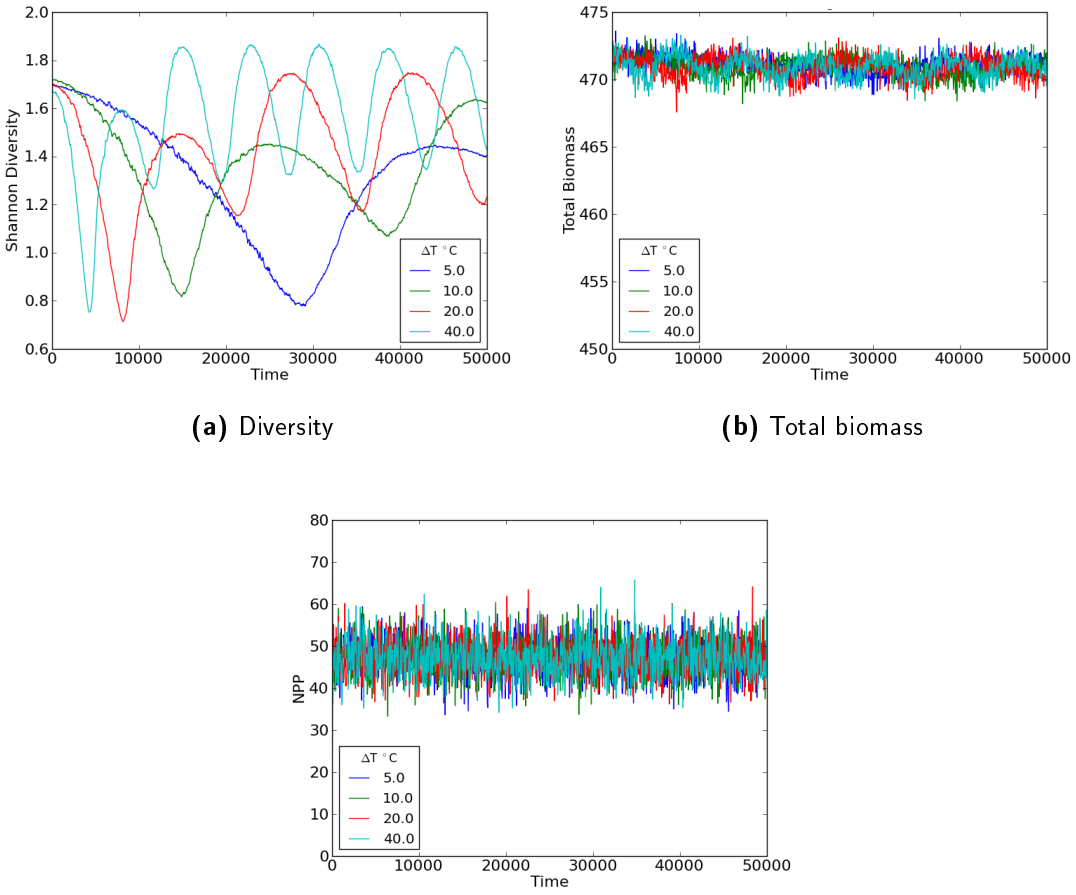

(a) Diversity

(b) Total biomass

(c) NPP

Figure 3.31: Variation in response with different rates of temperature change (measured as change in temperature for a run of 50,000 time units).

It can be seen in figure 3.31 that the NPP and biomass remain resilient up to a temperature increase of 40°C. Again there are significant effects on the diversity but overall very little clear indication that greater rates of change cause any worse

effects on the diversity than slower rates of change. In fact the lowest rate of change (5°C) has the biggest drop in diversity before recovering, this though could be down to the choice of a linear trend as the system goes from spinning up with a constant mean temperature to suddenly experiencing an increasing mean temperature. This discontinuity could lead to some transient effects.

3.7 Conclusions and Discussion

The model presented in this section has been successful in generating a diversity of temperature traits, maintained by temperature noise. Furthermore, such diversity in these circumstances is robust (in terms of NPP and biomass), to any additional imposed climate change.

However, it is not trivial to understand the relationship between the nature of the temperature noise properties and the diversity seen. Certainly there are some interesting patterns in the diversity with respect to the noise parameters (figures 3.14, 3.15, 3.16) but so far efforts to fully understand the nature of the diversity mathematically have not been fully successful and is left as an avenue for future work. All that can said is that the fate of a species depends on it never being so far from its optimum temperature long enough to die out.

To get meaningful results the model must be run several times and the results averaged to get the expected mean dynamics. This is costly in time as the model needs to be run 100 times or more. This is could be impractical for use in time critical modelling such as the land surface components of climate models due to the computational cost and complexity but is still useful in advancing the theoretical understanding of how diversity arises.

The work in this chapter has three possible of avenues of future work. Firstly, the complex relationship between diversity and the noise parameters needs to be better understood to allow this model to more definitively study the relationship between diversity and stability. Secondly, it would also be interesting to compare the noise

seen in real temperature observations to see if there is any correlation between real world temperature variability and diversity. Finally it may be interesting to investigate a resource model without the temperature noise but instead have species compete for more than one resource which can allow coexistence and then assign each species environmental traits either randomly or from observational data.

Chapter 4

Trait Diffusion Model

In Chapters 2 and 3 it was seen that both the Lotka-Volterra (LV) and single resource models will competitively exclude all but the dominant species and therefore do not produce ecosystem diversity. If heterogeneity is added in the form of temperature "noise" to the single resource model then species with different temperature traits can coexist. This latter model suffered from being complex and difficult to analyse and computationally intensive, which in a larger model such as a climate model would be harder to adapt, maintain and evaluate.

On the longer time-scales of evolution species will constantly diversify through genetic mutation and in a given ecosystem new species may invade from neighbouring areas. This means new species constantly appear and compete with already established species. As long as the rate of speciation matches the loss of species through competition diversity will be maintained (Rabosky, 2013).

The time-scale of anthropogenic climate change is quite short in evolutionary terms, so long-lived species will not have time to evolve into a completely distinct new species but there is time for micro-evolution, where new traits within species can evolve (Hendry and Kinnison, 2001). This means it is more useful to model traits (such as optimum growth temperature) rather than species. So the question changes from "what effect does species diversity have on ecosystem resilience

to environmental change?" to "what effect does existing trait diversity have on ecosystem resilience to climate change?".

As well as evolving, species undergoing climate change can also respond to climate change via plasticity/acclimation or by migration (Hoffmann and Sgrò, 2011; Gienapp et al., 2008). These processes are not mutually exclusive with evolution (Nicotra et al., 2010) and have led to difficulty in interpreting the mechanism of observed changes in traits (Hoffmann and Sgrò, 2011).

In this chapter the resource model used in Chapter 3 is modified to instead represent a set of temperature traits rather than species. Diversity of traits is modelled through a balance between traits evolving and competitively excluding each other. This model is then used to study the resilience of the system to increasing rates of temperature change.

The work in this chapter only includes the effects of trait evolution and leaves the effects of migration and acclimation for future work. The model also is kept simple by ignoring the temperature limitations seen in plants (i.e. infinite range of temperature traits). This allows the dynamics of the model to be more easily explored.

4.1 Model Equations

To model trait diversity the non-dimensionalised resource model from Chapter 3 is adapted by assuming that now each species is instead a different temperature trait value (optimum growth temperature) and that the biomass of any trait will diffuse into neighbouring traits at a constant rate ε.

The number of traits is fixed and each trait, as in the previous chapter, has a biomass value representing the total biomass of all individual members of the ecosystem with that trait.

The diffusion of trait biomass is a way of modelling the micro-evolution of traits

through mutation or cross breeding between diverse traits within a given species or set of species. As the resource model does not model individuals directly the only way of representing the evolution is by assuming that a proportion of biomass of any one trait "evolves" at a given rate to adjacent traits. The process assumes the population is large enough that the micro-evolution can be modelled as a continuous rather than a discrete process, i.e. the birth of individuals with specific mutations are not modelled, just the changes in relative total ecosystem biomass of each trait. The model assumes that most "mutations" are small changes and so limits the diffusion to adjacent traits.

This gives a modified equation set for n different trait values: -

$$\frac{db_0}{d\tau} = b_0 \left[\Gamma_0(\theta) \frac{r}{r+k} - 1 - \varepsilon \right] + \varepsilon b_1 \tag{4.1.1}$$

$$\frac{db_i}{d\tau} = b_i \left[\Gamma_i(\theta) \frac{r}{r+k} - 1 - 2\varepsilon \right] + \varepsilon (b_{i+1} + b_{i-1}) \tag{4.1.2}$$

$$\frac{db_n}{d\tau} = b_n \left[\Gamma_n(\theta) \frac{r}{r+k} - 1 - \varepsilon \right] + \varepsilon b_{n-1} \tag{4.1.3}$$

$$\frac{dr}{d\tau} = \mu(1-r) - \frac{r}{r+k} \sum_j \Gamma_j(\theta)\, b_j \tag{4.1.4}$$

This is for an n trait value system (where $1 \leq i \leq n$).

As in Chapter 3, this chapter uses non-dimensional variables 4.1.5 including time which is multiplied by the death rate γ to give a non-dimensional time variable where 1 unit is one trait lifetime $\frac{1}{\gamma}$. All traits are assumed to have the same death rate.

$$\begin{aligned} k &= \frac{K}{S} & r &= \frac{R}{S} & b_i &= \frac{Q\,B_i}{S} \\ \theta &= \frac{T}{T_w} & \theta_{OPT,i} &= \frac{T_{OPT,i}}{T_w} & \tau &= t\gamma \\ \mu &= \frac{a}{\gamma} & \Gamma_i &= \frac{g_i}{\gamma} \end{aligned} \tag{4.1.5}$$

The definitions of the dimensional variables such as R, S and K etc, which are not used in this chapter, can be found in Table 3.1 in Chapter 3.

Symbol	**Variable / Parameter**	**Unit**
b_i	Non-dimensional biomass trait i	-
Γ_i	Temperature dependent biomass growth:death rate ratio trait i	-
Γ_{max}	Maximum growth:death rate ratio	-
θ	Non-dimensional temperature (per T_w)	-
$\theta_{OPT,i}$	Non-dimensional optimum temperature of trait i	-
T_w	Temperature growth curve width	°C
r	Resource availability:supply ratio	-
k	Non-dimensional resource half saturation constant	-
μ	Conversion rate unavailable to available resource (per lifetime)	-
ε	Trait diffusion parameter (per lifetime)	-

Table 4.1: List of symbols for Chapter 4

The equations for the rate of change of resource availability:supply ratio r and the growth:death rate ratio of a trait $\Gamma_i(\theta)$ are unchanged from the previous chapter. The -2ε term inside the square brackets represents the proportion of biomass lost per lifetime to traits adjacent in optimum temperature, while the $\varepsilon(b_{i+1} + b_{i-1})$ term represents biomass gained by traits either side diffusing into this one.

4.2 Equilibrium Solution

Running the model numerically, using the Runge-Kutta 4th order method, shows that the numerical model always converges to a single equilibrium solution (see figures 4.1 and 4.2). The model was initialised by only the optimum trait having biomass at the start and all others zero.

4.2.1 Effect of Diffusion Rate and Trait Spacing

The diffusion rate changes the equilibrium solution. In figure 4.1 we can see that the equilibrium solution has a shape that appears very similar to a Gaussian. The equilibrium curve is sharper for low diffusion rates and flatter for higher diffusion rates. The diffusion effect means that biomass is transferred from a trait to the adjacent traits until a balance is reached as traits with an inferior growth rate will have a higher $\frac{db}{d\tau}$ due to the diffusion from adjacent traits with superior growth rate. So higher diffusion will tend to reduce the dominance of traits with a higher growth rate.

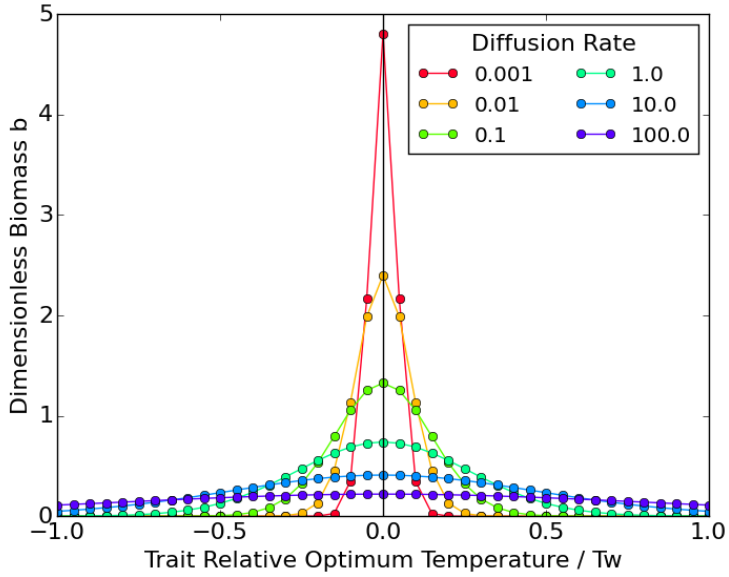

Figure 4.1: Equilibrium solutions to the trait diffusion model for differing values of diffusion rate ε. The model was run with 401 traits evenly spaced $0.05T_w$ apart for 1000 lifetimes to allow the model to reach equilibrium.

Lower diffusion rates take longer to come to equilibrium as the biomass will take longer to move from trait to trait (Figure 4.2a). The total biomass of the system though appears to remain constant (Figure 4.2b).

The diffusion therefore has an effect on diversity as the higher diffusion case has more evenly distributed biomass and is therefore more diverse (figure 4.3).

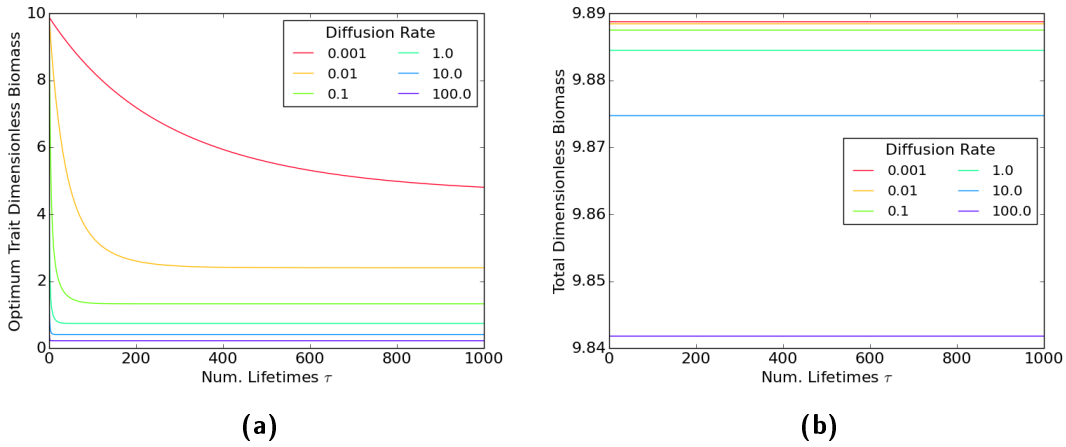

Figure 4.2: a) Time evolution of the biomass of trait matching environmental temperature (optimum trait) b) Time evolution of total system biomass.

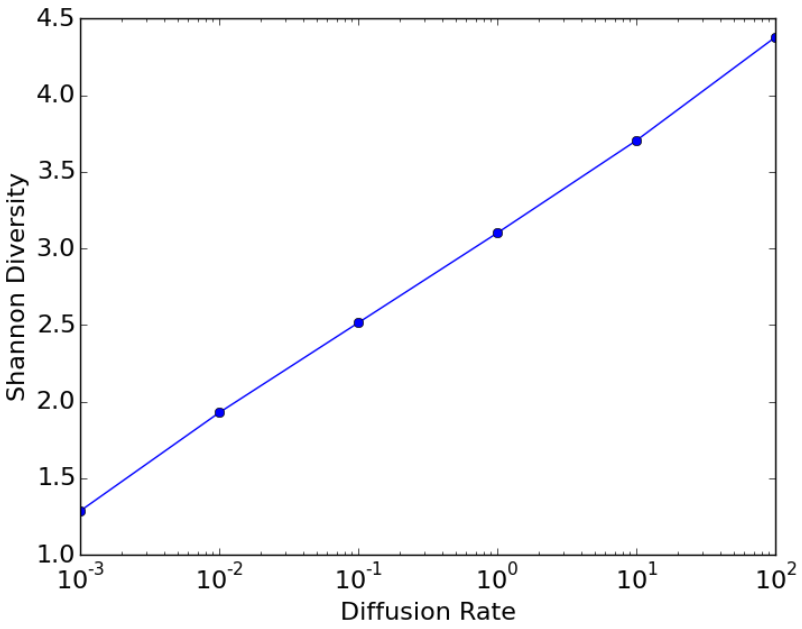

Figure 4.3: Shannon diversity at equilibrium for different diffusion rates, demonstrating that greater diffusion leads to greater diversity.

The diffusion rate has a very small influence on the system biomass (Figure 4.4) but a very pronounced effect on the biomass of the optimum trait, with larger diffusion reducing its magnitude.

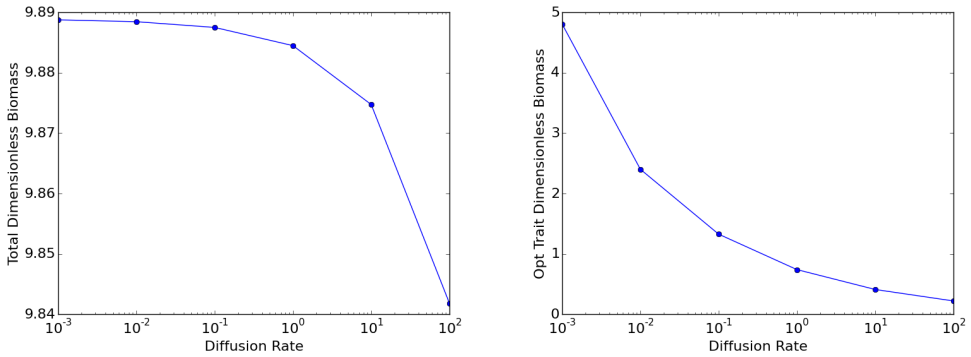

(a) **(b)**

Figure 4.4: Effect of diffusion rate on a) Total system biomass b) biomass of optimum trait.

The NPP (which is defined as $B_i g_i$) and the total system biomass both slightly reduce with increasing diffusion rate. Meanwhile the resource availability increases with increasing diffusion as the total biomass has decreased, meaning less resource has been used (Figure 4.5).

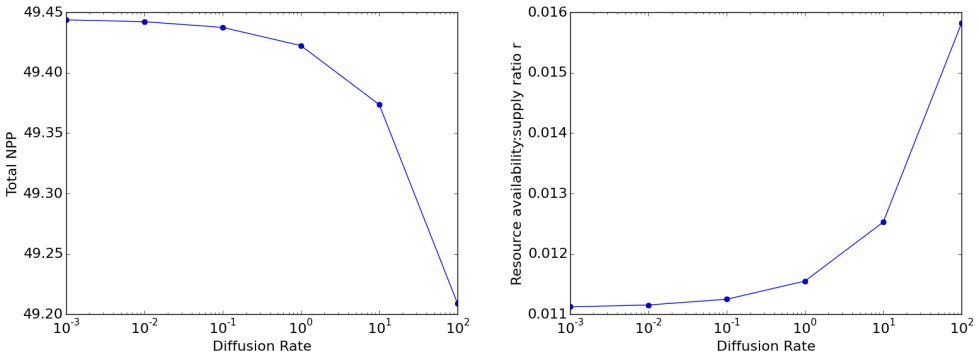

(a) **(b)**

Figure 4.5: Effect of diffusion rate on a) NPP b) resource availability.

The spacing of the optimum temperatures of the traits (Figure 4.6) has the effect to reduce the biomass of the dominant trait as the spacing is reduced. This is

due to traits closer to the dominant trait have optimum temperatures closer to the environmental temperature and therefore have a higher growth rate than a trait further away.

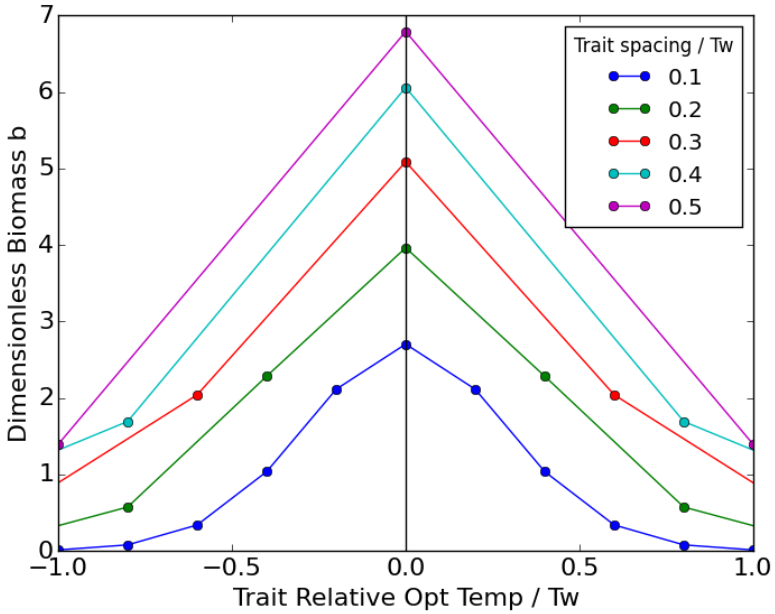

Figure 4.6: Equilibrium solutions to the trait diffusion model for differing spacing of trait optimum temperatures for diffusion rate of 0.1 dimensionless biomass per lifetime.

The trait spacing also has an effect on how quickly the optimum trait biomass achieves equilibrium (Figure 4.7a) with bigger spacing achieving equilibrium faster.

The diversity decreases with increasing trait spacing (Figure 4.8) as the biomass becomes more evenly spread across traits (Figure 4.6).

The total biomass decreases and the optimum trait biomass increases as the trait spacing increases (Figure 4.9).

Again the NPP correlates with the total system biomass and slightly reduces with increasing trait spacing, while the resource availability increases with increasing trait spacing as the total biomass has decreased, meaning less resource has been used (Figure 4.10).

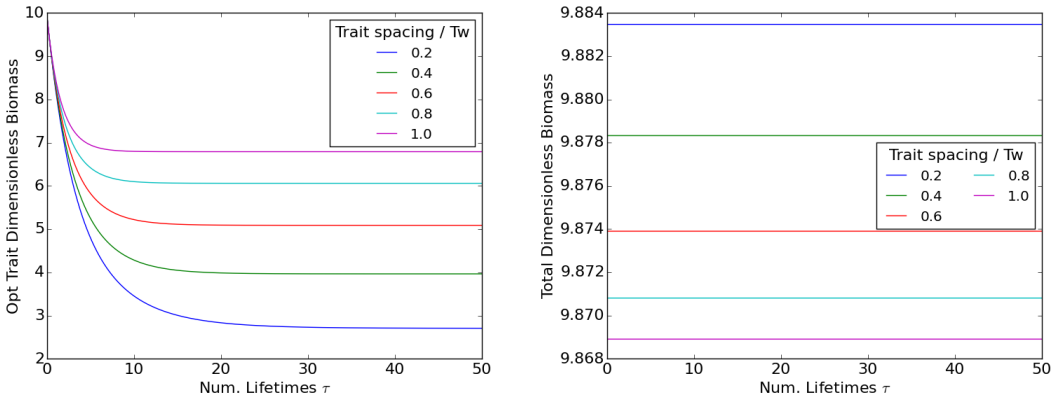

Figure 4.7: a) Time evolution of optimum trait biomass b) Time evolution of total system biomass for different trait spacings.

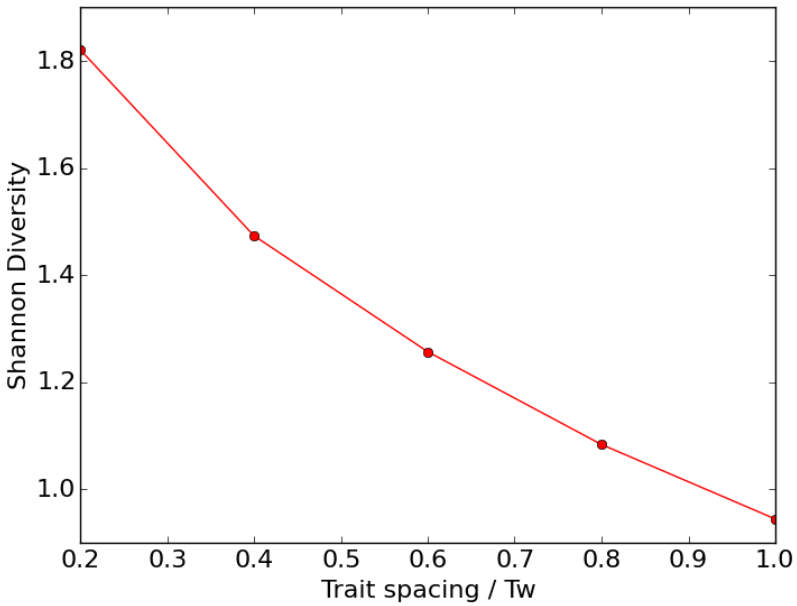

Figure 4.8: Shannon diversity (Equation 1.2.1) at equilibrium for different trait spacings.

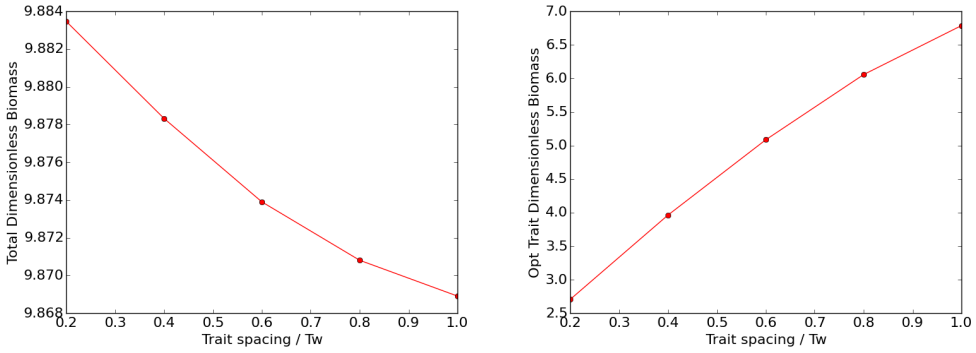

Figure 4.9: Effect of trait spacing on a) Total system biomass b) biomass of optimum trait.

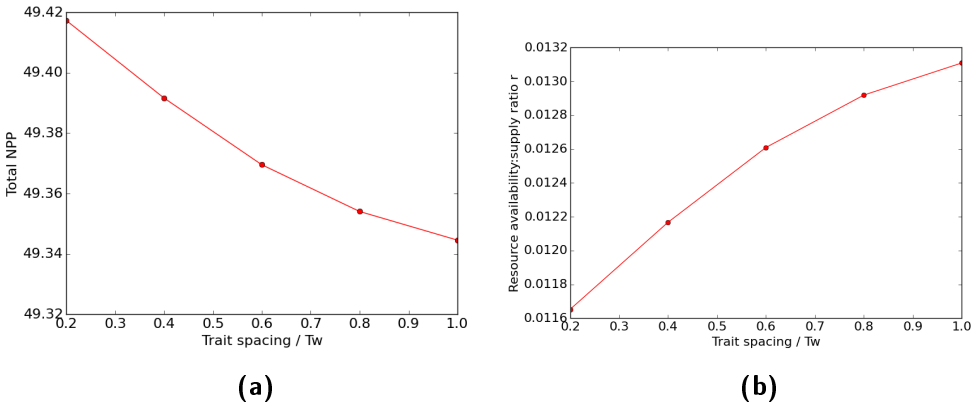

Figure 4.10: Effect of trait spacing on a) NPP b) resource availability.

4.2.2 Range of Traits

Before testing the effect of a temperature increase (e.g. climate change) on this model it important to know how many traits are needed to accurately model the biomass and NPP. It is assumed that the traits are arranged symmetrically around the environmental temperature and the trait range is the difference between the environmental temperature and the trait furthest from the environmental temperature. If the range of traits is too small then large inaccuracies would be introduced as the last trait would have a significant biomass relative to the optimum trait. As the trait biomass distribution is similar to a Gaussian in shape then as traits are added each one will have a smaller and smaller biomass until the effect of adding more traits becomes negligible.

This effect can be seen in Figure 4.11 where the biomass distribution converges as more traits are added. It is important that the trait range is large enough to accurately model both the total biomass and the individual trait biomasses.

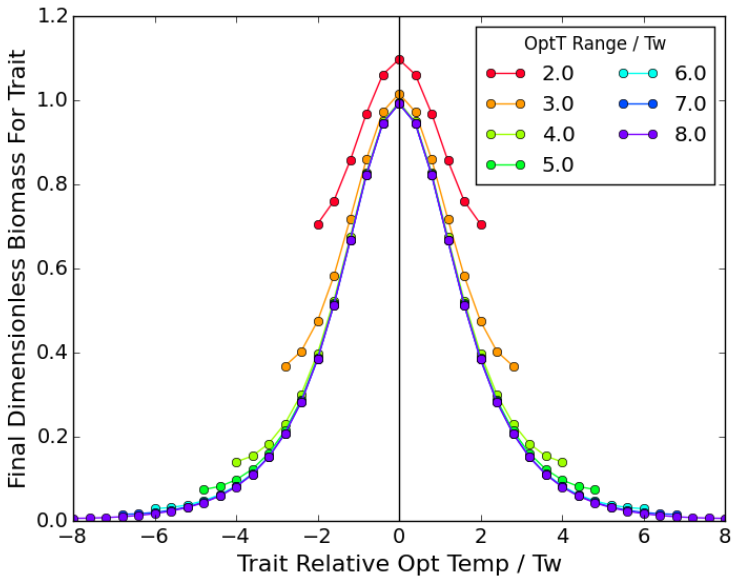

Figure 4.11: Shows the effect of trait range on biomass for diffusion rate 0.1 and trait spacing of 0.4 T_w. As the trait range increases then the biomass distribution converges. If the range is too short the result can deviate quite significantly.

Different values of diffusion and trait spacing will need a different number of traits to get an accurate representation. Figure 4.12 shows that the trait range needed increases as the diffusion rate is reduced as the biomass distribution becomes wider.

When the temperature is increased in a temperature change scenario then the trait range needed will have to be asymmetric with the lowest trait starting at starting temperature - trait range and the highest trait having temperature equal to final temperature + trait range. If a big enough trait range is used then the effect of the asymmetry will be negligible.

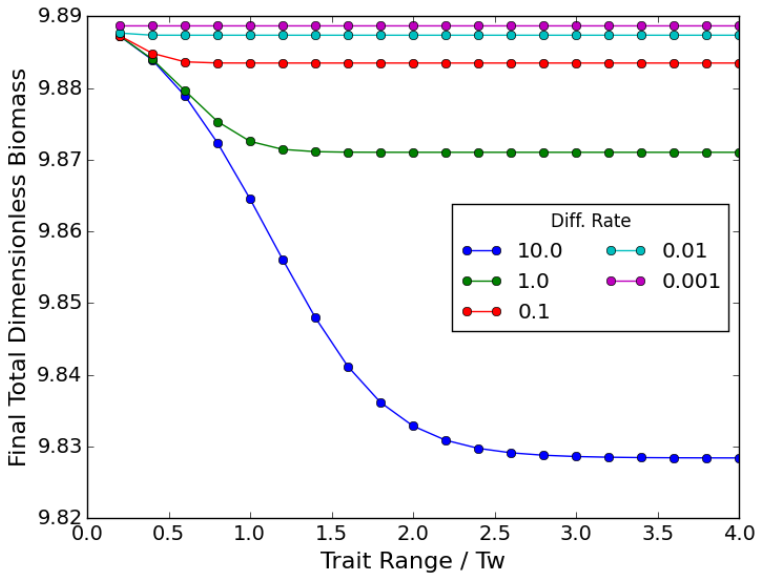

Figure 4.12: Shows the variation of total ecosystem biomass as the number of traits is increased in range with a trait spacing of 0.2 of the growth curve width T_w. For each value of trait diffusion the biomass converges as the number of traits increases. The variation in total biomass is quite small.

4.3 Effect of Temperature Change on the Trait Diffusion Model

To study the effects of temperature change the model was first spun up to equilibrium at the starting temperature and then the temperature was increased linearly for a fixed time period of 75 lifetimes (Figure 4.13). By repeating this for different temperature rates it is possible to see if there are any rate dependent effects on the total system biomass and NPP. To keep the model simple the range of traits is not limited, and so ignores the temperature limitations seen in real plants.

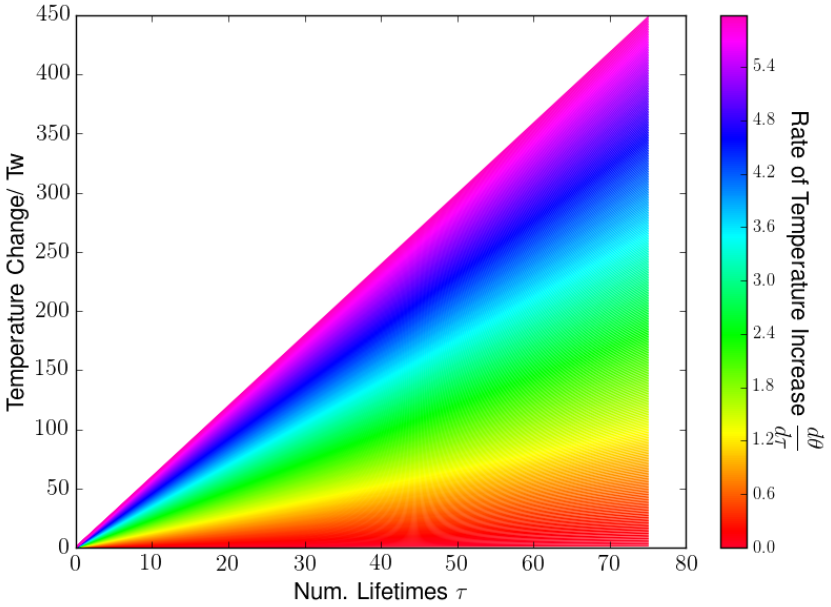

Figure 4.13: Shows the range of rates of temperature increase used to study rate dependent effects on the model. A total of 299 scenarios from 0.02 T_w per lifetime to 5.98 T_w per lifetime were used. In the plot each scenario has a colour as shown in the colour bar.

The rate of temperature increase has a critical value where the biomass collapses. In figure 4.14a the time evolution of the total system biomass can be seen, each scenario appears to settle down to fixed value despite the constantly increasing temperature and constantly changing trait biomasses. If the final biomass value of each scenario is plotted against the rate of temperature increase as in 4.14b a

collapse of the system biomass can be seen around a rate of 0.6 T_w per lifetime.

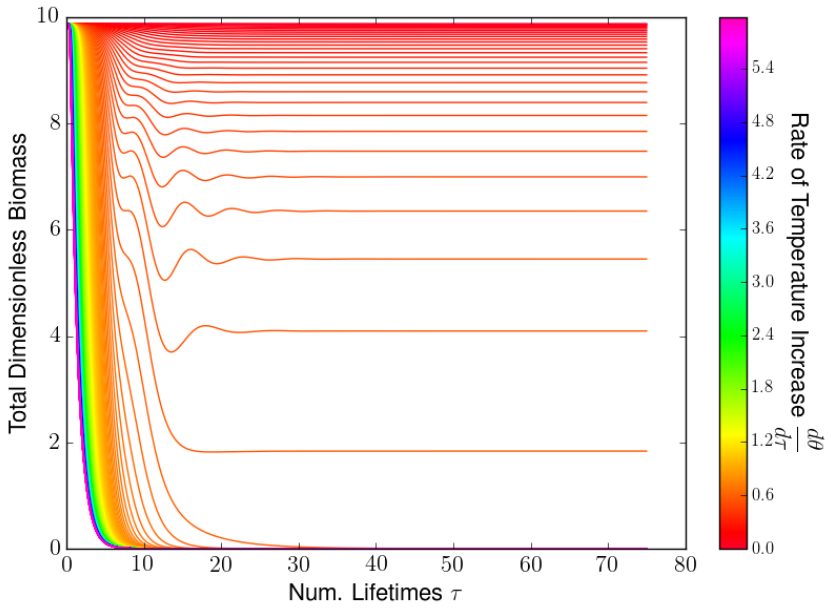

(a)

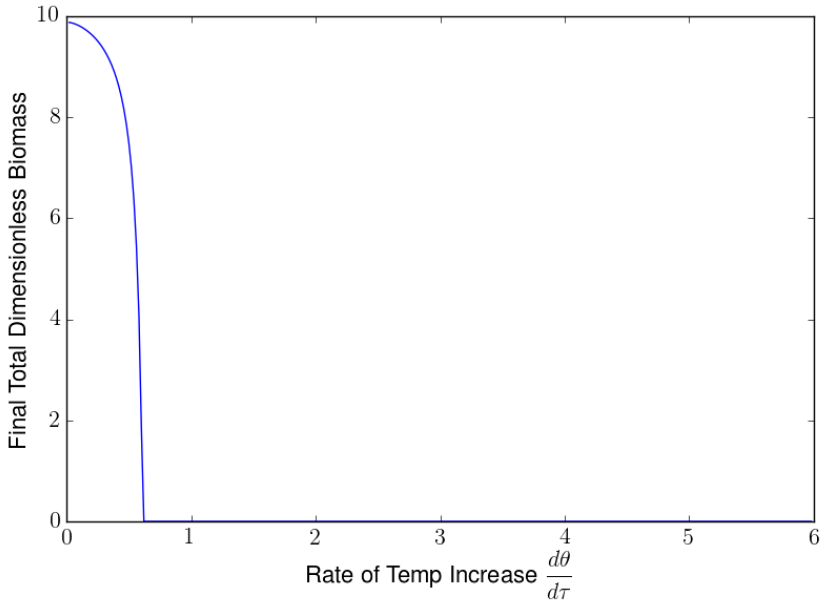

(b)

Figure 4.14: a) Shows the evolution of the system biomass for each rate of temperate change for diffusion of 0.1 (per lifetime) and spacing of 0.2 T_w. The colourbar shows the rate of temperate change for each plot. b) Shows the final biomass vs rate of temperature change, shows that there is a critical rate of 0.6 T_w per lifetime.

A very similar pattern is seen with NPP as this is closely related to the biomass (Figure 4.15).

Figures 4.14 and 4.15 only showed results for one particular choice of trait diffusion and trait spacing. The simulation was run many times for a range of diffusion and spacing values with over 2500 traits used to be sure of covering the range of temperatures. For each run the critical rate was defined as the rate where the NPP dropped to half its original value.

The critical rate can then be plotted against diffusion rate for a range of spacing values (Figure 4.16).

A higher diffusion rate makes the system more resilient to temperature changes as can be seen by systems with higher diffusion being able to withstand higher rates of temperature change before the NPP collapses.

We already know there is a relationship between the equilibrium diversity and the trait diffusion and trait spacing (figures 4.3 and 4.8). So we can replot figure 4.16 as critical rate vs starting diversity (figure 4.17), which shows that systems with a higher starting Shannon Diversity and evenness are for any particular spacing value more resilient to temperature change.

This result makes sense intuitively. More ability to diffuse allows better ability to keep up with imposed change.

4.3.1 Predictions of Critical $\frac{dT}{dt}$ based on species lifetime and diffusion

The results so far have all been plotted in terms of the non-dimensional equations and variables. To make real predictions of critical rates of change we can calculate $\frac{dT}{dt}$ from $\frac{d\theta}{d\tau}$ if we know the mortality rate γ and the growth curve width T_w and assume that growth rate g(T) = $\Gamma\gamma$ with a fixed value of Γ.

Figure 4.18 presents the results for $\frac{dT}{dt}$ in the case where $T_w = 2.0°\text{C}$ and $\Gamma = 10$.

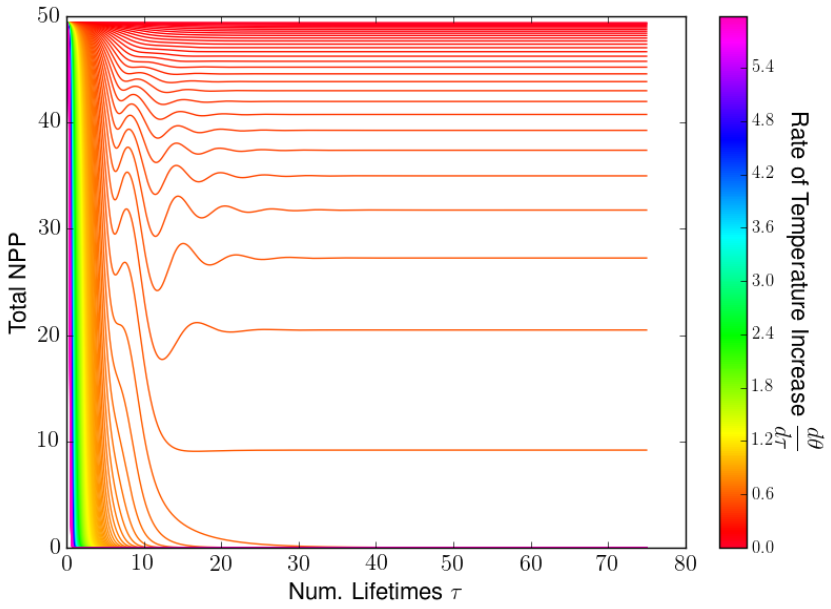

(a)

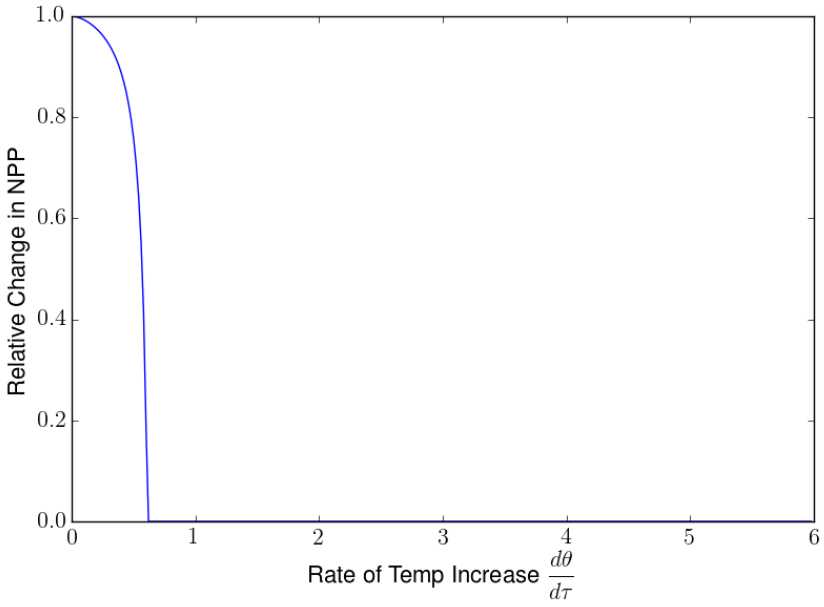

(b)

Figure 4.15: a) Shows the evolution of the system NPP for each rate of temperate change for diffusion of 0.1 (per lifetime) and spacing of 0.2 T_w. The colourbar shows the rate of temperate change for each plot. b) Shows the final NPP vs rate of temperature change, shows that there is a critical rate of 0.6 T_w per lifetime.

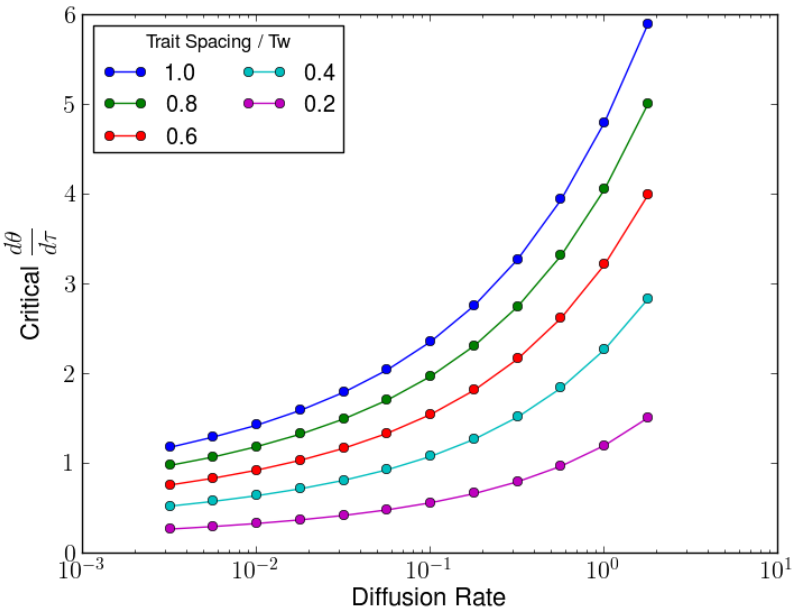

Figure 4.16: Shows the critical $\frac{d\theta}{d\tau}$ vs diffusion rate. Higher diffusion rate allows the system to maintain biomass and NPP with higher rates of temperature change.

The critical rate $\frac{dT}{dt}$ is proportional to the mortality rate and therefore reciprocal of the lifetime.

The results in Figure 4.18 suggest that for a tree of lifetime of 100 years the critical rate of change would be 0.054°C year^{-1}, for an annual plant 5.4°C year^{-1} and for a short-lived bacteria (lifetime 0.01 year / 3 days) would be 540°C year^{-1}. Obviously these results will change in different values are chosen for the trait spacing, diffusion/diversity, growth curve width and growth:death rate ratio Γ.

As forest ecosystems are of key importance, Figure 4.19 shows the critical rates of change for species with lifetime of order of 100 years, range from 0.01 to 0.3 °C year^{-1} for a diffusion rate in range 10^{-2} to $10^{0.25}$ per lifetime and spacing in range 1 to 5°C and $T_w = 5.0$°C.

The lower values of these predicted critical rates are within the rates of change predicted for anthropogenic warming (see IPCC (2013), temperature increase of between 2°C and 6°C globally by 2100 with maybe as much as 11°C for the arctic

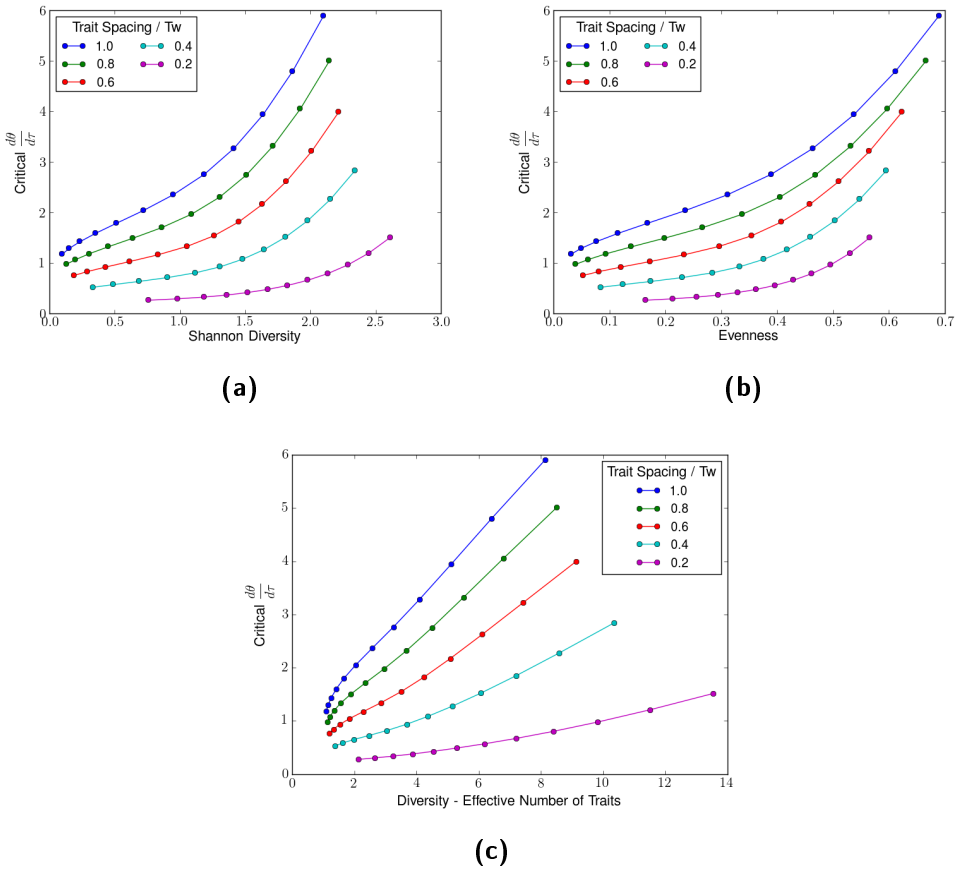

Figure 4.17: Shows the critical $\frac{d\theta}{d\tau}$ vs diversity. Measured by a) Shannon diversity b) Evenness. c) Effective number of traits. Higher diversity and evenness allows the system to maintain biomass and NPP with higher rates of temperature change.

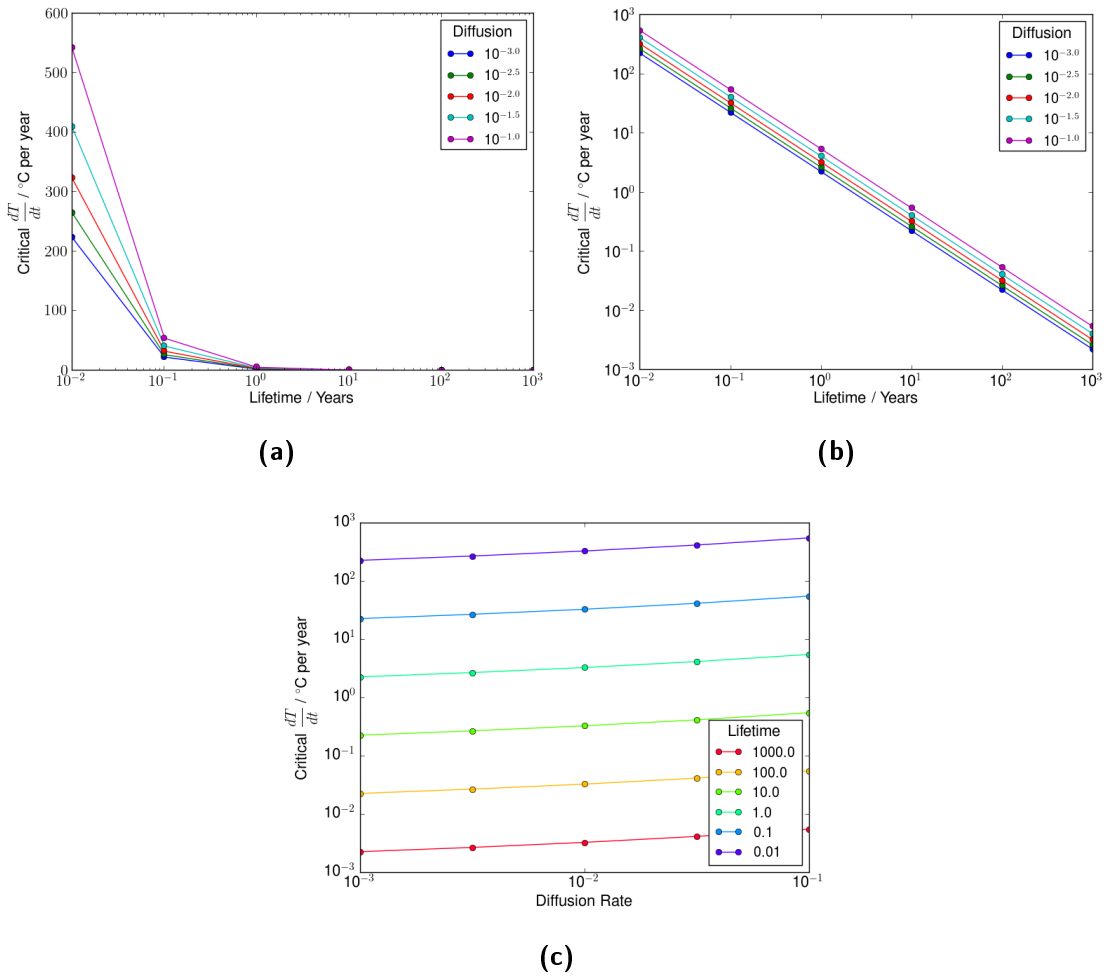

Figure 4.18: Shows the reciprocal relationship between critical $\frac{dT}{dt}$ and lifetime for $T_w = 5.0°C$, spacing 2.5°C and $\Gamma = 10$. a) Critical $\frac{dT}{dt}$ vs Lifetime for different diffusion rates b) same as a) with y axis also plotted logarithmically. c) $\frac{dT}{dt}$ vs diffusion for different lifetimes.

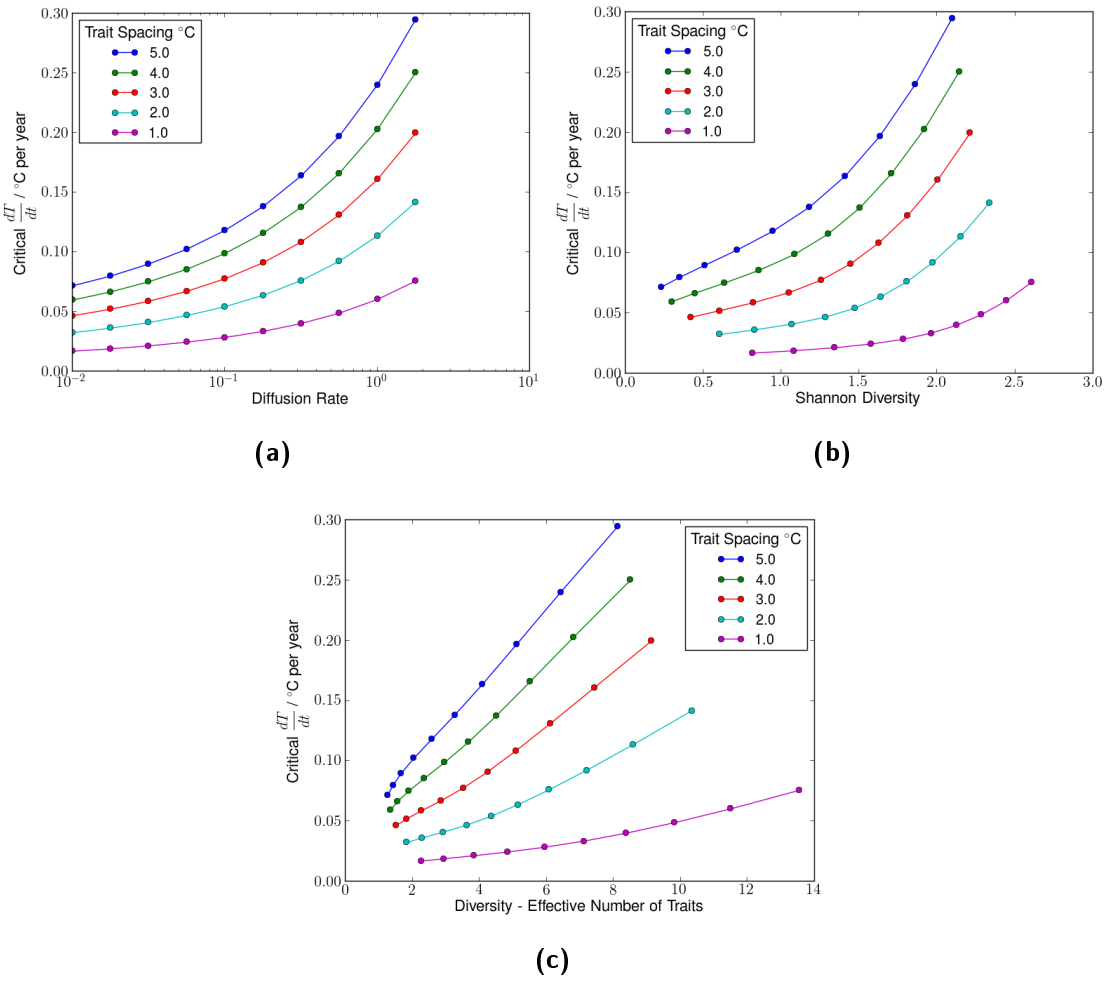

Figure 4.19: Critical rates of change for species of lifetime 100 years, which is representative of forest trees. a) Plotted vs diffusion b) Plotted vs Shannon diversity c) Plotted vs effective number of traits.

by this date - gives warming rates of 0.02, 0.0667 and 0.122 °C yr^{-1} respectively). So whether our forests can adapt to warming depends on the trait diversity, growth curve width and trait spacing of real forest ecosystems.

4.4 Discussion and Conclusions

The trait diffusion model is a simple yet effective way of representing diversity and avoids the difficulties of using stochastic effects to maintain diversity as in Chapter 3. The diffusion represents the natural tendency of an ecosystem to increase in trait diversity due to genetic mutation and evolution, while the single resource competition will reduce the biomass of traits less well suited to the environment.

This trade off between the diffusing and competitive effects leads to a distribution with a Gaussian like shape, with the peak centred around the temperature of the environment. Larger diffusion rates lead to a flatter and wider distribution and low diffusion rates give a sharper and taller distribution. So greater diffusion leads to higher trait diversity.

Due to the Gaussian like shape of the distribution the traits further from the environmental temperature have smaller and smaller biomass and so there comes a point where the effect of adding more traits on the total system biomass becomes negligible and converges on the biomass that would be obtained with an infinite range of traits. This allows the number of traits needed to accurately model the total system properties to be established.

If the environmental temperature is increased linearly for a system that has previously come to equilibrium at the starting temperature then the system will find a new constant lower level of biomass and NPP even though the temperature and the trait biomasses are constantly changing. The new biomass level is increasingly lower for higher rates for temperature increase.

Beyond a certain critical rate of temperature change the biomass and NPP collapse down to zero. This suggests that the system has an adaptation limit where it can

only keep up with temperature change if it is below the critical rate, as above this rate it can no longer adapt. This chapter has shown that an ecosystem with higher trait diversity maintains its biomass better for a given rate of temperature increase and therefore suggests that trait diversity makes an ecosystem more resilient to environmental changes.

This conclusion has implications for real ecosystems, suggesting that the ability of an ecosystem to adapt to environmental change and the rate of the change are the key factors in determining if a particular ecosystem can survive the changes.

For forest ecosystems the critical rates range from 0.01 to 0.3 °C year^{-1} for a diffusion rate in range 10^{-2} to $10^{0.25}$ per lifetime and spacing in range 1 to 5°C and $T_w = 5.0$°C. This means that if real forest ecosystems have critical rates that correspond to the lower end of this range, they could very well experience rates of change that are greater than their critical rate.

Hence understanding the diffusion rates, growth curve widths and trait spacing of real ecosystems would allow this model to make more specific predictions as to whether ecosystems can withstand current and forecast rates of change. So understanding the real values of these parameters is a very important avenue of future work.

This is especially true if on-going industrialisation causes faster warming rates, or as the planet emerges from what some have called the warming "hiatus" (Kosaka and Xie, 2013).

The model assumes that only temperature trait diffusion determines the trait diversity and ignores any other possible mechanisms that may influence the temperature trait diversity. It would be useful validation of this model to perform an in-depth study of plant traits to see if there is a link between the range of environmental traits (such as temperature) in an ecosystem and the variance of the corresponding environmental variable.

Currently the trait spacing has an effect on the diversity and also on the resilience

that cannot be explained purely through the diversity alone. This suggests that the model might be more or less resilient in a continuous form where the trait spacing is no longer a factor but this isn't a trivial thing to do, so is very much an avenue of future work.

Chapter 5

Theory of Vegetation Demography

This chapter is the start of the second part of the thesis, which develops a new Dynamic Global Vegetation Model (DGVM). This first chapter of this part of the thesis focuses on the theoretical basis for the model.

Estimating the rate forests accumulate (or lose) carbon is an important issue for large-scale land surface models whose purpose is estimating the land carbon sink (Moorcroft et al., 2001; Fisher et al., 2010). Stephenson et al. (2014) have shown that the rate of carbon accumulation tends to increase with tree size and so this has implications for the accuracy of predictions of large-scale vegetation models which do not model different plant sizes, especially should such models be used for policy applications to determine how much terrestrial ecosystems are capable of offsetting anthropogenic emissions.

Many forests are subject to the effects of land use and land cover change and forest management (Lambin et al., 2003). These processes can selectively remove trees of some sizes and leave others or result in an area being cleared for crops but then later falling out of use and forest regrowing (Bellassen et al., 2010; Lambin et al., 2003; Zaehle et al., 2006). So it is desirable to be able to account for such size-dependent processes in DGVMs.

This chapter will present the underlying theoretical concept of a vegetation demog-

raphy model that includes size dependent growth and also analyses some idealised analytical solutions to the model. Chapter 6, will then expand upon this theoretical basis to create a full numerical vegetation model.

5.1 Basic Model Concept - Continuity

The distribution of tree sizes in a forest is shaped by three factors in the form of growth, death and recruitment of seedlings. This means that the change in number of trees in a particular size range is simply governed by the number of trees smaller than that range growing into it minus the number of trees lost from that size range to death or by growing bigger. This is simple case of continuity or conservation with an additional loss term associated with mortality.

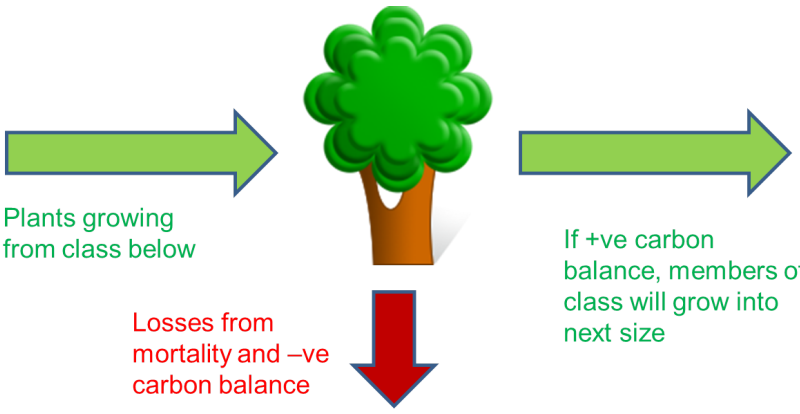

Figure 5.1: The growth of each size class is determined by the flow of trees into and out of the class. Trees can grow from smaller size classes into this one, can grow out of this size class or be lost due to mortality.

To model such a system we can use the continuity equation from physics, often used in fluid flow as well as areas such as electromagnetic theory. The continuity equation simply describes the transport of a conserved quantity. In the case of fluid flow, the fluid is conserved and also flows spatially.

$$\frac{\partial \rho}{\partial t} + \boldsymbol{\nabla} \cdot (\rho \boldsymbol{u}) = 0 \tag{5.1.1}$$

where ρ is the fluid density and $\boldsymbol{u}$ is the velocity vector field. If flow is just in one dimension, then we can simplify to the below, which is the one-dimensional advection equation: -

$$\frac{\partial \rho}{\partial t} + \frac{\partial}{\partial x}(\rho u) = 0 \tag{5.1.2}$$

For a forest the equation is modified so the state variable becomes the tree density n with units of trees m^{-2} kg^{-1}. The spatial variable is m, and this is the tree dry carbon mass with units kg of carbon, hereafter denoted kg C. The velocity becomes the carbon mass growth rate of trees as a function of size m. In addition there is a loss or sink term, on the right hand side, representing tree mortality γ.

This is very similar to the model used in Kohyama (1991) except the size variable chosen is the tree dry carbon mass m rather than trunk diameter. This is convenient for modelling both tree physiology and the carbon cycle. The physiology model can just directly calculate the rate of CO_2 fixation to give $\frac{dm}{dt}$. A tree's carbon mass is in the range 46% to 50% of kiln dry mass for hardwood trees and 47% to 55% for softwood (conifer) trees (Lamlom and Savidge, 2003).

$$\frac{\partial n}{\partial t}(m,t) + \frac{\partial}{\partial m}\left(n(m,t)\,\frac{\partial m}{\partial t}(m,t)\right) = -\gamma n(m,t) \tag{5.1.3}$$

The recruitment of new seedlings to the lowest mass class m_0, determines the lower boundary condition: -

$$\left[n(m,t)\,\frac{\partial m}{\partial t}(m,t)\right]_{m=m_0} = \text{Recruitment} \tag{5.1.4}$$

To convert the size distribution from in terms of mass m to another size variable y (such as trunk diameter or height), then the following relation is used as derived in Appendix D.

$$n(y,t) = \frac{dm}{dy} n(m,t) \tag{5.1.5}$$

5.2 Equilibrium Solution to Continuity Equation

To understand the dynamics of the forest continuity equation, the model is simplified to have time independent growth rate that is approximated by a simple mathematical function of mass and to assume the recruitment is constant.

These solutions assume no shading of shorter trees by taller ones, so these solutions are more applicable to open canopies. The next chapter will add recruitment and shading competition to the model but the extra complexity will require them to be solved numerically.

At equilibrium the forest continuity equation is: -

$$\frac{\partial n}{\partial t}(m,t) = -\frac{\partial}{\partial m}\left(n(m,t)\,\frac{\partial m}{\partial t}(m,t)\right) - \gamma n(m,t) = 0 \tag{5.2.6}$$

This can be written more compactly using g(m) = $\frac{\partial m}{\partial t}(m)$ and then multiplying out by the product rule.

$$n(m)\frac{dg}{dm}(m) + g(m)\frac{dn}{dm}(m) = -\gamma n(m) \tag{5.2.7}$$

Which simplifies to : -

$$\frac{1}{n(m)}\frac{dn}{dm}(m) = -\frac{1}{g(m)}\left[\frac{dg}{dm}(m) + \gamma\right] \tag{5.2.8}$$

5.2.1 Power Law Growth Rate Case

The first case considered is to assume the growth rate follows a power law dependence on size: -

$$g(m) = am^b \tag{5.2.9}$$

where a and b are constants.

Integrating equation 5.2.8 for this case yields:-

$$\int_{n_0}^{n} \frac{dn}{n(m)} = -\Big[\ln g(m)\Big]_{m_0}^{m} - \gamma \int_{m_0}^{m} \frac{1}{am^b} dm \tag{5.2.10}$$

where m_0 is the lowest mass class and n_0 is the number of trees in the lowest mass class.

$$\ln \frac{n(m)}{n_0} = -\left[b \ln |am| + \frac{\gamma m^{1-b}}{a(1-b)}\right]_{m_0}^{m} \tag{5.2.11}$$

$$n(m) = n_0 \exp\left[-b \ln \left|\frac{m}{m_0}\right| - \frac{\gamma}{a(1-b)}\left(m^{1-b} - {m_0}^{1-b}\right)\right] \tag{5.2.12}$$

Giving the size distribution of

$$n(m) = \frac{k}{m^b} \exp\left[-\frac{\gamma}{a(1-b)} m^{1-b}\right] \tag{5.2.13}$$

where

$$k = n_0 \, {m_0}^b \exp\left[\frac{\gamma \, {m_0}^{1-b}}{a(1-b)}\right] \tag{5.2.14}$$

For $b = 0$, which corresponds to a constant growth rate of magnitude a, this general form (Equation 5.2.13) reduces to

$$n(m) = n_0 \exp\left(-\frac{\gamma}{a}\left[m - m_0\right]\right) \tag{5.2.15}$$

Idealised Self-Thinning

If the above power law solution is used to represent an idealised case where $b = \frac{2}{3}$ then the growth rate is: -

$$g(m) = am^{2/3} \tag{5.2.16}$$

This corresponds to a case where the trees are self-similar with a constant mass density and with growth proportional to the crown area A. The self-similarity and constant density implies that the crown area is a circle of radius r and the tree mass is proportional to volume V, which in turn is proportional to the crown radius cubed r^3. The growth rate is assumed to be proportional to the crown area A.

$$g \propto A \propto r^2 \tag{5.2.17}$$
$$m \propto V \propto r^3$$

Rewriting the above equation by substituting mass m into the relation for g, leads to Equation 5.2.16

If the mortality is negligible so $\gamma \to 0$, then Equation 5.2.13 reduces to

$$n = \frac{k}{m^{2/3}} \tag{5.2.18}$$

where $k = n_0 \, {m_0}^{2/3}$.

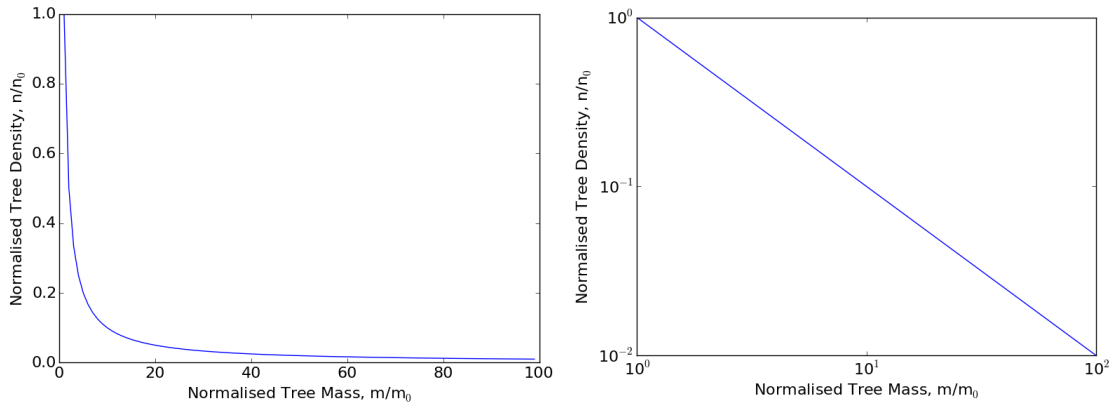

(a) **(b)**

Figure 5.2: The self-thinning trajectory as a solution to the forest continuity equation in the idealised case of g(m) $\propto$ a $m^{2/3}$ a) Linear axes b) logarithmic axes

This then corresponds to the trajectory an even aged stand will follow during self-thinning (Westoby, 1984). This is only an approximation as real forest growth function increases up to a maxima then then decreases back down to zero as size increases. The above approximation can seen to be valid for small sizes before the growth maxima.

5.2.2 Quadratic Growth Rate Case

A more complex functional form for $g(m)$ that still allows the equilibrium solution to be found easily by direct integration is to assume quadratic dependence of $g(m)$ on mass. This approximates to tree growth rates in a situation that while the photosynthesis is a monotonic function of size, the respiration and litter losses increase more slowly but eventually overtake photosynthesis meaning there is both a turning point in the growth rate and a maximum size where growth rate has fallen to zero. This pattern can be seen in some studies of forest growth (Kohyama, 1987, 1991), particularly for faster growing species in canopy gaps.

$$g(m) = g_{max}\left[1 - \left(\frac{m}{m_{max}} - 1\right)^2\right] \tag{5.2.19}$$

A non-dimensional form of the tree mass is used to simplify the mathematics: -

$$x = \frac{m}{m_{max}} \tag{5.2.20}$$

$$g(x) = \frac{\partial m}{\partial t}(x) = g_{max} x\,(2 - x) \tag{5.2.21}$$

The differential is

$$\frac{dg}{dm} = \frac{g_{max}}{m_{max}} 2\,(1 - x) \tag{5.2.22}$$

Again we integrate Equation 5.2.8 to get the analytical expression for n: -

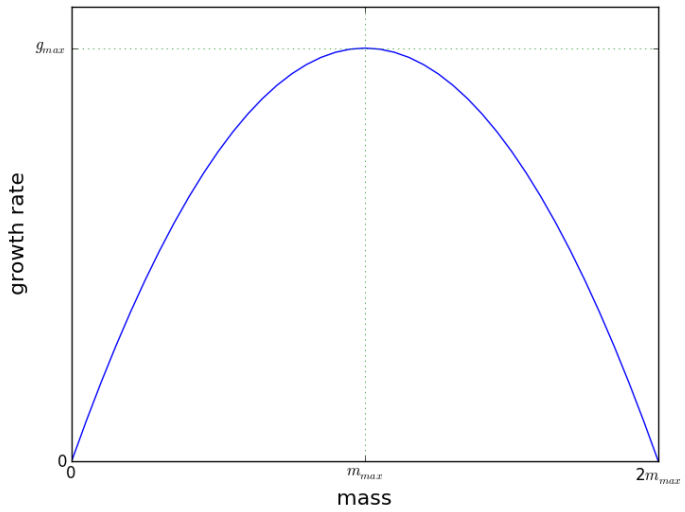

Figure 5.3: Quadratic growth rate as function of mass

$$\int_{n_0}^{n} \frac{dn}{n(m)} = -\Big[\ln g(x)\Big]_{x_0}^{x} - \frac{\gamma\, m_{max}}{g_{max}} \int_{x_0}^{x} \frac{1}{x\,(2-x)} dx \tag{5.2.23}$$

$$\ln \frac{n}{n_0} = -\Big[\ln |x\,(2-x)|\Big]_{x_0}^{x} - \frac{\gamma\, m_{max}}{2g_{max}} \left[\ln \left|\frac{2-x}{x}\right|\right]_{x_0}^{x} \tag{5.2.24}$$

We can make the simplifying substitution of : -

$$z = \frac{\gamma\, m_{max}}{2g_{max}} \tag{5.2.25}$$

$$n = n_0 {x_0}^{z+1} (2-x_0)^{1-z} \frac{(2-x)^{z-1}}{x^{z+1}} \tag{5.2.26}$$

If we gather all the constant terms into a constant D, we get

$$n = \begin{cases} D\,\frac{(2-x)^{z-1}}{x^{z+1}}, & \text{for } x \leq 2 \\ 0 & \text{for } x > 2 \end{cases} \tag{5.2.27}$$

If $x > 2$ the solution (Equation 5.2.27) is then only real if z is an integer and is complex if z is a multiple of 0.5 and is undefined if z is neither an integer nor a

multiple of 0.5. As you would not expect trees to grow beyond $x > 2$ as the growth rate $g \leq 0$ then the solution is defined to be zero for $x > 2$.

The differential of the above solution is : -

$$\frac{dn}{dm} = \frac{dn}{dx} = \frac{2D\,(2-x)^{z-2}}{x^{z+2}}\,(x-1-z) \tag{5.2.28}$$

Effect of z parameter on analytical solutions

The z parameter is an important determinant of the distribution shape seen. Figure 5.4, shows the different distribution shapes for different values of z.

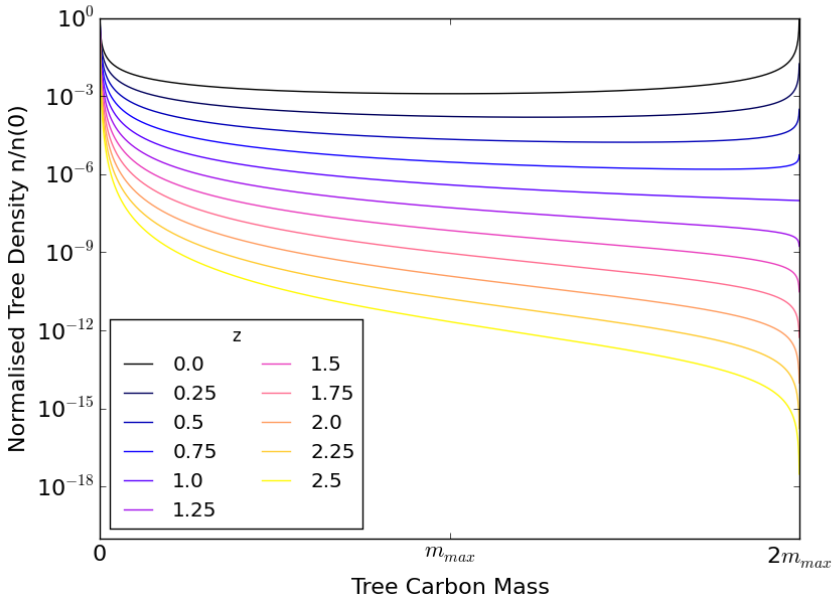

Figure 5.4: Shows different analytical solutions assuming a quadratic growth rate for different values of z. Clearly shows that as z increases past 1 the solutions no longer have a minima in the middle and instead are monotonically decreasing.

This shows that the distribution is "U-shaped" with a minima between $1 < x < 2$ ($m_{max} < m < 2m_{max}$) if $0 < z < 1$, this means that the tree density is larger for both smaller and larger trees compared to medium sized trees. If $z \geq 1$ the tree density is a monotonically decreasing function of size and for $z > 1$ follows the

rotated sigmoid shape commonly seen in observed forest size distributions (Zenner, 2005; Rubin et al., 2006).

When $0 < z < 1$, the medium sized trees grow quickly and therefore trees spend the least time at these sizes and the top of the canopy is densely populated. When $z \geq 1$ then the death rate is becoming large enough to have a significant effect on the distribution and the forest has a decreasing number of trees with increasing size, as represented through mass m.

This can be understood mathematically if the continuity equation (Equation 5.1.3) is rearranged in terms of $\frac{\partial n}{\partial m}(m)$ and g(m) is substituted for $\frac{\partial m}{\partial t}$

$$\frac{\partial n}{\partial m}(m) = -\frac{n(m)}{g(m)}\left(\gamma + \frac{\partial g}{\partial m}(m)\right) \tag{5.2.29}$$

From this it can be seen that the gradient of the distribution will be positive where $\left(\gamma + \frac{\partial g(m)}{\partial m}\right)$ is negative. This means the positive slope seen for $m > m_{max}$ and $z < 1$ corresponds to: -

$$\frac{\partial g}{\partial m}(m) < -\gamma \tag{5.2.30}$$

So if the steepest negative slope at $x = 2$ ($m = 2m_{max}$) is less than $-\gamma$ the distribution will be "U-shaped". From Equation 5.2.22 it can be seen that the greatest slope of the growth function is

$$\left|\frac{dg}{dm}\right|_{max} = 2\frac{g_{max}}{m_{max}} \tag{5.2.31}$$

So z is described by the ratio of the mortality to the greatest slope of g: -

$$z = \frac{\gamma\, m_{max}}{2g_{max}} = \frac{\gamma}{\left|\frac{dg}{dm}\right|_{max}} \tag{5.2.32}$$

5.3 Discussion

The continuity equation has been previously used successfully as a way of modelling forest ecology by Kohyama (1991, 1993, 2006) and ecosystem demography (Moorcroft et al., 2001). These earlier studies only focused on producing numerical simulations based on empirical data.

This chapter has shown that a simplified time independent growth rate that is described by simple mathematical functions of tree size itself, can be used to obtain approximate analytical solutions to the forest continuity equation.

Two useful solutions were found. The first was using a power law growth rate, which allowed the idealised self-thinning trajectory to be reproduced.

The second solution was that with a quadratic growth rate increasing from the origin to a maxima before decaying back to zero at the largest tree size, which approximates the variation of growth rate observed by Kohyama (1987) for forest gaps. This showed two distinct size distributions, the first having a rotated sigmoid size distribution (as also seen in observational studies such as Zenner (2005); Rubin et al. (2006)) and the second was a "U-shape" distribution. The "U-shape" distribution corresponds to a forest with a very dense upper storey with very few medium sized trees.

The determinant of which distribution shape being seen was the ratio of the maximum slope of the growth function to the death rate γ. If the death rate is higher than the maximum growth rate slope then a rotated sigmoid solution is seen, otherwise the solution will be the "U-shape" distribution.

In the next chapter the model will be improved to include competition through shading, growth rate based on plant physiology and recruitment based on primary productivity.

Chapter 6

Numerical Model of Robust Ecosystem Demography (R.E.D.)

As mentioned in Chapter 5, estimating land use and land cover change and forest regrowth after a disturbance is an important issue for large-scale land surface models whose purpose is estimating the land carbon sink. The TRIFFID (Cox, 2001; Best et al., 2011; Clark et al., 2011) dynamic global vegetation model (DGVM) does not model differing tree sizes and this is a contributing factor to the reason that its regrowth time-scales are often longer than those seen in observations (see Figure 6.1).

The model presented in Chapter 5 is extended in this chapter with a physiology model from TRIFFID used to calculate the growth rate and also introducing representations of light competition and recruitment.

6.1 Discretisation

To make a practical model we need to discretise this equation into a set of mass classes. The mass classes are defined as equally spaced with the mean mass (midpoint) of the class used to represent the mass of all individuals in that class. The

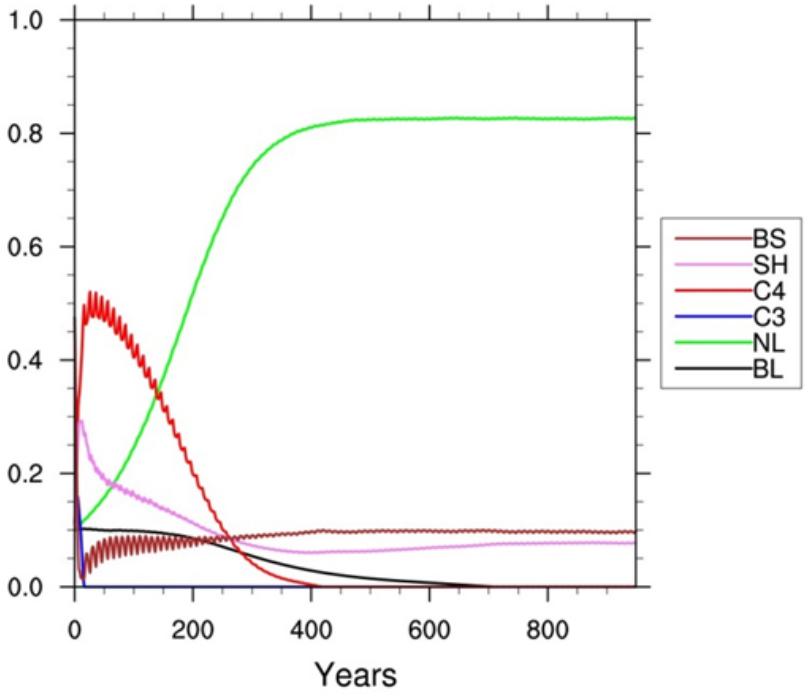

Figure 6.1: Output from TRIFFID for Hyytiala in Finland. Shows the time evolution of the fractional coverage of each PFT where BS is bare soil, SH is shrub, C4 is C4 grass, C3 is C3 grass, NL is needleleaf trees and BL is broadleaf trees. The dominant PFT of needle leaf takes ∼300 years to regrowth whereas observations show this should be ≤∼100 years timescale (Staaland et al., 1998).

Table 6.1: List of symbols for Chapter 6

Symbol	Variable / Parameter	Unit
m	Tree carbon mass	kg C
$n(m,t)$	Tree density	trees m^{-2} kg^{-1}
γ	Tree mortality	$year^{-1}$
C	Tree carbon mass per unit crown area	kg C m^{-2}
C_l	Leaf carbon mass per unit crown area	kg C m^{-2}
C_f	Fine root carbon mass per unit crown area	kg C m^{-2}
C_w	Wood carbon mass per unit crown area	kg C m^{-2}
L	Leaf area index	-
A	Tree crown area	m^2
D	Tree trunk diameter (breast height)	m
B	Tree basal area	m^2
H	Tree height	m
σ_l	Specific leaf carbon density	kg C m^{-2}
ρ	Tree wood density	kg C m^{-2}
m_l	Tree leaf carbon mass	kg C
m_r	Tree root (fine and coarse) carbon mass	kg C
m_s	Tree stem (woody aboveground) carbon mass	kg C
m_f	Tree fine root carbon mass	kg C
m_w	Tree woody (above and below ground) carbon mass	kg C
Π	Net Primary Productivity	kg C m^{-2} $year^{-1}$
Π_G	Gross Primary Productivity	kg C m^{-2} $year^{-1}$
R_p	Respiration per unit tree crown area	kg C m^{-2} $year^{-1}$
R_{pm}	Maintenance respiration	kg C m^{-2} $year^{-1}$
R_{pg}	Growth respiration	kg C m^{-2} $year^{-1}$
r_g	Growth respiration coefficient	-
f_{PAR}	Fraction of photosynthetically active radiation	-
k	extinction coefficient	-
f_l	fraction of light reaching particular depth in canopy	-
Λ_l	Litter rate per unit tree crown area	kg C m^{-2} $year^{-1}$
λ_l	Leaf litter rate	$year^{-1}$
λ_r	Root litter rate	$year^{-1}$
λ_w	Wood litter rate	$year^{-1}$
f_R	Fraction of NPP going to reproduction	-
f_S	Fraction of reproduction NPP going to seedlings	-

mass of each class is then expressed mathematically as:-

$$m_j = \Delta m \left(\frac{1}{2} + j \right) \tag{6.1.1}$$

where j is an integer defined so that m_0 is the class with the smallest mass and higher values of j correspond to classes of higher mass. Also the smallest class m_0 is assumed to represent trees with masses between 0 and Δm (see Figure 6.2).

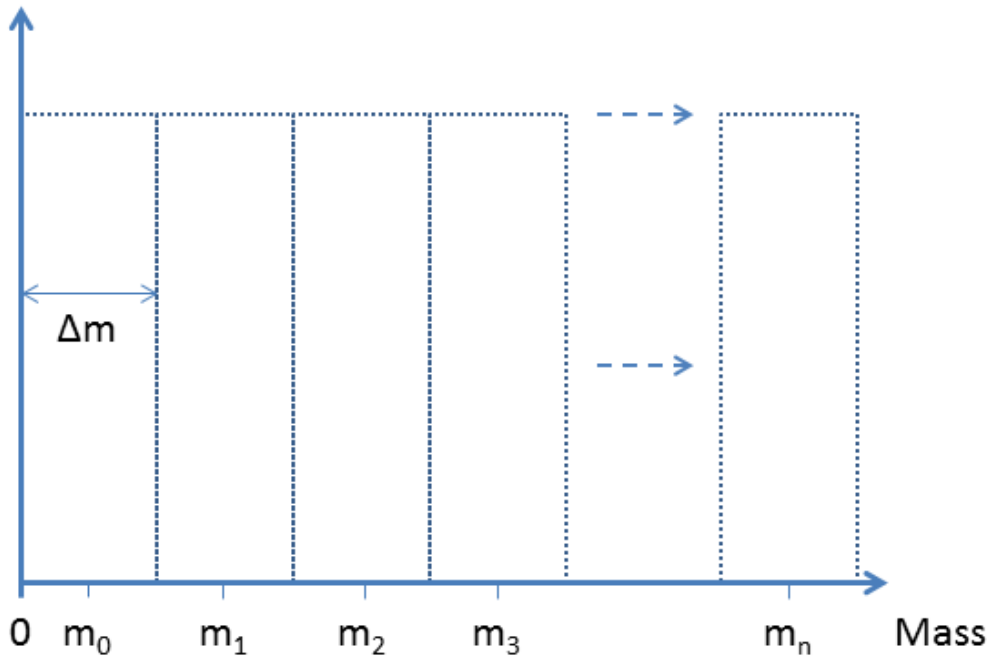

Figure 6.2: Shows how to mass classes are defined in RED. Each class has a width of Δm and has a value corresponding to the mid-point value. The first class covers the range from mass of 0 to Δm and has a value of $m_0 = \frac{\Delta m}{2}$.

For a mass class j with growth rate $\frac{\partial m_j}{\partial t}$ then we get: -

$$\frac{\partial n_j}{\partial t} = -\frac{1}{\Delta m} \left(n_j \frac{\partial m_j}{\partial t} - n_{j-1} \frac{\partial m_{j-1}}{\partial t} \right) - \gamma n_j \tag{6.1.2}$$

where n_j is the number density (trees m^{-2} kg^{-1}).

This equation has three terms that correspond respectively to growth out of the class, growth into the class and losses due to trees dying.

$$\frac{\partial n_j}{\partial t} = growout_j + growin_j + death_j \tag{6.1.3}$$

$$growout_j = -\frac{n_j}{\Delta m}\frac{\partial m_j}{\partial t} \tag{6.1.4}$$

$$growin_j = -growout_{j-1} \tag{6.1.5}$$

$$death_j = -\gamma n_j \tag{6.1.6}$$

Each of these terms will be described in more detail later in this chapter, as they will be modified at the upper and lower boundary conditions and where the growth rate is negative ($\frac{\partial m}{\partial t} < 0$).

6.2 Allometry

The scaling relationship between different tree dimensions and properties are important in determining both the outcome of competition and for accurately estimating the amount of carbon locked up in a forest. Trees compete via shading each other, so how tall a tree is and its crown size are important factors in its ability to capture light and shade its rivals. In a DGVM it is also crucial to know the canopy height, fractional coverage and Leaf Area Index (LAI) of each plant functional type (PFT), as a climate model needs to be able to calculate vegetation-dependent biophysical surface parameters, such as albedo and roughness.

Based on the work of Niklas and Spatz (2004), West et al. (2009) and Poorter et al. (2006) simple scaling power laws are used.

6.2.1 Leaf mass

The relationship between leaf mass and tree mass follows that of Niklas and Spatz (2004): -

$$m_l = k_{ml} m^{\phi_{ml}} \tag{6.2.7}$$

where $\phi_{ml} = 3/4$.

6.2.2 Trunk Diameter

The trunk diameter at breast height is defined as (Niklas and Spatz, 2004):

$$D = k_D {m_l}^{\phi_D} \tag{6.2.8}$$

where $\phi_D = 1/2$.

If it is assumed that the leaf mass m_l is proportional to leaf area and that the area of transport tissue is proportional to trunk diameter squared, then the above leaf mass to trunk diameter relationship can also be seen to be consistent with the pipe model (Shinozaki et al., 1964a,b), where each unit of leaf area is assumed to require the support of a corresponding area of transport tissue. Wang et al. (2010) has shown the sapwood area scales with the trunk diameter with an exponent in the range 1.3-2.2.

6.2.3 Root mass (both coarse and fine)

The root mass m_R is considered to be a fixed fraction of the stem mass m_s: -

$$m_r = k_{rs} m_s \tag{6.2.9}$$

where k_{RS} corresponds to the root:shoot ratio.

6.2.4 Stem mass (woody aboveground mass)

The stem mass is estimated from the tree volume

$$m_s = k_{ms} D^2 H \tag{6.2.10}$$

$$k_{ms} = F\rho\frac{\pi}{4} \tag{6.2.11}$$

where F is the form factor which is taken to be 0.6 in broad-leaf species (Chave et al. (2005), value in this chapter adjusted for different units) and ρ the trunk wood carbon density (oven dry mass over green volume, kg C m^{-3}).

6.2.5 Roots and Stem

To be consistent with TRIFFID (Cox, 2001) the above allometry is modified by splitting roots in fine and coarse and to merge coarse roots and stem into a term representing the wood in the tree.

For simplicity the mass of fine roots is assumed to be equal to the leaf mass (Cox, 2001). This simplified model does not include water availability, which can alter the leaf to root mass ratio Sitch et al. (2003).

$$m_f = m_l \tag{6.2.12}$$

The woody mass is then equal to the sum of the coarse roots and stem mass

$$m_w = m_r + m_s - m_f = m_s(1 + k_{rs}) - m_l \tag{6.2.13}$$

6.2.6 Height

Niklas and Spatz (2004) derived a relationship between tree height and trunk diameter.

$$H = k_H D^{\phi_H} - c_H \approx k_H D^{2/3} \tag{6.2.14}$$

where $\phi_H = 2/3$.

Typically $c_H << k_H D^{\phi_H}$ so usually c_H can be ignored. Note the value of ϕ_H is usually lower than 2/3. Feldpausch et al. (2011) found it to vary regionally in the range 0.48 to 0.65 with a value globally of 0.53, but the reasons for this are so far poorly understood. The 2/3 exponent appears to represent the hydraulic limit and trees do not always grow to the limit due to many other factors such as altitude, fire, tree density (ie light competition), water availability and storm frequency that can all modify tree allometry.

The constant derived in Niklas and Spatz (2004) is

$$k_H = \frac{1}{(1 + k_{rs}) k_{ms} k_{ml}^{\frac{1}{\phi_{ml}}} k_D^{\frac{1}{\phi_D}}} \tag{6.2.15}$$

6.2.7 Crown area

The crown area is assumed to scale with the square of the tree height. This is because it has been found that the crown radius scales linearly with height (Poorter et al., 2006; West et al., 2009; Enquist et al., 2009).

$$A = k_A H^{\phi_A} \tag{6.2.16}$$

where $\phi_A = 2$.

6.2.8 Leaf area index (LAI)

LAI is the total leaf area above each unit area of the forest floor. For a single tree this is: -

$$L = \frac{m_l}{\sigma_l A} \tag{6.2.17}$$

where m_l is the tree leaf carbon mass and σ_l is the specific leaf carbon density and A the crown area of the tree.

6.2.9 Carbon mass density

This is the carbon density of a tree averaged over its canopy area

$$C = \frac{m}{A} \tag{6.2.18}$$

where C is the tree carbon mass and A the tree crown area.

6.2.10 Basal area

Basal area is the cross-sectional area of the trunk measured at breast height.

$$B = \frac{\pi D^2}{4} \tag{6.2.19}$$

where D is the tree trunk diameter.

6.2.11 Allometry Parameters

A set of parameter values is given in Table 6.2. The values are based on those in Niklas and Spatz (2004) and are used to represent a generic tree type. When RED

is extended to include multiple Plant Functional Types (PFTs) then parameter values will be defined for each PFT based on observational data sets.

Table 6.2: Allometry parameter values based on Niklas and Spatz (2004)

Parameter	Value	Unit
k_{ml}	0.137	$\text{kg}^{1/4}$
k_D	0.085	$\text{m kg}^{-1/2}$
k_{rs}	0.423	-
k_{ms}	202.3	kg m^{-3}
k_A	0.167	-
ϕ_{ml}	$\frac{3}{4}$	-
ϕ_D	$\frac{1}{2}$	-
ϕ_H	$\frac{2}{3}$	-
ϕ_A	2	-

6.3 Growth Rate

The growth rate of a tree is related to the Net Primary Productivity (NPP) Π, which is the net fixation of CO_2 via photosynthesis, and the effect of loss of leaves, roots, and twigs called litter Λ_l. The carbon density growth rate is simply the NPP minus the litter.

$$\frac{\partial C}{\partial t} = \Pi(1 - f_R) - \Lambda_l \tag{6.3.20}$$

where f_R is the fraction of NPP allocated to reproduction.

So the growth rate in terms of mass is

$$\frac{\partial m}{\partial t} = \frac{\partial m}{\partial C}\frac{\partial C}{\partial t} = \frac{\partial m}{\partial C}\Big(f_l(m)\Pi(1 - f_R) - \Lambda_l\Big) \tag{6.3.21}$$

where $f_l(m)$ is the shading term representing the fraction of light lost due to shading through the canopy. Note that when carbon balance is negative the growth rate

is not allowed to go below zero and instead the mortality is increased (see section 6.4.1).

6.3.1 Net Primary Productivity

The Net Primary Productivity (NPP) is defined as the Gross Primary Productivity(GPP) Π_G minus the plant respiration R_p: -

$$\Pi = \Pi_G - R_p \tag{6.3.22}$$

For the purposes of this study, photosynthesis is assumed to follow a "Big Leaf" canopy model, with leaf nitrogen concentration scaling with light (Cox et al., 1998).

$$\Pi_G = \Pi_{G_{TOP}} \frac{f_{PAR}}{k} \tag{6.3.23}$$

and

$$R_p = R_{pm} + R_{pg} \tag{6.3.24}$$

where $\Pi_{G_{TOP}}$ is the maximum GPP (at the top of the canopy), f_{PAR} the fraction of photosynthetically active radiation, R_{pm} the maintenance respiration and R_{pg} the growth respiration.

The growth respiration is assumed to be a fixed fraction r_g (growth respiration coefficient) of the GPP minus maintenance respiration (Cox, 2001), thus: -

$$R_{pg} = r_g \left\{\Pi_G - R_{pm}\right\} \tag{6.3.25}$$

So the NPP is then

$$\Pi = (1 - r_g) \left[\Pi_G - R_{pm}\right] \tag{6.3.26}$$

The maintenance respiration represents the CO_2 lost by the vegetation as it burns stored chemical energy to maintain its tissues. The maintenance respiration term is a combination of respiration of leaves, fine roots and woody (stem and coarse roots) components.

Plant respiration is modelled in a similar way to TRIFFID. For more details see Appendix E

$$R_{pm} = R_d \left(1 + \left(\frac{\mu_{rl} m_f + a_{ws} \mu_{sl} m_w}{m_l}\right)\right) \frac{f_{PAR}}{k} \tag{6.3.27}$$

In Figure 6.3 the variation in GPP with size can be seen which is predominantly due to the fact that the LAI changes as a function of crown area and leaf mass (see equation 6.2.17).

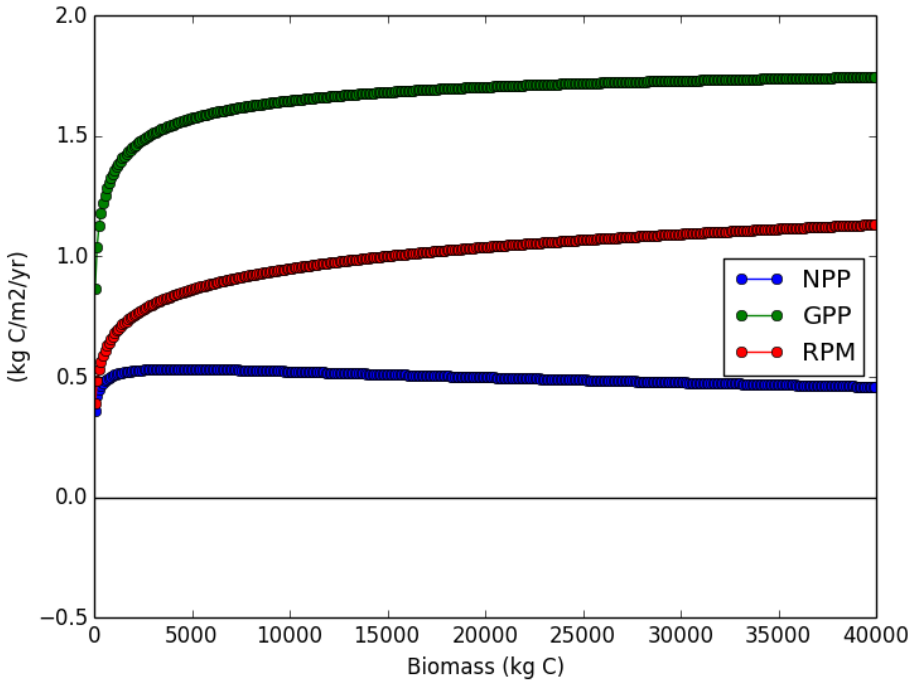

Figure 6.3: Shows the GPP, NPP and respiration as a function of class size (carbon mass) for $\Pi_{G_{TOP}} = 0.9$ kg C m^{-2} yr^{-1}.

6.3.2 Litter

The litterfall is defined as: -

$$\Lambda_l = \lambda_l m_l + \lambda_r m_r + \lambda_w m_w \tag{6.3.28}$$

where m_l, m_r and m_w are the carbon masses of leaf, fine root and wood and λ_l, λ_r and λ_w are constants with units of year^{-1}.

6.3.3 Shading

Smaller trees are shaded by larger ones, and reduce the light available to trees or branches below. Models of a whole canopy suggest that light reaching the forest floor is an exponential function of the leaf area index (LAI) above (Beer-Lambert Law, see Monsi and Saeki (1953) and Hirose (2005)). In RED the canopy is split up into size classes where each class shades smaller size classes. Each tree size class is modelled as a canopy following the Beer-Lambert law but where the amount of light reaching the top of each size class is reduced by shading from larger classes.

RED does not explicitly model spatial distribution, so some way is needed to calculate how much light reaches a particular size class to know how much the growth rate of that size class is suppressed by shading.

Two opposing limiting assumptions for the overlap of the canopy are minimum overlap (i.e. trees grow in gaps wherever possible) or that trees are randomly arranged (i.e. trees always partly overlap). It is likely that neither assumption is completely true and real forests will have overlaps that are between the two.

Random Overlap Shading

RED uses random overlap shading as this is very simple conceptually and does not have the complexity of keeping record of the shaded and unshaded fraction of each class. It also does not have any problem with keeping track of gap formation due to mortality, which could be an issue for any shading scheme that tries to explicitly account for how much of size class is shaded and how much is unshaded or partly shaded. This latter issue is particularly a problem for a minimum overlap shading scheme.

The amount of light that is transmitted through both the vegetated and unvegetated fraction of the class above is calculated and then it is assumed the light level reaching the next class below is the mean of the shaded and unshaded light levels.

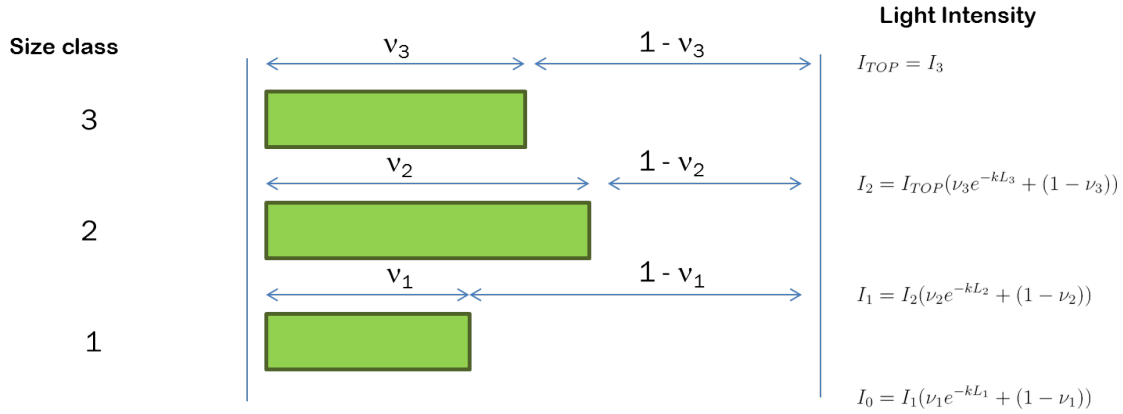

Figure 6.4: Shows the shading in the model. Each level represents a size class, which has a fractional coverage ν_j of the grid-box area. Each class has LAI L_j and is assumed to absorb in accordance with Beer's law. The light reaching the class below is assumed to be the mean of the light getting through the vegetated and unvegetated fractions.

The fraction of light incident on the canopy reaching the top of class j

$$f_{lj} = \prod_{k>j}^{n} (1 - f_{PAR,k}\,\nu_k) \tag{6.3.29}$$

where ν_j is the fraction of area covered by class j

This does have the drawback that there is always some overlap (and hence shading) even in a sparsely vegetated area, this could have a slight impact on regrowth rates as small trees will lose some light even when the canopy is not yet closed. So this model is less applicable to semi-arid or dry regions. This effect should be small though and this shading scheme has the advantage of modelling the dominant mechanism of competition while remaining mathematically simple.

Another simplification is that RED does not currently model the overlapping (or co-competition) of tree crowns, so the crown is effectively modelled as an infinitely thin disc of leaves with corresponding LAI.

The latest version of JULES (Clark et al., 2011), includes an advanced shading model that includes the effects of changing sun angle and also diffuse lighting and scattered direct lighting in a multi-layer canopy model (Mercado et al., 2007; Dai et al., 2004). This model could be adapted in future to RED, with the layers replaced by RED size classes.

6.4 Mortality

Tree mortality is due to several causes including senescence, competitive suppression (shading and crowding) and disturbance (fire, storms etc).

For simplicity at this stage, the mortality term γ in RED is assumed to be a constant independent of tree-mass and currently does not include disturbance or direct competitive effects. This is the simplest way of modelling mortality and Kohyama (1991) found in a similar model that explicitly including the effect of competitive suppression in the mortality term (i.e. density dependence) was very much secondary to growth suppression in determining the stationary size distribution.

Coomes and Allen (2007) suggests that the mortality of a forest with size follows a u-shape with high mortality at the largest and smallest tree sizes and lowest mortality in the middle. This comes about due to increasing age related mortality with size combined with higher mortality of small trees due to shading and competition for space.

This suggests that the mortality term may, in a future version of RED, represent senescence better if the mortality term is age related. As RED has no direct modelling of age then the best proxy for age is size and so the mortality term could be modified in future to be an increasing function of size.

6.4.1 Negative Carbon Balance

What if the carbon balance of a particular mass class is negative (i.e. $\frac{\partial m_j}{\partial t} < 0$)? To conserve carbon either trees must shrink (which is unrealistic), or some trees in the mass class must die (through carbon balance mortality). RED assumes the latter.

The additional mortality from negative carbon balance is assumed to be proportional to the negative growth rate:-

$$death_j = \begin{cases} -n_j\gamma & \text{For } \frac{\partial m_j}{\partial t} \geq 0 \\ -n_j\left[\gamma - \frac{1}{\Delta m}\left(\frac{\partial m_j}{\partial t}\right)\right] & \text{For } \frac{\partial m_j}{\partial t} < 0 \end{cases} \tag{6.4.30}$$

This approach was also used by Kohyama (1991), albeit in a different form.

6.5 Recruitment and Seedling Establishment

Recruitment of seedlings is calculated by taking a fraction, f_R, of NPP to represent reproductive activity of the plant and then taking a fraction of this, f_S, to represent the NPP that actually makes it to seedlings. This is suppressed by available space in the lowest mass class by considering how much room is left after the current fractional coverage ν_0 is taken into account and then further suppressed by the shading from above by multiplying by the fraction of light making it through to the forest floor f_{l0}.

$$growin_0 = f_{l0}\left(1-\nu_0\right)\frac{f_R\, f_S\, \Pi_{TOT}}{m_0} \tag{6.5.31}$$

where $nu_0 = n_0 A_0$ is the area coverage of the lowest mass class, f_{l0} the amount of light reaching the forest floor and m_0 the mass of the lowest mass class. The $(1-\nu_0)$ term represents density dependent competition between members of the lowest mass class.

The NPP per tree of each class is calculated as follows

$$\Pi_{TOT,j} = \Pi_j \, n_j \, A_j \tag{6.5.32}$$

Where Π_j is the NPP per unit crown area for a given class from equation 6.3.22, and A_j is the crown area of trees of the class in question. So the total NPP per unit ground area is simply the sum: -

$$\Pi_{TOT} = \sum_{j>0} \Pi_{TOT,j} = \sum_{j>0} \Pi_j \, n_j \, A_j \tag{6.5.33}$$

Model Initialisation

The model can be initialised in several ways: -

1. Initiate the lowest mass class with a tree density that equates to a fractional coverage of 100%. All other mass classes will be set to zero. This represents the forest being started off with a dense crop of seedlings.

2. Prescribe a distribution from the start. If an analytical or approximate solution to RED including shading can be found then we can start the model with little or no spin up. This would be useful in a coupled DGVM.

3. Have seeding from outside the grid-box i.e. migration. In a spatially resolved DGVM then RED would simulate the vegetation in each grid-box and could then model some seeds travelling from grid-box to grid-box. When running RED in a point mode (zero dimensional case as presented here) we could add a fixed term in equation 6.5.31 representing seeding from outside the model area.

Currently we initialise the model using the first method and then run the model to equilibrium.

6.6 Time-step Size Constraints

The model has a stability condition for the time step size based on the mass class width and maximum growth rate. The model can become unstable if any tree can grow by more than one mass class in one time step.

This creates a time step requirement: -

$$\Delta t < \frac{\Delta m}{(\frac{dm}{dt})_{max}} \tag{6.6.34}$$

While the mass class width Δm is defined by the user-defined mass classes, the maximum growth rate $(\frac{dm}{dt})_{max}$ is more complex as it depends on climate conditions. It is therefore important to be aware of the highest possible growth rate when selecting the mass class and timestep sizes. If Δt is constrained by other factors then Δm must instead be changed instead, so the above condition is met.

6.7 Results

6.7.1 Tree PFT Simulations

Figure 6.5 shows the distribution and light availability as a function of mass class for both Broadleaf and Needleleaf PFTs. The two simulations were started with seedlings (lowest mass class) covering the whole area and no other size classes present and then run until the total system biomass reached equilibrium. The parameter set used for these simulations is given in Table 6.3.

The simulation (Figure 6.6) shows a much shorter regrowth time-scale compared to TRIFFID (Figure 6.1) of about 39 years for Broadleaf and 63 years for Needleleaf.

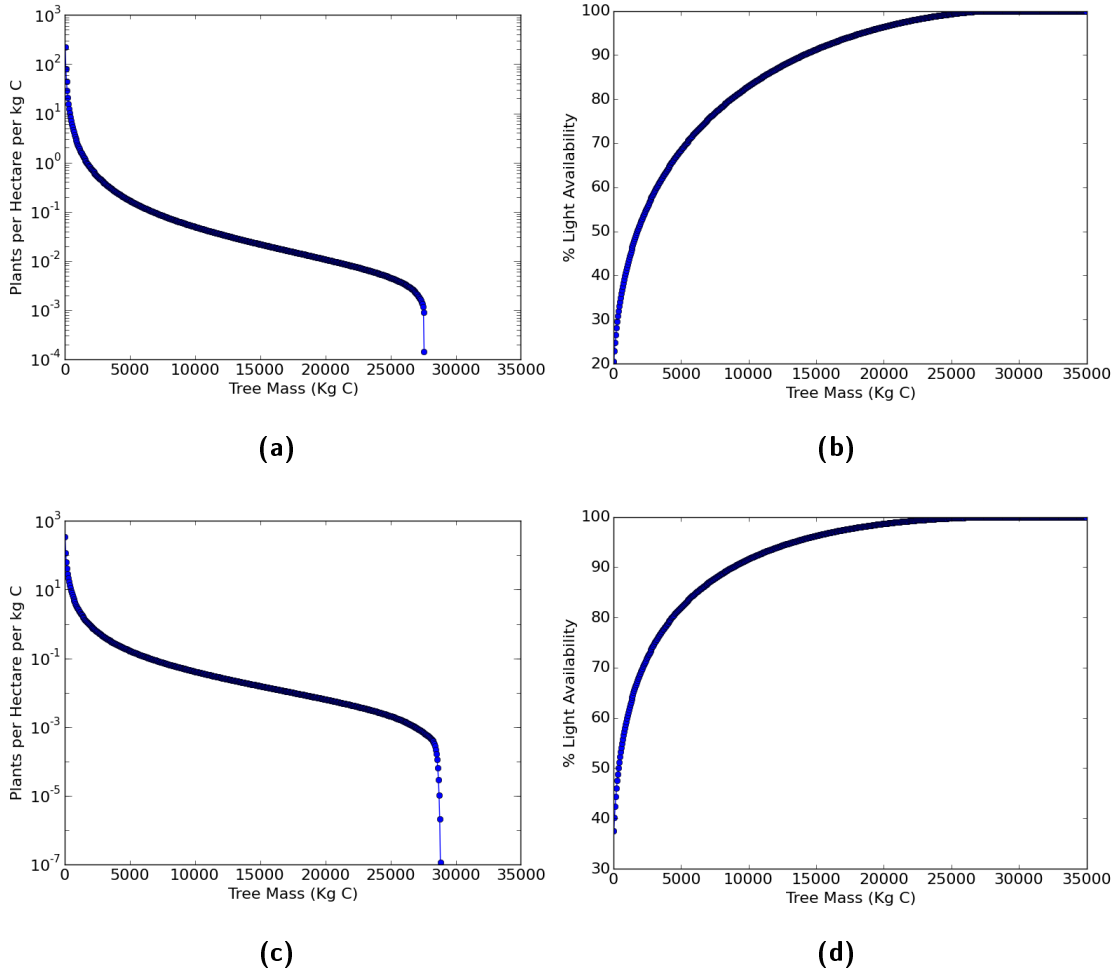

Figure 6.5: Shows a) the mass distribution and b) the light availability for Broadleaf PFT c) mass distribution and d) light availability for Needleleaf PFT

Table 6.3: Parameter values used in Broadleaf and Needleleaf PFT simulations, based on those used in latest version of TRIFFID

Parameter	**Broadleaf**	**Needleleaf**
r_g	0.25	0.25
k_{PAR}	0.5 LAI^{-1}	0.5 LAI^{-1}
γ_l	0.25 yr^{-1}	0.25 yr^{-1}
γ_w	0.01 yr^{-1}	0.01 yr^{-1}
γ_r	0.25 yr^{-1}	0.25 yr^{-1}
n_l	0.04 kg N $(\mathrm{kg\ C})^{-1}$	0.03 kg N $(\mathrm{kg\ C})^{-1}$
R_d	0.1816 kg C m^{-2} yr^{-1}	0.1362 kg C m^{-2} yr^{-1}
μ_{rl}	1.0 kg C m^{-2}	1.0 kg C m^{-2}
μ_{sl}	0.1 kg C m^{-2}	0.1 kg C m^{-2}
a_{ws}	10	10
σ_l	0.0824 kg C m^{-2}	0.2263 kg C m^{-2}
γ	0.01 yr^{-1}	0.01 yr^{-1}
$\Pi_{G_{TOP}}$	0.9 kg C m^{-2} yr^{-1}	0.9 kg C m^{-2} yr^{-1}
m_0	25 kg C	25 kg C
Δm	50 kg C	50 kg C

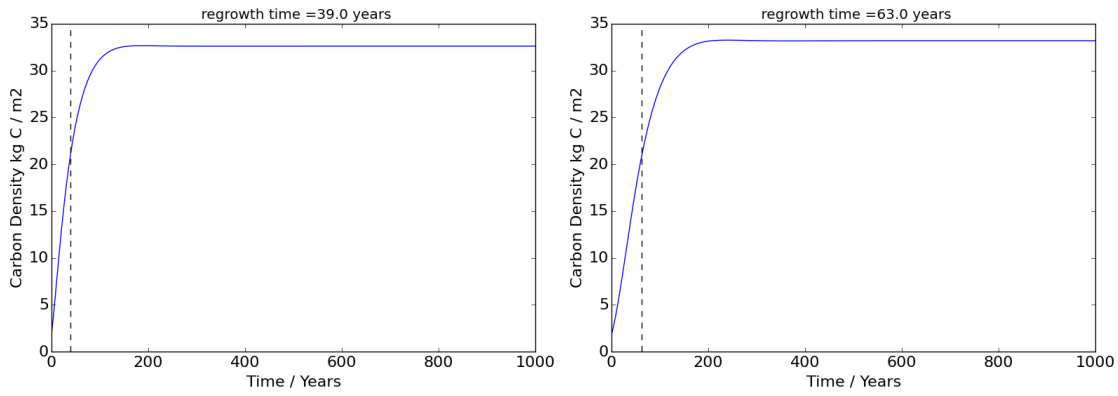

(a) **(b)**

Figure 6.6: Shows the regrowth rate for a) Broadleaf PFT is 39 years and b) Needleleaf PFT is 63 years.

6.7.2 Mortality Parameter

By repeating the Broadleaf simulation for different values of the mortality term it is possible to see the effect this term has on the distribution. Figure 6.7 shows that increasing mortality (shortening lifetime) reduces the number of plants reaching the highest mass classes considerably. Conversely a long lifetime leads to a more even size distribution with more plants reaching the size limits imposed by their GPP, respiration and litter.

This pattern can be explained by the basic theory presented in section 5.2.2 where the z parameter which is proportional to the mortality term γ determines the shape of distribution seen. Shading (that is neglected in our analytical solution) does not change this pattern appreciably.

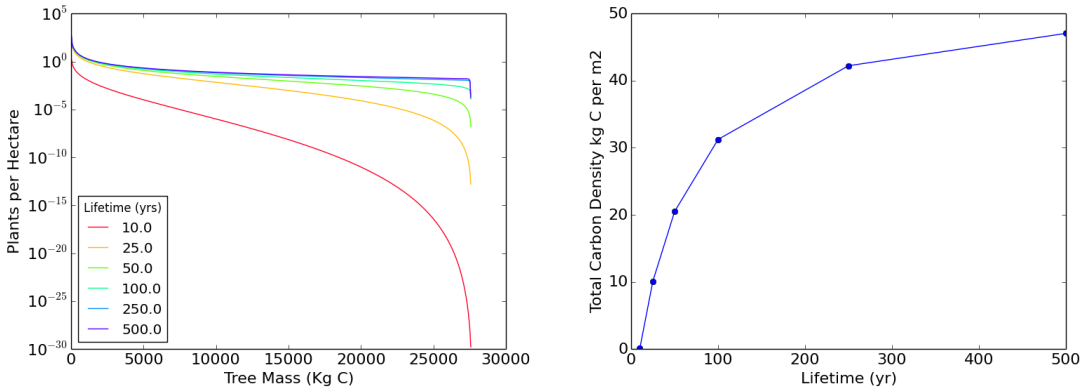

Figure 6.7: Shows the effect of changing the mortality term in RED on a) the size distribution b) the final total biomass.

6.7.3 Self-Thinning

The model does approach the self-thinning limit (Westoby, 1984; Hamilton et al., 1995) if background mortality is excluded, seeding is switched off and the model started with a "pulse" of seedlings (see Figure 6.8). This is done by setting the

mortality term to zero, setting f_R and f_S also to zero and initialising the model with 100% coverage of seedlings in the smallest mass class and all others with zero tree density.

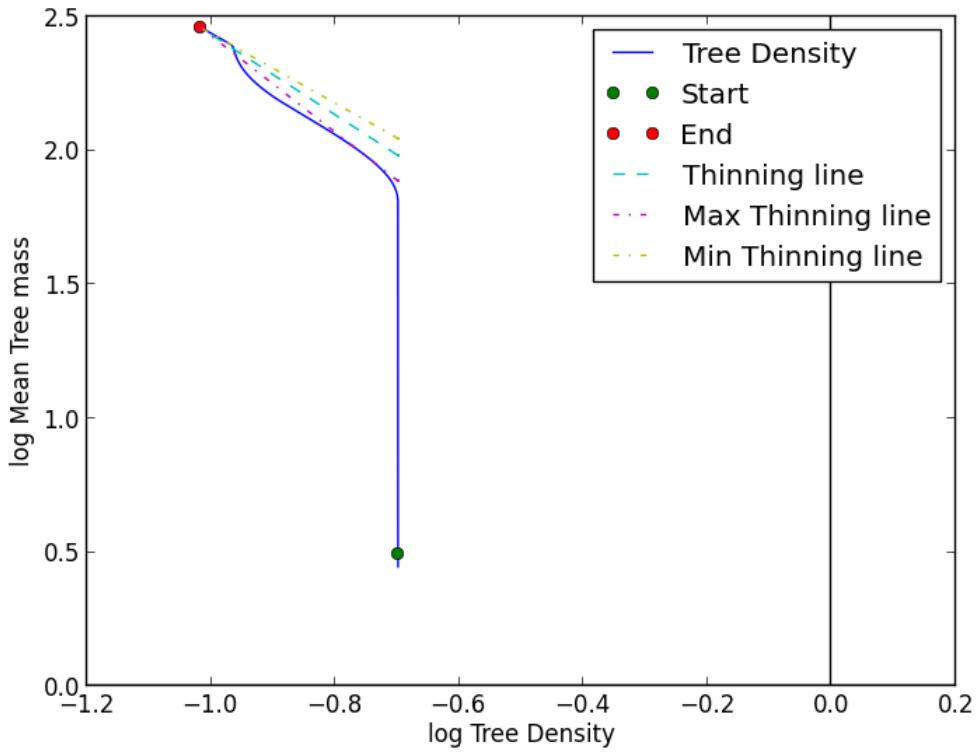

Figure 6.8: Shows the self-thinning trajectory of RED running with no background mortality. The maximum and minimum thinning lines correspond to the expected range of exponent from -1.3 to -1.8 (Lonsdale, 1990).

The self-thinning comes about as the pulse of seedlings grow and the trees in the smaller classes get increasingly shaded until they go into negative carbon balance. If background mortality is non-zero then this will deplete the number of trees over time and the model will evolve to a near horizontal trajectory as the trees stop growing but continue to be lost through the mortality term. So setting the background mortality to zero allows the self-thinning effect to be isolated.

This agrees with the assertion of Hamilton et al. (1995) that self-thinning only exactly follows the -$\frac{3}{2}$ scaling law when competition for light is the only cause of

mortality.

6.8 Proportion of NPP allocated to reproduction

The proportion of NPP going into reproduction is an important determinant of ecosystem behaviour. Resources diverted from growth will limit a plants ability to compete for light but without reproduction the forest would exist for only one generation.

To investigate the effect of this parameter on the behaviour of RED the model was run with a range of values of the proportion of NPP going into reproduction (f_R). To simplify the analysis it was assumed that all the NPP allocated to reproduction is available to new seedlings ($f_S = 1$).

In figure 6.9 the total forest biomass (sum of all mass classes) is plotted as a function of the proportion of NPP allocated to reproduction, for different mean plant lifetimes. The plot shows that there is a peak in biomass with respect to proportion of NPP allocated to reproduction. This peak occurs at lower reproductive NPP proportion for longer lifetimes, because a slow growing forest with low mortality will need less seedlings coming through to replace those lost to mortality.

If this plot is repeated for different measures of forest function such as total forest NPP, cumulative fractional coverage and the forest floor light level (Figure 6.10) a similar pattern is seen with an optimum value of f_R for each measure.

The optimum value of NPP to reproduction is though different for each measure as can be seen in Figure 6.11.

Malhi et al. (2011) suggests reproductive NPP is typically between 5–15% of canopy NPP for tropical forests. This model is showing (Figure 6.11) that the optima occur in this range for some lifetime cases (40-180 years for biomass maxima, 240-640 years for fractional coverage maxima, 60-320 for NPP maxima and 180-640 years for forest floor light minima). This suggests that biomass is least likely variable

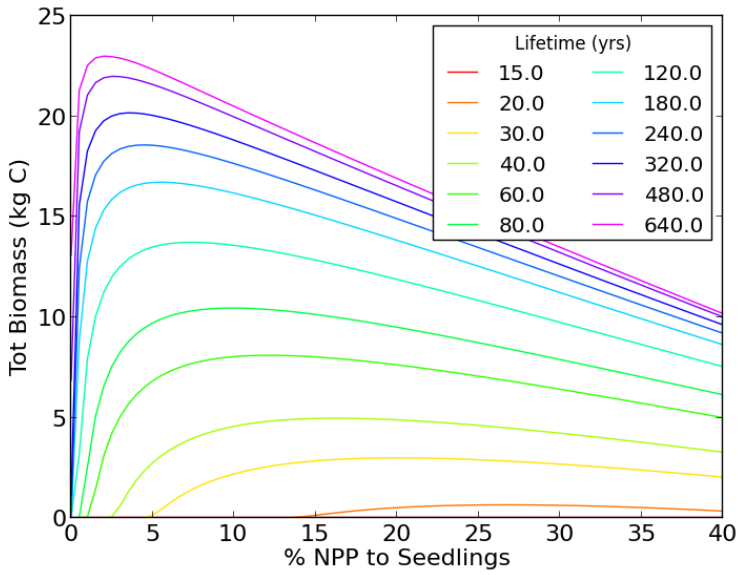

Figure 6.9: Total Forest Biomass as a function of proportion of NPP allocated to reproduction for different lifetimes. Clearly shows that there is an optimum proportion to reproduction for a given tree lifetime/mortality. As the lifetime of the trees increase (ie lower mortality rate) the smaller the optimum proportion of NPP to reproduction and the higher the biomass peak.

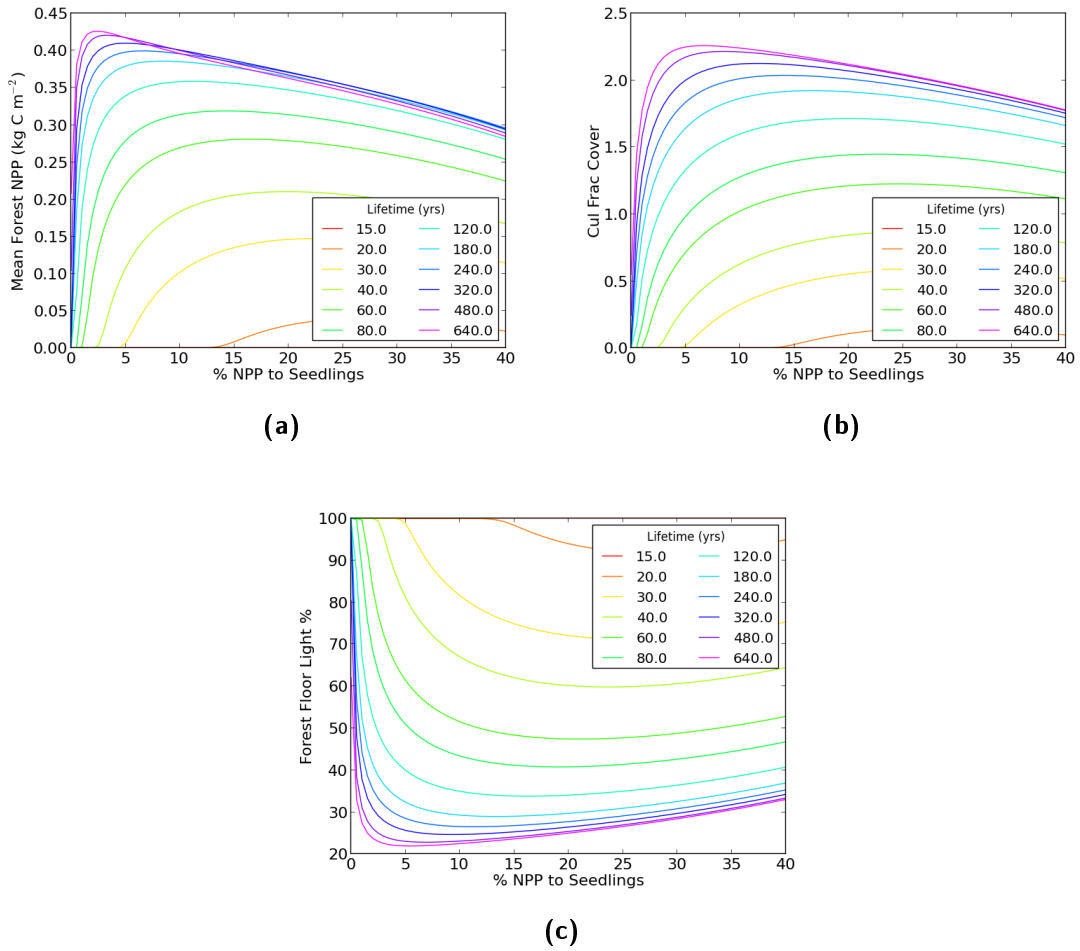

Figure 6.10: a) Total forest NPP as a function of proportion of NPP allocated to reproduction for different lifetimes. b) Cumulative fractional coverage as a function of proportion of NPP allocated to reproduction for different lifetimes. c) The portion of light reaching the forest floor as a function of proportion of NPP allocated to reproduction for different lifetimes. All these optima occurs at different NPP values.

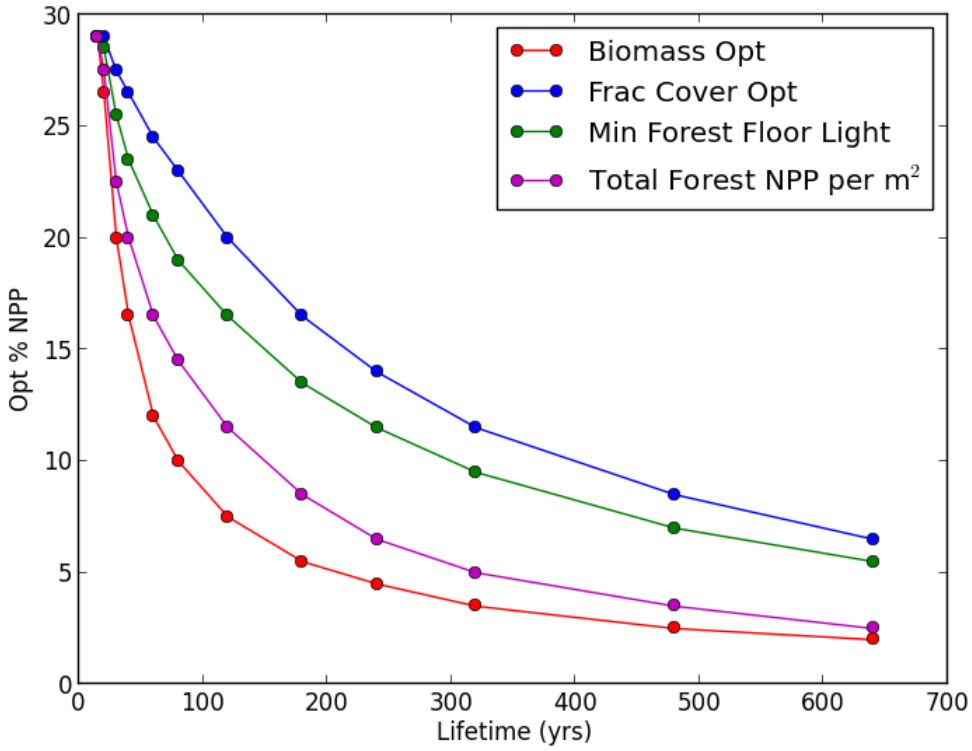

Figure 6.11: Shows the optimum proportion of NPP allocated to reproduction in terms of biomass, total NPP, forest floor light level and cumulative fractional coverage.

for reproduction optimisation as tropical trees can be long-lived (Chambers et al. (1998) suggest maybe as much as 1000 years for the oldest trees in the Amazon), and suggests that it is competition for light (fractional coverage or forest floor light) that could be determining the optimum proportion of NPP to reproduction for trees of a given lifetime. Investigating this further could be an interesting avenue of future work.

6.9 Discussion

This study presents a new DGVM called RED, that is not as complex as gap and individual based models, but includes size dependence in the form of mass classes. The model is based on the principle of continuity, where the number of individuals in each mass class is governed by the number growing in from the class below, minus the number growing out, or lost due to mortality.

The RED model is an important step forward compared to previous DGVMs (such as TRIFFID) as the size dependence through mass classes allows the differing growth rates with tree size to be modelled. The inclusion of the forest demography, through size classes, means the regrowth time-scales are therefore better represented compared to TRIFFID. RED also has benefits in terms of simplicity compared to many gap and individual based DGVMs and so should be expected to require less simulation overhead to execute.

This study has also for the first time shown that there is an optimum proportion of NPP allocated to reproduction. The optimum depends on lifetime/mortality with forests with lower mortality expending much less NPP on reproduction than those with higher mortality.

6.10 Full Mathematical Description of Discretised Model

$$\frac{\partial n_j}{\partial t} = growout_j + growin_j + death_j \tag{6.10.35}$$

$$growout_j = \begin{cases} \frac{-1}{\Delta m} n_j \frac{\partial m_j}{\partial t} & \text{For } \frac{\partial m_j}{\partial t} \geq 0 \\ 0 & \text{For } \frac{\partial m_j}{\partial t} < 0 \end{cases} \tag{6.10.36}$$

$$growin_j = \begin{cases} f_{l0}\left(1-\nu_0\right) \frac{f_R f_S \Pi_{TOT}}{m_0} & j = 0 \\ -growout_{j-1} & \text{For } j > 0 \end{cases} \tag{6.10.37}$$

$$death_j = \begin{cases} -n_j \gamma & \text{For } \frac{\partial m_j}{\partial t} \geq 0 \\ -n_j \left[\gamma - \frac{1}{\Delta m}\left(\frac{\partial m_j}{\partial t}\right)\right] & \text{For } \frac{\partial m_j}{\partial t} < 0 \end{cases} \tag{6.10.38}$$

Chapter 7

Conclusions

This chapter provides an overview of the main findings presented in this PhD thesis and discusses how the work may be extended by future research.

7.1 Overview

Chapter 1 summarised the current understanding of biodiversity and stability in ecological models. While trade-offs, complexity, niches, and neutral theory all seem to have a role to play in creating the diversity we see, there is no definitive theoretical understanding of diversity. Stability also has no single definition, so for the purposes of this thesis the principle of resilience is used - which is how far a system characteristic such as biomass or net primary productivity (NPP) changes as a system is undergoing an environmental change.

The development of Dynamic Global Vegetation Models (DGVMs) was also discussed, showing how the models have increased in complexity but that current models either do not model differing tree sizes and therefore struggle to model size-dependent aspects of land use and land cover change and regrowth or solve this in ways that make the models complex and hard to maintain.

Building on the Lotka-Volterra based equations used in the TRIFFID DGVM,

chapter 2 models the effect of increasing temperature on the NPP of a system which consists of species with a range of temperature optima. The system was initially in a equilibrium state with the starting temperature, but once the temperature started increasing linearly underwent transient oscillations in NPP until settling down to a steady 'pseudo-equilibrium' level. Introducing a smoother non-linear temperature increase that has heat capacity (analogous to the Earth undergoing climate change) the transient oscillations in the NPP are reduced suggesting the transient is a result of the system being pushed out of its initial steady state when the temperature increase suddenly starts. Changing the equations to use competition coefficients broke conservation of both individual species and total coverage, suggesting the equations are not a useful way to model diversity and so cannot be used to study the effect of diversity on the systems resilience to change.

To provide a clearer mechanism of competition chapter 3 used a single resource model and stochastic temperature "noise" to successfully model diversity (again using a system with a range of temperature optima) and found diversity varied with the choice of noise parameters. The relationship between noise parameters and diversity was found to be complex (see Figures 3.14, 3.15, 3.16 in section 3.5.3).

To overcome the problems of generating diversity, chapter 4 introduced trait diffusion to a non-stochastic version of the single resource model, whereby biomass diffuses to adjacent traits due to genetic mutation. This model successfully modelled coexistence and found that a sudden collapse in NPP occurred if the rate of temperature change exceeded a critical value (see Figure 4.15 in Section 4.3). The critical rate was found to increase with increasing initial diversity, implying a more diverse system a higher resilience to environmental change.

Chapter 5 presented a simple model of vegetation demography based on a continuity equation that models size distribution of plants. This chapter therefore deals with modelling of size diversity. Analytical solutions were found for the case where the growth rate was time independent and was a simple function of size. Two useful solutions were found for the case where plant growth rate was (i) a power law of

mass and (ii) the case where it was an inverted quadratic. The power law solution can be reduced to to the trajectory an even aged stand will follow during self-thinning. The quadratic solution reproduces the rotated sigmoid size distribution often seen in observations if the death rate is higher than the maximum growth rate slope, otherwise the solution will be a "U-shape" distribution.

Chapter 6 builds on the previous chapter by expanding the model into the basis for a DGVM called the Robust Ecosystem Demography (RED). Plant growth rate as a function of plant mass is based-on equations used in JULES for NPP, respiration and litter. Simple random overlap shading is added to simulate one-sided competition for light and a fraction of total system NPP is allocated to recruitment, which is further limited by forest floor light and space availability. The inclusion of size classes allowed better representation of regrowth time-scales compared to TRIFFID. It was also found that there is an optimum proportion of NPP to allocate to reproduction (or "recruitment") in order to maximise properties such as biomass and total ecosystem NPP. This optimum depends on mortality, with lower mortality plants expected to devote a smaller fraction of NPP to reproduction.

7.2 Future Work

There are a number of different areas of possible future research that could build on the work in this thesis. The stochastic resource model in chapter 3 would particularly benefit from a deeper mathematical understanding of how diversity varies with the nature of the environmental noise. It would also be interesting to compare the noise seen in real temperature observations to see if there is any correlation between real world temperature variability and diversity.

The Trait Diffusion model would also benefit from a study of how the trait diffusion parameter relates to real processes such as genetic variation (mutation etc) between generations. Another avenue of investigation is to compare the trait model to an individual based evolution model where new individuals appear with traits that are

randomly mutated from those already in the system. It would be useful validation of the Trait model to perform an in-depth study of plant traits to see if there is a link between the range of environmental traits in an ecosystem and the range of the environmental variable. For example, do a wider range of plant temperature traits occur in ecosystems that experience greater variations in temperature than those which experience smaller temperature variations?

The work of chapter 5, would most usefully be extended by looking for more complex functions of size for the time independent growth rate, that are still simple enough to allow an analytical solution of the continuity equation. In particular, it would be useful to look for a polynomial function that better replicates the asymmetric growth rate curves seen in observations.

The RED model presented in chapter 6 is the area of the thesis with the most potential for future work. The most pressing extension is to add multiple Plant Functional Types (PFTs), and competition between these PFTs. This may need RED to be fully coupled into the UK land surface model JULES for a more complete comparison. An important validation would be to compare the size distributions produced by RED to real observations of mature forest. One challenge here is obtaining a size distribution that uses tree mass as the size variable or that can easily be converted to tree mass. It is also necessary to tune the allometry parameters for every PFT. Currently the mortality rate in RED is constant for all size classes. This is a crude simplifying assumption which needs to be improved by looking at observational data to infer size-dependent mortality. A particular issue here will be to separate the age/size related mortality from the competition related mortality, as these are dealt with differently in RED.

The final area of future work is better understanding the optimum proportions of NPP into reproduction/recruitment as currently what determines the optimum nor why the optima differ for different variables is fully understood.

Appendices

Appendix A

Lotka-Volterra Competition Coefficients

It is a standard result of Lotka-Volterra competition theory uses competition coefficients to model the strength of competition between individuals both of the same species and other species.

A.1 2 Species Theory

The effect of other species on a particular species is modified by using competition coefficients c and k. If both c and k are set to 1 then this is equivalent to the original model. To get coexistence then c and k must not be equal to each other.

So equation 2.1.2 is modified to give: -

$$\begin{aligned} \frac{d\nu_1}{dt} &= a_1 \left(\Gamma_1(\theta)(1 - k\nu_1 - c\nu_2) - 1\right) \\ \frac{d\nu_2}{dt} &= a_2 \left(\Gamma_2(\theta)(1 - c\nu_1 - k\nu_2) - 1\right) \end{aligned} \tag{A.1.1}$$

For there to be steady-state with both species having non-zero coverage then we need to solve the following

$$\begin{aligned}\Gamma_1(\theta)(1-k\nu_1-c\nu_2)-1=0\\ \Gamma_2(\theta)(1-c\nu_1-k\nu_2)-1=0\end{aligned} \tag{A.1.2}$$

Then we get the equations of the null-clines in phase space

$$\begin{aligned}\nu_1=\frac{1-\frac{1}{\Gamma_1(\theta)}-c\nu_2}{k}\\ \nu_2=\frac{1-\frac{1}{\Gamma_2(\theta)}-c\nu_1}{k}\end{aligned} \tag{A.1.3}$$

From the null-clines the steady-state coverages can be obtained in terms of growth, death and competition parameters.

$$\begin{aligned}\nu_1=\frac{k\left(1-\frac{1}{\Gamma_1(\theta)}\right)-c\left(1-\frac{1}{\Gamma_2(\theta)}\right)}{k^2-c^2}\\ \nu_2=\frac{k\left(1-\frac{1}{\Gamma_2(\theta)}\right)-c\left(1-\frac{1}{\Gamma_1(\theta)}\right)}{k^2-c^2}\end{aligned} \tag{A.1.4}$$

This leads to the conditions for stable equilibrium

$$\frac{k}{c}>\begin{cases}\dfrac{1-\frac{1}{\Gamma_1}}{1-\frac{1}{\Gamma_2}}, & \text{For } \Gamma_1>\Gamma_2\\ \dfrac{1-\frac{1}{\Gamma_2}}{1-\frac{1}{\Gamma_1}}, & \text{For } \Gamma_2>\Gamma_1\end{cases} \tag{A.1.5}$$

with the implied condition $k \neq c$.

A.2 Multiple Species Theory

For an n species system the equations are

$$\frac{d\nu_i}{d\tau} = a_i \left[\left(1 - k\nu_i - c \sum_{j \neq i} \nu_j \right) \Gamma_i(\theta) - 1 \right] \tag{A.2.6}$$

The non-trivial steady-state solution where all species have non-zero coverage is then

$$\left[\left(1 - k\nu_i - c \sum_{j \neq i} \nu_j \right) \Gamma_i(\theta) - 1 \right] = 0 \tag{A.2.7}$$

this can be reformulated into matrix notation

$$\begin{pmatrix} \Gamma_1 k & \Gamma_1 c & \cdots & \Gamma_1 c \\ \Gamma_2 c & \Gamma_2 k & \cdots & \Gamma_2 c \\ \vdots & \vdots & \ddots & \vdots \\ \Gamma_n c & \Gamma_n c & \cdots & \Gamma_n k \end{pmatrix} \begin{pmatrix} \nu_1 \\ \nu_2 \\ \vdots \\ \nu_n \end{pmatrix} = \begin{pmatrix} \Gamma_1 - 1 \\ \Gamma_2 - 1 \\ \vdots \\ \Gamma_n - 1 \end{pmatrix} \tag{A.2.8}$$

Inverting the matrix allows the solution for the species coverages to be found

$$\begin{pmatrix} \nu_1 \\ \nu_2 \\ \vdots \\ \nu_n \end{pmatrix} = \frac{1}{(k + (n-1)c)(k-c)} \begin{pmatrix} \frac{k+(n-2)c}{\Gamma_1} & \frac{-c}{\Gamma_2} & \cdots & \frac{-c}{\Gamma_n} \\ \frac{-c}{\Gamma_1} & \frac{k+(n-2)c}{\Gamma_2} & \cdots & \frac{-c}{\Gamma_n} \\ \vdots & \vdots & \ddots & \vdots \\ \frac{-c}{\Gamma_1} & \frac{-c}{\Gamma_2} & \cdots & \frac{k+(n-2)c}{\Gamma_n} \end{pmatrix} \begin{pmatrix} \Gamma_1 - 1 \\ \Gamma_2 - 1 \\ \vdots \\ \Gamma_n - 1 \end{pmatrix} \tag{A.2.9}$$

This gives the ith species coverage

$$\nu_i = \frac{1}{(k + (n-1)c)(k-c)} \left[(k + (n-2)c) \left(1 - \frac{1}{\Gamma_i} \right) - c \sum_{j \neq i} \left(1 - \frac{1}{\Gamma_j} \right) \right] \tag{A.2.10}$$

It can clearly be seen that there is no multiple species solution if k = c and that this case reverts to a single species competitively excluding all others. It is also a well known result of Lotka-Volterra competition models that the solution is only stable if the intra-species competition is stronger than the interspecies competition

(k > c) (Silvertown, 1987; May and McLean, 2007). While the solution still exists for k < c, the steady-state is an unstable saddle point.

One thing to note is that the above solution only applies for species who have a positive fractional coverage as it ignores the a_i term in Equation 2.5.22.

Any species for which

$$\left(1 - k\nu_i - c\sum_{j\neq i}\nu_j\right)\Gamma_i(\theta) - 1 < 0 \tag{A.2.11}$$

must be eliminated and the solution equation 2.5.23 written only in terms of the species which can maintain a positive coverage. The system would be reduced by the number of species which have zero coverage.

For example a three species system which species 3 has too small a growth rate would result in the coexistence of just species 1 and 2 with the solution

$$\nu_1 = \frac{1}{(k+c)(k-c)}\left[k\left(1-\frac{1}{\Gamma_1}\right) - c\left(1-\frac{1}{\Gamma_2}\right)\right] \tag{A.2.12}$$

$$\nu_2 = \frac{1}{(k+c)(k-c)}\left[k\left(1-\frac{1}{\Gamma_2}\right) - c\left(1-\frac{1}{\Gamma_1}\right)\right] \tag{A.2.13}$$

$$\nu_3 = 0 \tag{A.2.14}$$

If this process is not followed the solution calculated analytically with Equation 2.5.23 would not match that found numerically using Equation 2.5.22, as the analytical solution would have some species with negative coverage, whereas the numerical solution would have these species with zero coverage.

A.3 Constraints

Coverage needs to be constrained to be between 0 and 1 both for each individual coverage and the total coverage must also be in the same range. Real forests can

have overlapping coverage but this can only meaningfully be included where the size distribution of the forest is also modelled.

So

$$0 \geq \nu_i \geq 1 \tag{A.3.15}$$

$$0 \geq \nu_{tot} \geq 1 \tag{A.3.16}$$

The total coverage is

$$\nu_{tot} = \sum_i \nu_i = \frac{1}{k + (n-1)c} \sum_i \left(1 - \frac{1}{\Gamma_i}\right) \tag{A.3.17}$$

So the constraint for the total coverage is

$$0 \geq \frac{1}{k + (n-1)c} \sum_i \left(1 - \frac{1}{\Gamma_i}\right) \geq 1 \tag{A.3.18}$$

These constraints are very difficult to enforce in any simple way that guarantees both will always be met regardless of the growth rate and competition coefficient values. This means that conservation of coverage can be broken as the competition coefficients mean the term multiplying the growth term Γ is no longer the bare soil and it is this that allows the original model to conserve the fractional area.

Appendix B

Resource Model Stability Analysis

B.1 Linear Stability Analysis - One Species System with Fixed Temperature

The equations for this system are: -

$$\begin{aligned} f_r = \frac{dr}{dt} &= a(1-r) - \frac{r}{r+k} g\, b \\ f_b = \frac{db}{dt} &= b\left[g\,\frac{r}{r+k} - \gamma\right] \end{aligned} \tag{B.1.1}$$

This system has 2 equilibria (r,b) = (1,0) and (r,b) = (r^*,b^*), with $r^* = \dfrac{kd}{g-\gamma}$ and $b^* = \dfrac{a}{d}(1-r^*)$. The Jacobian for this system is: -

$$J = \begin{pmatrix} \dfrac{\partial f_r}{\partial r} & \dfrac{\partial f_r}{\partial b} \\ \dfrac{\partial f_b}{\partial r} & \dfrac{\partial f_b}{\partial b} \end{pmatrix} = \begin{pmatrix} -a - gb\,\dfrac{k}{(r+k)^2} & -g\,\dfrac{r}{(r+k)} \\ gb\,\dfrac{k}{(r+k)^2} & g\,\dfrac{r}{(r+k)} - \gamma \end{pmatrix} \tag{B.1.2}$$

B.1.1 (r,b) = (1,0) Equilibrium

For this equilibrium the Jacobian becomes: -

$$J = \begin{pmatrix} -a & \dfrac{-g}{(1+k)} \\ 0 & \dfrac{g}{(1+k)} - \gamma \end{pmatrix} \tag{B.1.3}$$

We then can find the eigenvalues via: -

$$\begin{vmatrix} -a-\lambda & \dfrac{-g}{(1+k)} \\ 0 & \dfrac{g}{(1+k)} - \gamma - \lambda \end{vmatrix} = 0 \tag{B.1.4}$$

Giving: -

$$\lambda_1 = -a,\ \lambda_2 = \frac{g}{(1+k)} - \gamma \tag{B.1.5}$$

λ_1 is always stable as all quantities a, g, k and γ are always positive by definition. λ_2 can be rearranged in terms of r^* so that $\lambda_2 = \dfrac{(g-\gamma)(1-r^*)}{(1+k)}$. λ_2 is then negative when $g < \gamma(1+k)$ ($r^* > 1$ or $r^* < 0$), noting that when $g < \gamma$ then $r^* < 0$. So this equilibrium is either a sink or unstable saddle, depending on the parameters g, γ and k.

B.1.2 (r,b) = (r^*,b^*) Equilibrium

For this equilibrium the Jacobian becomes: -

$$J = \begin{pmatrix} -a - gb^* \dfrac{k}{(r^*+k)^2} & -\gamma \\ gb^* \dfrac{k}{(r^*+k)^2} & 0 \end{pmatrix} \tag{B.1.6}$$

We then can find the eigenvalues via: -

$$\begin{vmatrix} -a - gb^* \dfrac{k}{(r^*+k)^2} - \lambda & -\gamma \\ gb^* \dfrac{k}{(r^*+k)^2} & -\lambda \end{vmatrix} = 0 \tag{B.1.7}$$

This gives a characteristic equation for lambda: -

$$\lambda^2 + [a+Z]\lambda + Z\gamma = 0 \tag{B.1.8}$$

where

$$Z = gb^* \frac{k}{(r^*+k)^2} = \frac{agk(1-r^*)}{\gamma(r^*+k)^2} = \frac{a}{gk\gamma}(g-\gamma)(g-\gamma(1+k)) \tag{B.1.9}$$

So λ is

$$\lambda = \frac{-(a+Z) \pm \sqrt{(a+Z)^2 - 4Z\gamma}}{2} \tag{B.1.10}$$

So both values of λ are negative (and equilibrium a stable sink) if $Z > 0$ and this is true if $r^* < 1$. This can be seen in equation for Z (Equation B.1.9). If not this equilibrium is an unstable saddle point. Even the equilibrium appears to be a stable sink if $R^* < 0$, note that a negative resource level can never be reached as $\frac{dr}{dt} = a$ at r=0.

It is also important to notice that the same conditions leading this equilibrium to be stable or not are the reverse of the conditions for the previous trivial equilibrium (r,b)=(1,0). So only one is ever stable under any set of parameters.

B.2 Linear Stability Analysis - Two Species System with Fixed Temperature

This system has two competing species who interact only through their competition for the one limiting resource.

$$
\begin{aligned}
f_r &= \frac{dr}{dt} = a(1-r) - \frac{r}{r+k}(g_1\, b_1 + g_2\, b_2) \\
f_{b1} &= \frac{db_1}{dt} = b_1 \left[g_1 \frac{r}{r+k} - \gamma \right] \\
f_{b2} &= \frac{db_2}{dt} = b_2 \left[g_2 \frac{r}{r+k} - \gamma \right]
\end{aligned}
\tag{B.2.1}
$$

This system has 3 equilibria (r,b1,b2) = (1,0,0), (r,b1,b2) = (r_1^*,b_1^*,0) and (r,b1,b2) = (r_2^*,0,b_2^*), with $r_i^* = \dfrac{kd}{g_i - \gamma}$ and $b_i^* = \dfrac{a}{d}(1 - r_i^*)$. The Jacobian for this system is: -

$$
\begin{aligned}
J &= \begin{pmatrix}
\frac{\partial f_r}{\partial r} & \frac{\partial f_r}{\partial b_1} & \frac{\partial f_r}{\partial b_2} \\
\frac{\partial f_{b_1}}{\partial r} & \frac{\partial f_{b_1}}{\partial b_1} & \frac{\partial f_{b_1}}{\partial b_2} \\
\frac{\partial f_{b_2}}{\partial r} & \frac{\partial f_{b_2}}{\partial b_1} & \frac{\partial f_{b_2}}{\partial b_2}
\end{pmatrix} \\
&= \begin{pmatrix}
-a - \frac{k}{(r+k)^2}(g_1\, b_1 + g_2\, b_2) & -g_1 \frac{r}{(r+k)} & -g_2 \frac{r}{(r+k)} \\
g_1\, b_1 \frac{k}{(r+k)^2} & g_1 \frac{r}{(r+k)} - \gamma & 0 \\
g_2\, b_2 \frac{k}{(r+k)^2} & 0 & g_2 \frac{r}{(r+k)} - \gamma
\end{pmatrix}
\end{aligned}
\tag{B.2.2}
$$

B.2.1 (r,b_1,b_2) = (1,0,0) Equilibrium

For this equilibrium the Jacobian becomes: -

$$J = \begin{pmatrix} -a & \frac{-g_1}{(1+k)} & \frac{-g_2}{(1+k)} \\ 0 & \frac{g_1}{(1+k)} - \gamma & 0 \\ 0 & 0 & \frac{g_2}{(1+k)} - \gamma \end{pmatrix} \tag{B.2.3}$$

We then can find the eigenvalues via: -

$$\begin{vmatrix} -a-\lambda & \frac{-g_1}{(1+k)} & \frac{-g_2}{(1+k)} \\ 0 & \frac{g_1}{(1+k)} - \gamma - \lambda & 0 \\ 0 & 0 & \frac{g_2}{(1+k)} - \gamma - \lambda \end{vmatrix} = 0 \tag{B.2.4}$$

Giving: -

$$\lambda_1 = -a,\ \lambda_2 = \frac{g_1}{(1+k)} - \gamma,\ \lambda_3 = \frac{g_2}{(1+k)} - \gamma \tag{B.2.5}$$

So this equilibrium is stable if for each species if $g_i < \gamma(1+k)$ which is equivalent to $r_i^* > 1$ or $r_i^* < 0$. If this is not true for any species then this an unstable equilibrium.

B.2.2 (r,b_1,b_2) = $(r_1^*, b_1^*, 0)$ and $(r, b_1, b_2) = (r_2^*, 0, b_2^*)$ Equilibria

For the $(r, b_1, b_2) = (r_1^*, b_1^*, 0)$ equilibrium the Jacobian becomes: -

$$J = \begin{pmatrix} -a - (g_1\, b_1^*)\frac{k}{(r_1^*+k)^2} & -d & \frac{-g_2}{g_1}\gamma \\ (g_1\, b_1^*)\frac{k}{(r_1^*+k)^2} & 0 & 0 \\ 0 & 0 & \gamma\left(\frac{g_2}{g_1} - 1\right) \end{pmatrix} \tag{B.2.6}$$

$$\begin{vmatrix} -a-(g_1\,b_1^*)\dfrac{k}{(r_1^*+k)^2}-\lambda & -d & \dfrac{-g_2}{g_1}\,\gamma \\ (g_1\,b_1^*)\dfrac{k}{(r_1^*+k)^2} & -\lambda & 0 \\ 0 & 0 & \gamma\left(\dfrac{g_2}{g_1}-1\right)-\lambda \end{vmatrix} = 0 \tag{B.2.7}$$

This gives a characteristic equation for lambda: -

$$\left(\gamma\left[\frac{g_2}{g_1}-1\right]-\lambda\right)(\lambda^2+[a+Z_1]\lambda+Z_1\gamma)=0 \tag{B.2.8}$$

Where $Z_1=\dfrac{g_1\,b_1^*\,k}{(r_1^*+k)^2}$

So λ is: -

$$\lambda_1=\gamma\left(\frac{g_2}{g_1}-1\right),\ \lambda_{2,3}=\frac{-(a+Z)\pm\sqrt{(a+Z_1)^2-4Z_1\gamma}}{2} \tag{B.2.9}$$

So this is stable only if $g_1>g_2$ and $g_1>\gamma(k+1)$

$$J=\begin{pmatrix} -a-(g_2\,b_2^*)\dfrac{k}{(r_2^*+k)^2} & \dfrac{-g_1}{g_2}\,\gamma & -d \\ 0 & \gamma\left(\dfrac{g_1}{g_2}-1\right) & 0 \\ (g_2\,b_2^*)\dfrac{k}{(r_2^*+k)^2} & 0 & 0 \end{pmatrix} \tag{B.2.10}$$

$$\begin{vmatrix} -a-(g_2\,b_2^*)\dfrac{k}{(r_2^*+k)^2}-\lambda & \dfrac{-g_1}{g_2}\,\gamma & -d \\ 0 & \gamma\left(\dfrac{g_1}{g_2}-1\right)-\lambda & 0 \\ (g_2\,b_2^*)\dfrac{k}{(r_2^*+k)^2} & 0 & -\lambda \end{vmatrix} = 0 \tag{B.2.11}$$

This gives a characteristic equation for lambda: -

$$\left(\gamma\left[\frac{g_1}{g_2}-1\right]-\lambda\right)(\lambda^2+[a+Z_2]\lambda+Z_2\gamma)=0 \tag{B.2.12}$$

Where $Z_2 = \dfrac{g_2\, b_2^*\, k}{(r_2^* + k)^2}$

So λ is: -

$$\lambda_1 = \gamma\left(\frac{g_1}{g_2} - 1\right),\ \lambda_{2,3} = \frac{-(a + Z_2) \pm \sqrt{(a+Z)^2 - 4Z_2\gamma}}{2} \tag{B.2.13}$$

So this is stable only if $g_2 > g_1$ and $g_2 > \gamma(k+1)$

B.3 Linear Stability Analysis - System with n Species

For equilibrium (r,b_1,b_2, ... ,b_i, ... ,b_n) = $(r_i^*, 0, 0, ..., b_i^*, ..., 0)$, i.e. when species i is the only one left.

$$J = \begin{pmatrix} -a-\frac{g_i\, b_i^*\, k}{(r_i^*+k)^2} & \frac{-g_1}{g_i}\gamma & \cdots & \frac{-g_{i-1}}{g_i}\gamma & -\gamma & \frac{-g_{i+1}}{g_i}\gamma & \cdots & \frac{-g_n}{g_i}\gamma \\ 0 & \gamma\left(\frac{g_1}{g_i}-1\right) & \cdots & 0 & 0 & 0 & \cdots & 0 \\ \vdots & \vdots & \ddots & \vdots & \vdots & \vdots & & \vdots \\ 0 & 0 & \cdots & \gamma\left(\frac{g_{i-1}}{g_i}-1\right) & 0 & 0 & \cdots & 0 \\ \frac{g_i\, b_i^*\, k}{(r_i^*+k)^2} & 0 & \cdots & 0 & 0 & 0 & \cdots & 0 \\ 0 & 0 & \cdots & 0 & 0 & \gamma\left(\frac{g_{i+1}}{g_i}-1\right) & \cdots & 0 \\ \vdots & \vdots & & \vdots & \vdots & \vdots & \ddots & \vdots \\ 0 & 0 & \cdots & 0 & 0 & 0 & \cdots & \gamma\left(\frac{g_n}{g_i}-1\right) \end{pmatrix} \tag{B.3.14}$$

The characteristic equation of this system is: -

$$(\lambda^2 + [a + Z_i]\lambda - \gamma Z_i) \prod_{j=1\, j\neq i}^{n} \left(\gamma\left[\frac{g_j}{g_i} - 1\right] - \lambda\right) = 0 \tag{B.3.15}$$

Where $Z_i = \dfrac{g_i\, b_i^*\, k}{(r_i^*+k)^2}$

For the resulting eigenvalues to be all negative and this equilibrium to be stable then g_i must be greater than all other species growth rates and $g_i > \gamma(k+1)$.

Appendix C

Resource Model Diversity vs Noise Plots

This appendix shows larger versions of the plots from Section 3.5.3 in Chapter 3.

C.1 Constant α Slices

Slices of constant α from Figure 3.14

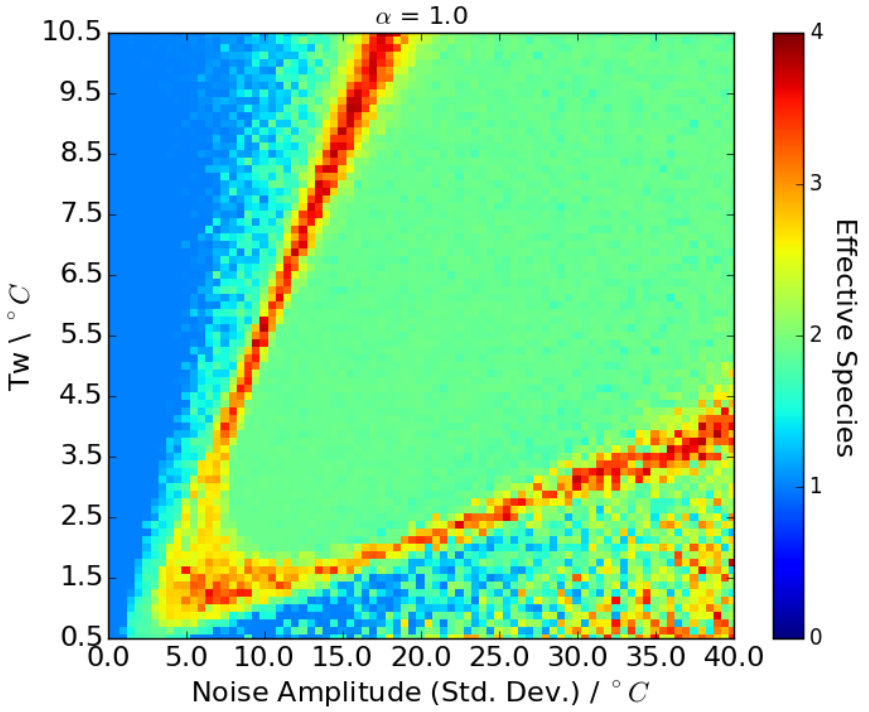
α = 1.0
Tw \ $^\circ C$
10.5
9.5
8.5
7.5
6.5
5.5
4.5
3.5
2.5
1.5
0.5
0.0
5.0
10.0
15.0
20.0
25.0
30.0
35.0
40.0
Noise Amplitude (Std. Dev.) / $^\circ C$
Effective Species
4
3
2
1
0

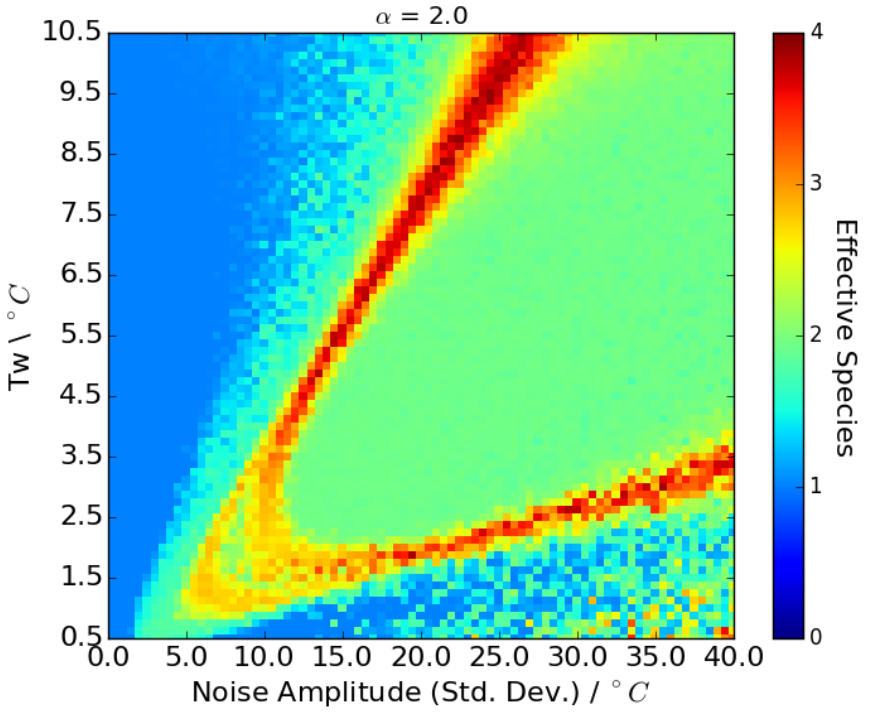
α = 2.0
Tw \ $^\circ C$
10.5
9.5
8.5
7.5
6.5
5.5
4.5
3.5
2.5
1.5
0.5
0.0
5.0
10.0
15.0
20.0
25.0
30.0
35.0
40.0
Noise Amplitude (Std. Dev.) / $^\circ C$
Effective Species
4
3
2
1
0

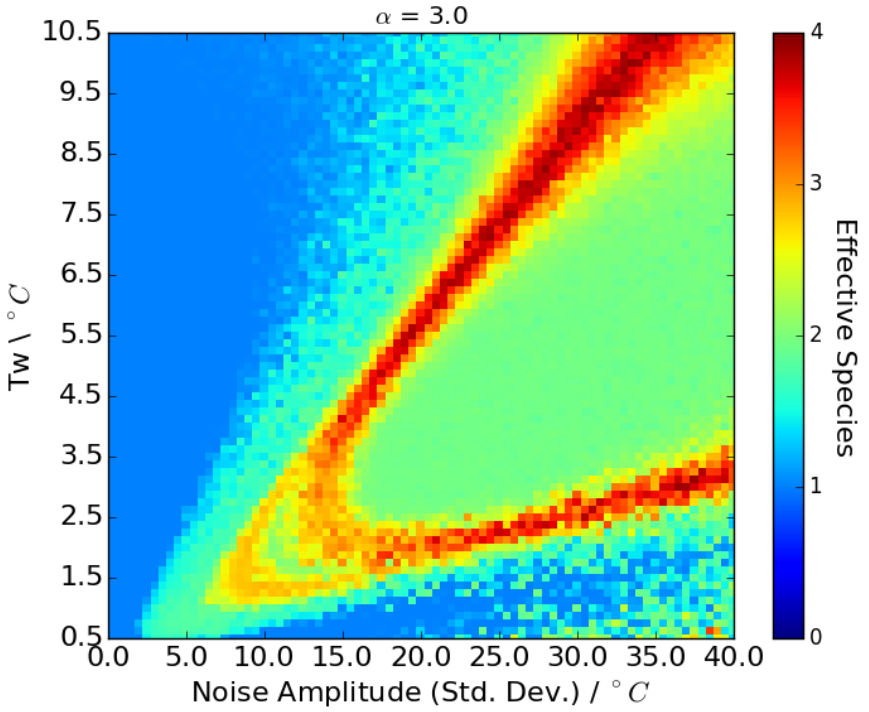
α = 3.0
Tw \ $^\circ C$
Noise Amplitude (Std. Dev.) / $^\circ C$
Effective Species
10.5
9.5
8.5
7.5
6.5
5.5
4.5
3.5
2.5
1.5
0.5
0.0
5.0
10.0
15.0
20.0
25.0
30.0
35.0
40.0
0
1
2
3
4

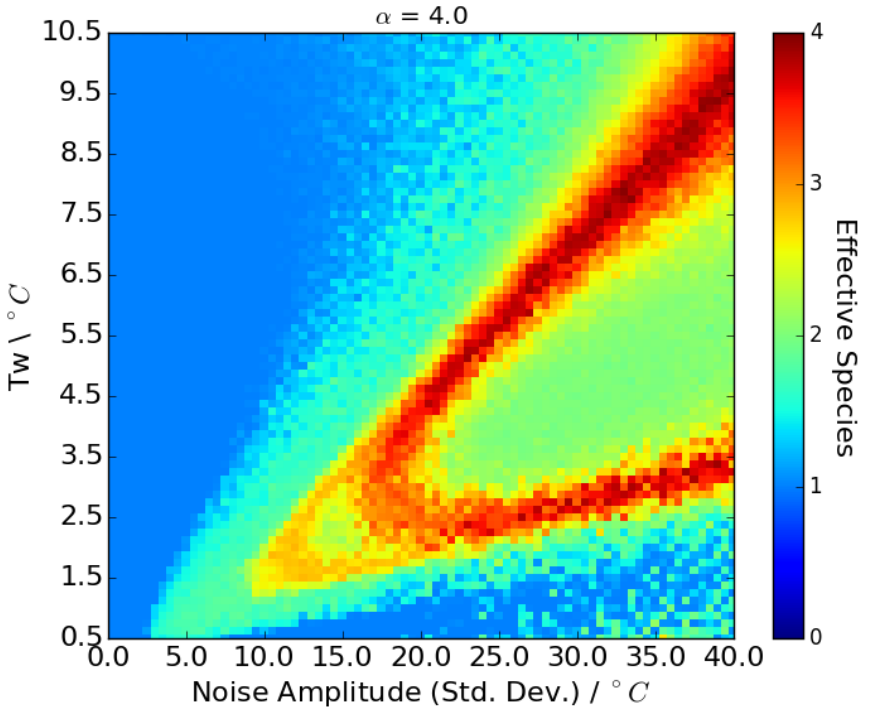
α = 4.0
Tw \ $^\circ C$
Noise Amplitude (Std. Dev.) / $^\circ C$
Effective Species
10.5
9.5
8.5
7.5
6.5
5.5
4.5
3.5
2.5
1.5
0.5
0.0
5.0
10.0
15.0
20.0
25.0
30.0
35.0
40.0
0
1
2
3
4

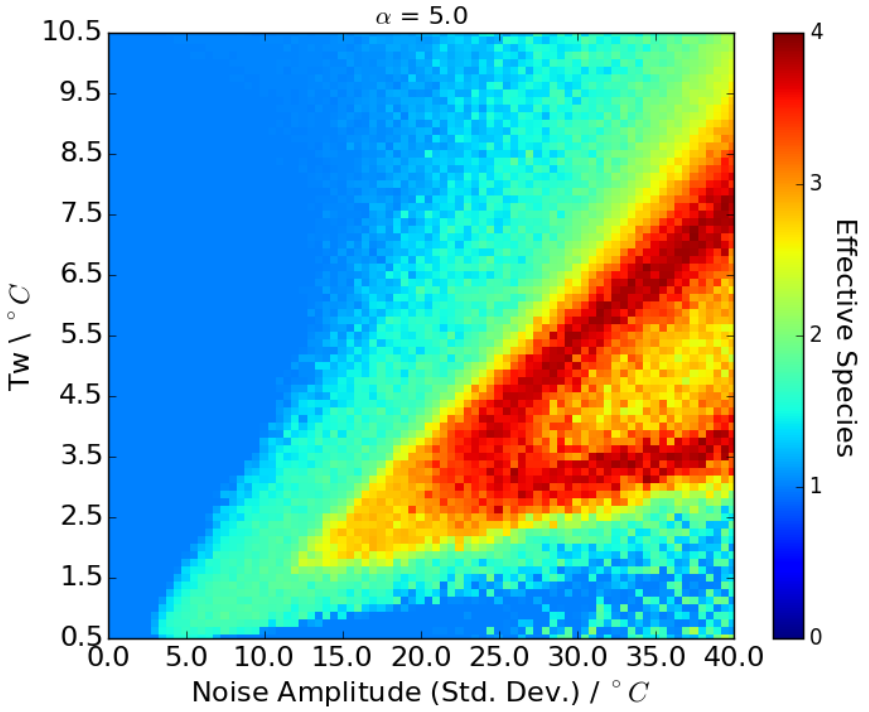
α = 5.0
Tw \ °C
Noise Amplitude (Std. Dev.) / °C
Effective Species
10.5
9.5
8.5
7.5
6.5
5.5
4.5
3.5
2.5
1.5
0.5
0.0
5.0
10.0
15.0
20.0
25.0
30.0
35.0
40.0
4
3
2
1
0

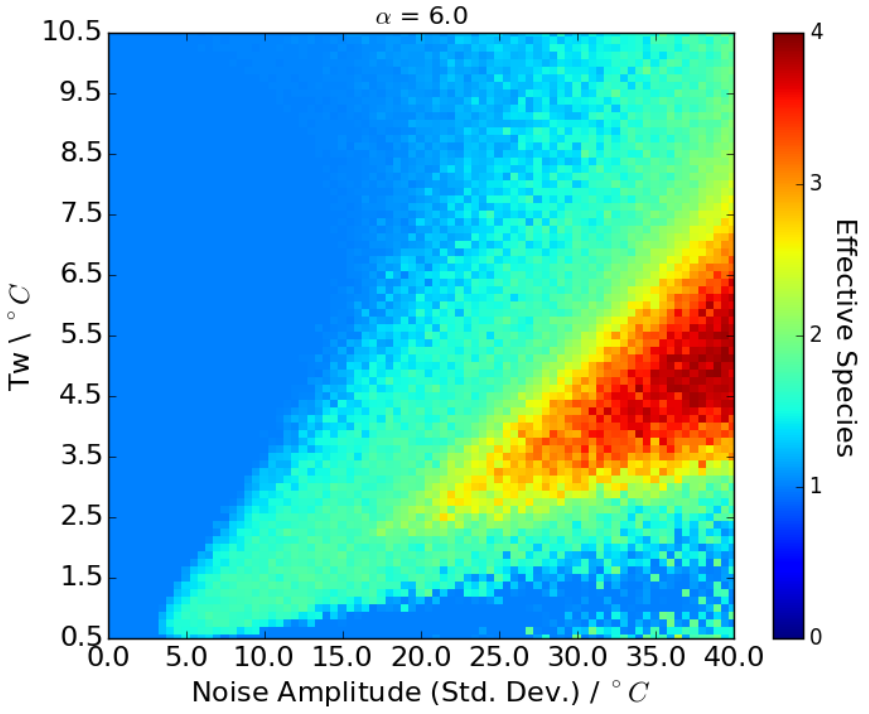
α = 6.0
Tw \ °C
Noise Amplitude (Std. Dev.) / °C
Effective Species
10.5
9.5
8.5
7.5
6.5
5.5
4.5
3.5
2.5
1.5
0.5
0.0
5.0
10.0
15.0
20.0
25.0
30.0
35.0
40.0
4
3
2
1
0

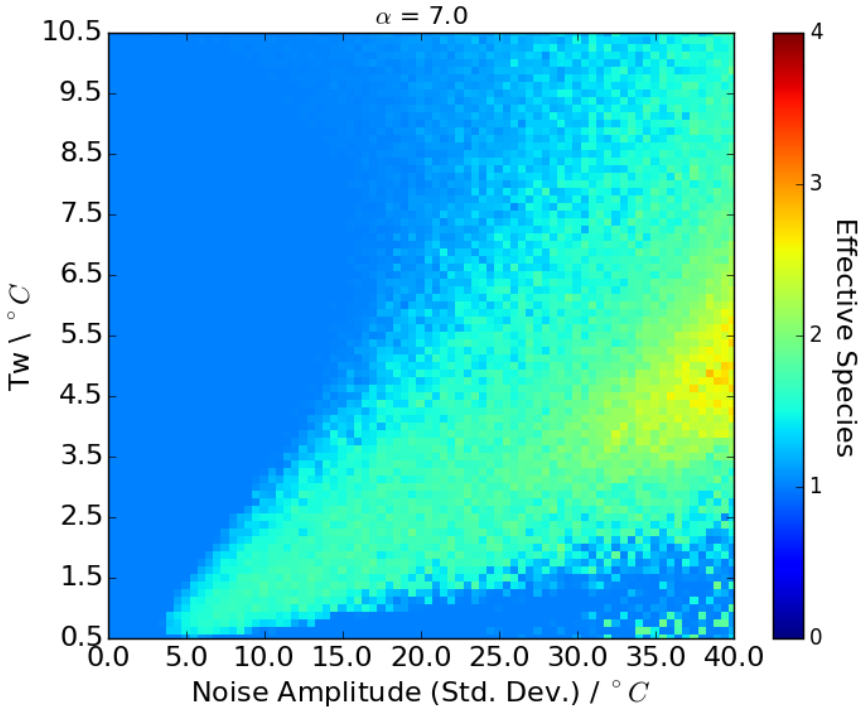
α = 7.0
Tw \ $^\circ C$
Noise Amplitude (Std. Dev.) / $^\circ C$
Effective Species
10.5
9.5
8.5
7.5
6.5
5.5
4.5
3.5
2.5
1.5
0.5
0.0
5.0
10.0
15.0
20.0
25.0
30.0
35.0
40.0
0
1
2
3
4

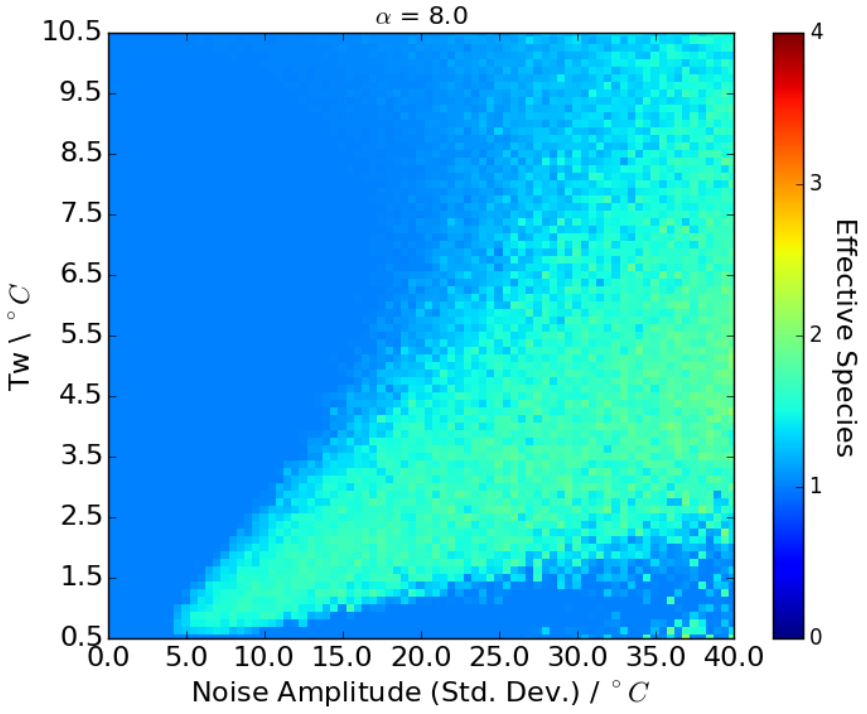
α = 8.0
Tw \ $^\circ C$
Noise Amplitude (Std. Dev.) / $^\circ C$
Effective Species
10.5
9.5
8.5
7.5
6.5
5.5
4.5
3.5
2.5
1.5
0.5
0.0
5.0
10.0
15.0
20.0
25.0
30.0
35.0
40.0
0
1
2
3
4

C.2 Constant σ Slices

Slices of constant σ from Figure 3.15

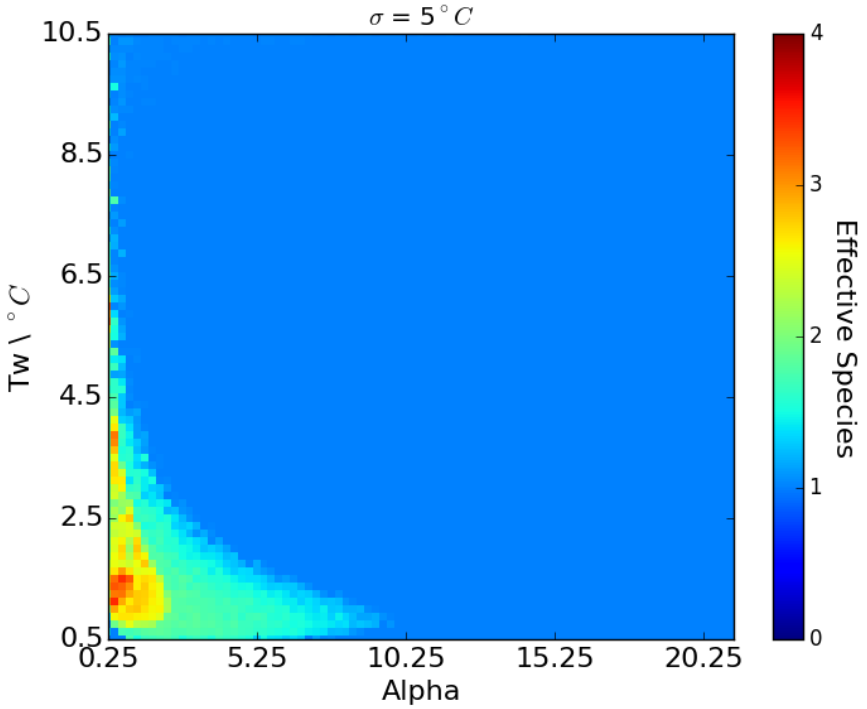

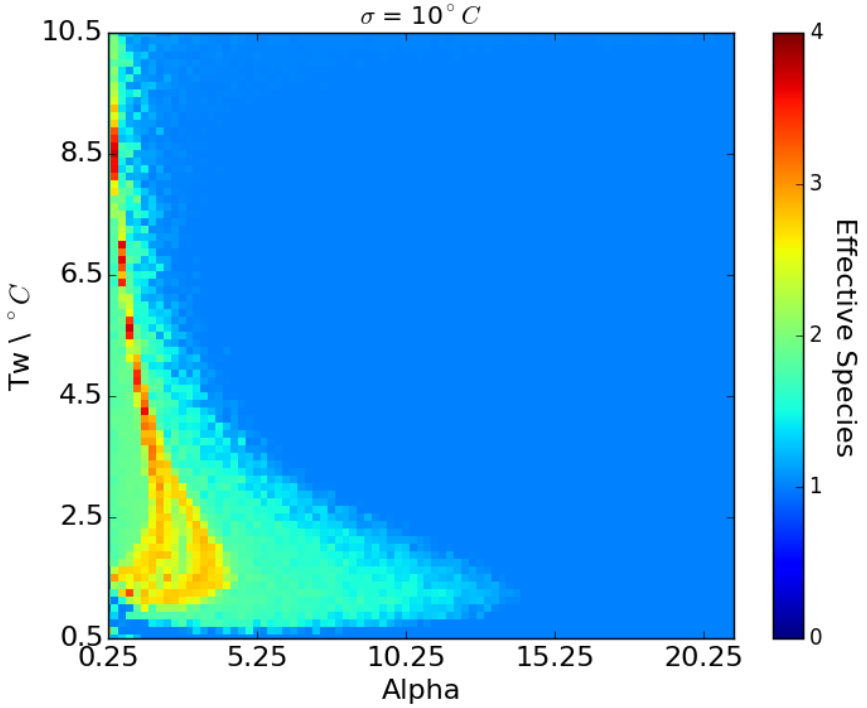

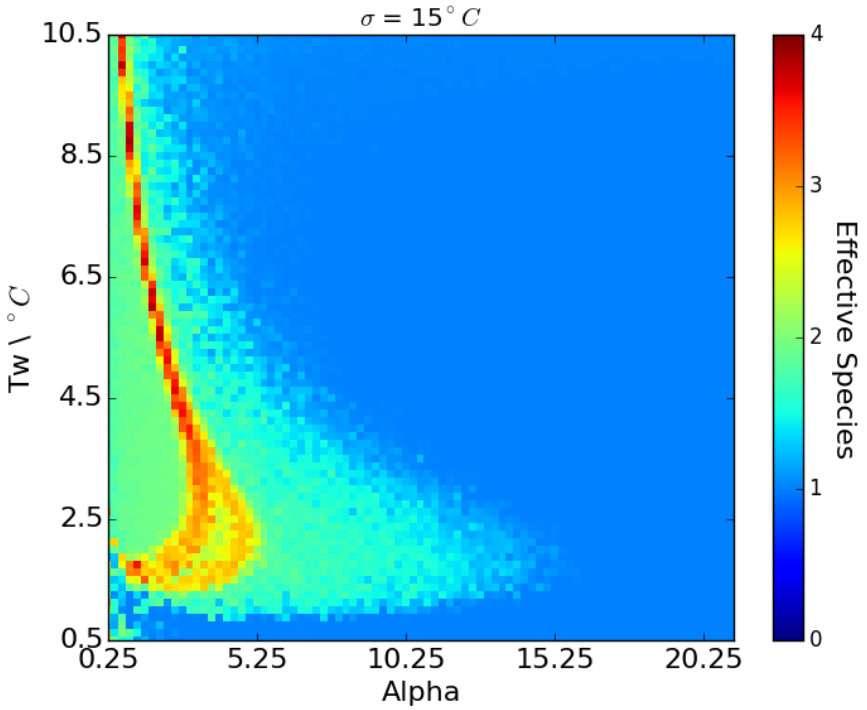
$\sigma = 15^\circ C$
10.5
8.5
6.5
4.5
2.5
0.5
Tw \ $^\circ C$
0.25
5.25
10.25
15.25
20.25
Alpha
4
3
2
1
0
Effective Species

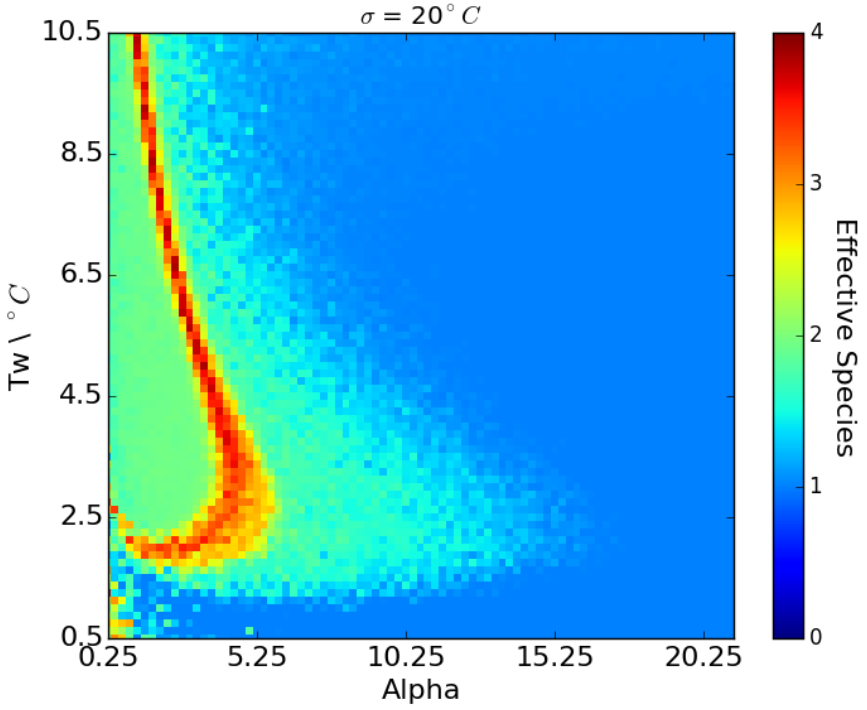
$\sigma = 20^\circ C$
10.5
8.5
6.5
4.5
2.5
0.5
Tw \ $^\circ C$
0.25
5.25
10.25
15.25
20.25
Alpha
4
3
2
1
0
Effective Species

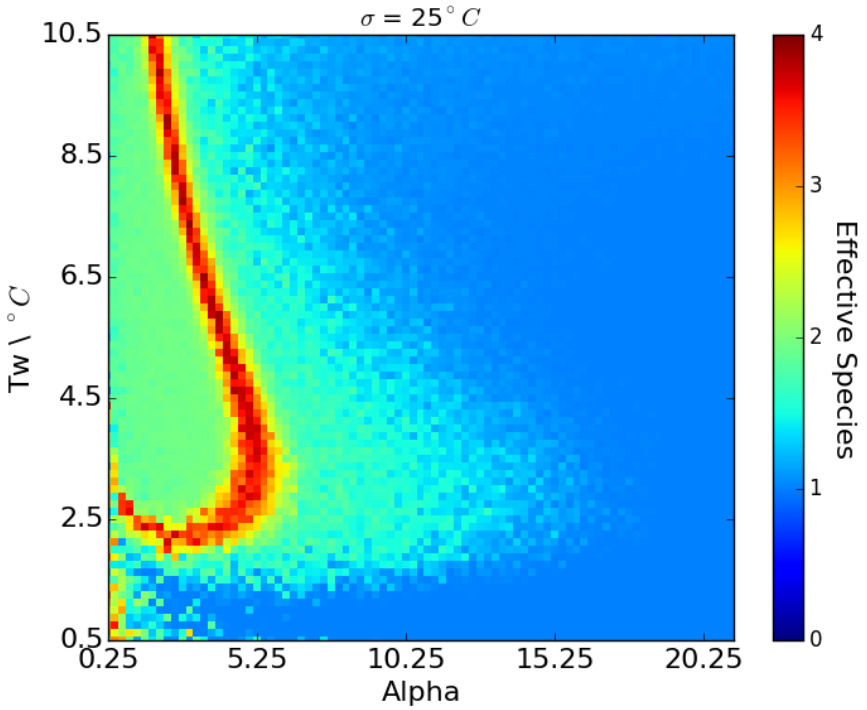
$\sigma = 25^\circ C$
10.5
8.5
6.5
4.5
2.5
0.5
Tw \ $^\circ C$
0.25
5.25
10.25
15.25
20.25
Alpha
4
3
2
1
0
Effective Species

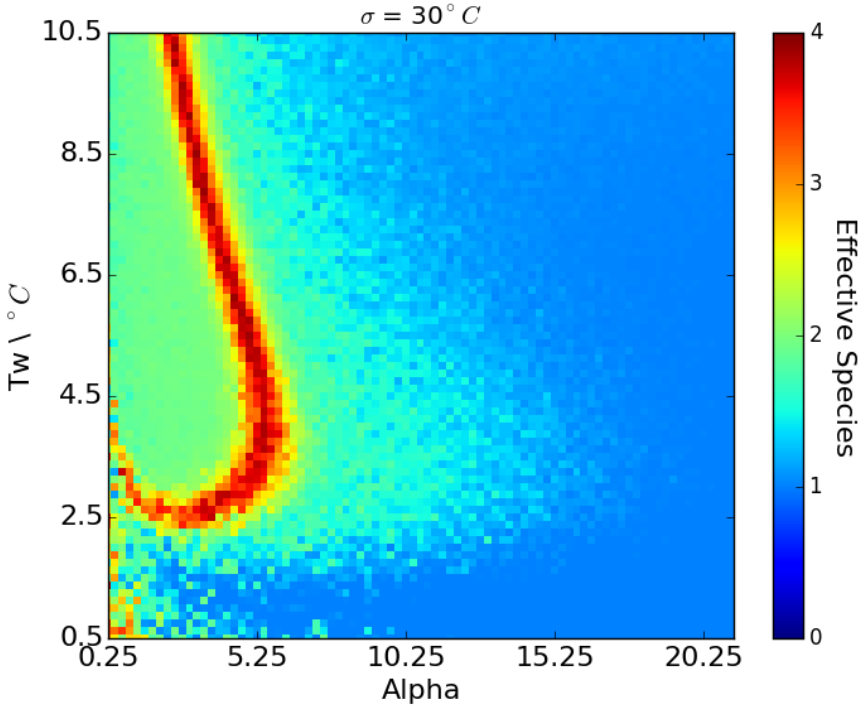
$\sigma = 30^\circ C$
10.5
8.5
6.5
4.5
2.5
0.5
Tw \ $^\circ C$
0.25
5.25
10.25
15.25
20.25
Alpha
4
3
2
1
0
Effective Species

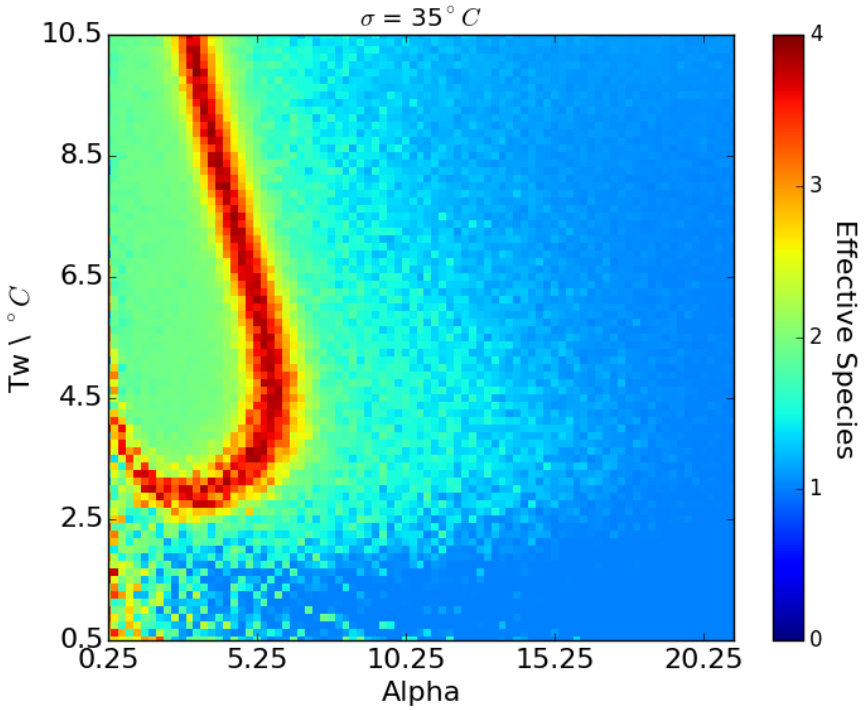
$\sigma = 35^\circ C$
10.5
8.5
6.5
4.5
2.5
0.5
Tw \ $^\circ C$
0.25
5.25
10.25
15.25
20.25
Alpha
4
3
2
1
0
Effective Species

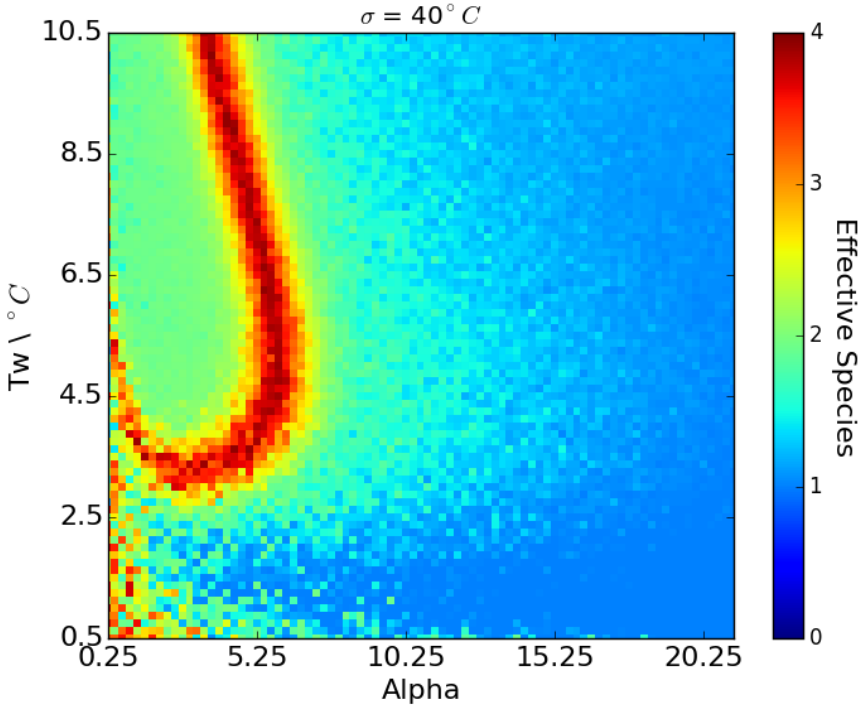
$\sigma = 40^\circ C$
10.5
8.5
6.5
4.5
2.5
0.5
Tw \ $^\circ C$
0.25
5.25
10.25
15.25
20.25
Alpha
4
3
2
1
0
Effective Species

C.3 Constant T_w Slices

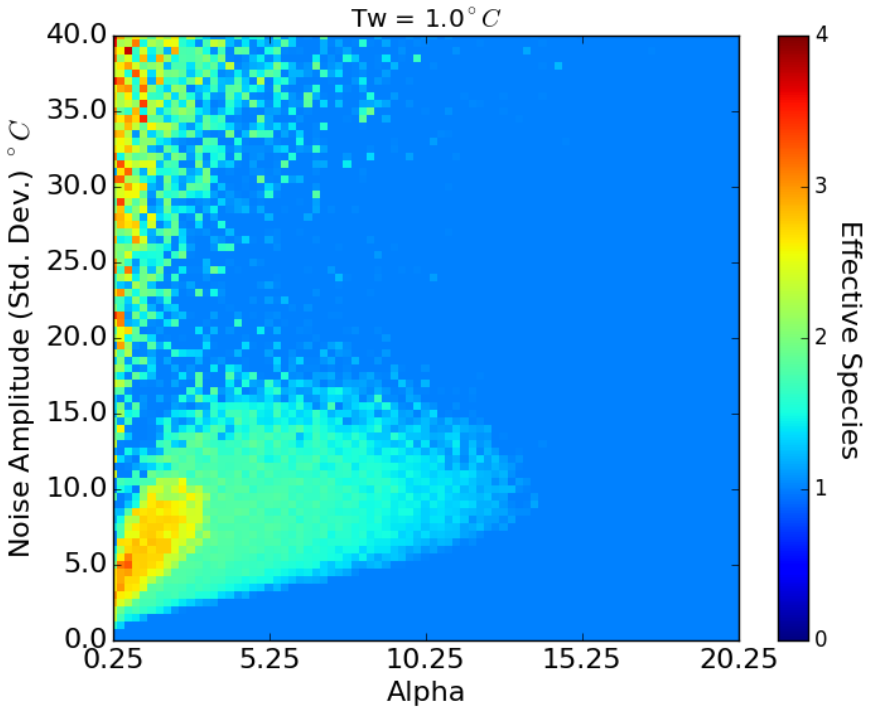

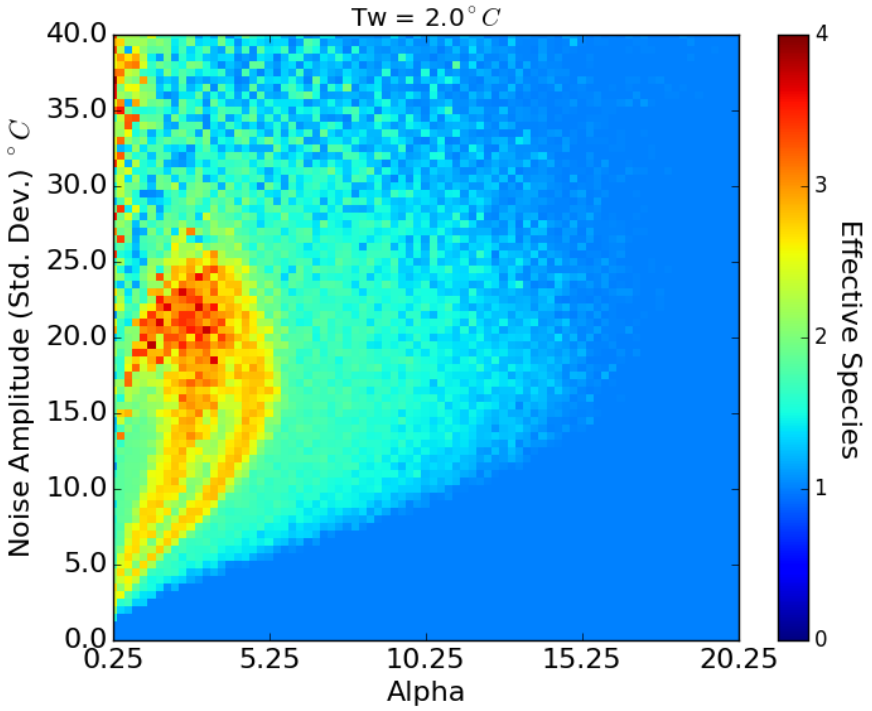

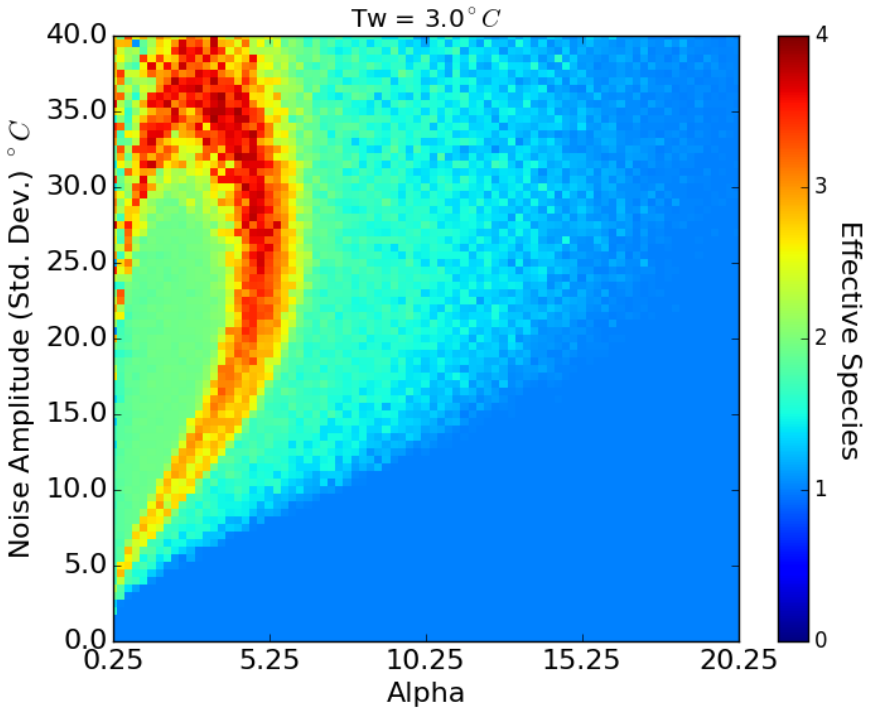
Tw = 3.0°C
Noise Amplitude (Std. Dev.) °C
Alpha
Effective Species
0.0
5.0
10.0
15.0
20.0
25.0
30.0
35.0
40.0
0.25
5.25
10.25
15.25
20.25
0
1
2
3
4

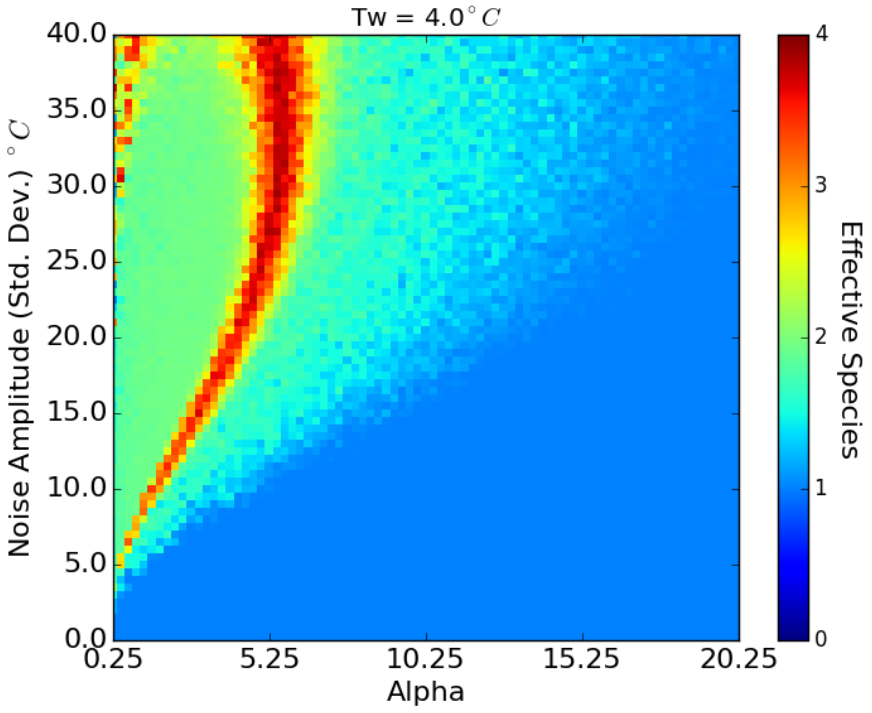
Tw = 4.0°C
Noise Amplitude (Std. Dev.) °C
Alpha
Effective Species
0.0
5.0
10.0
15.0
20.0
25.0
30.0
35.0
40.0
0.25
5.25
10.25
15.25
20.25
0
1
2
3
4

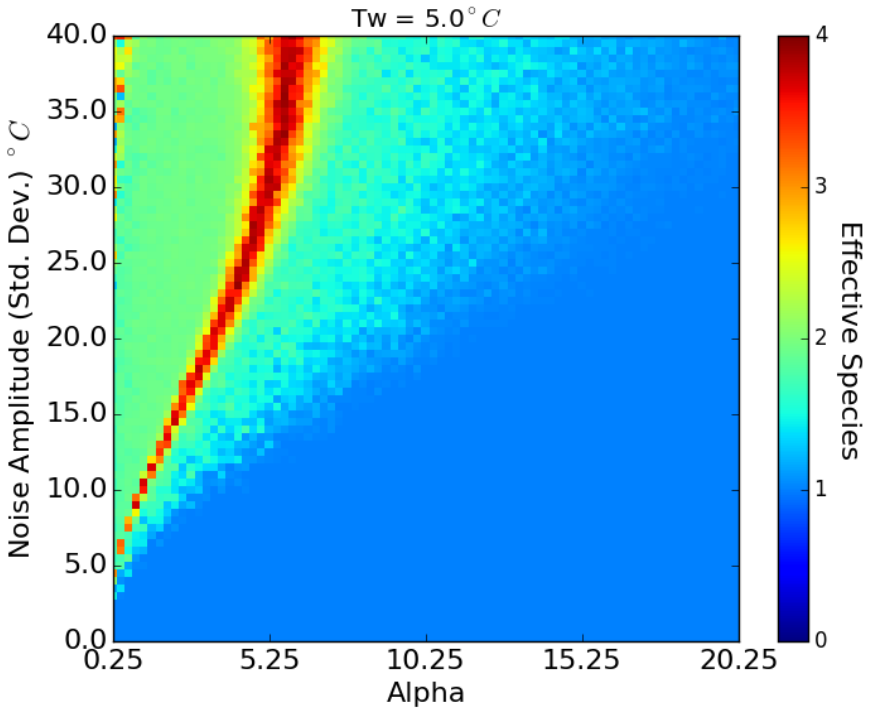
Tw = 5.0°C
Noise Amplitude (Std. Dev.) °C
40.0
35.0
30.0
25.0
20.0
15.0
10.0
5.0
0.0
0.25
5.25
10.25
15.25
20.25
Alpha
Effective Species
4
3
2
1
0

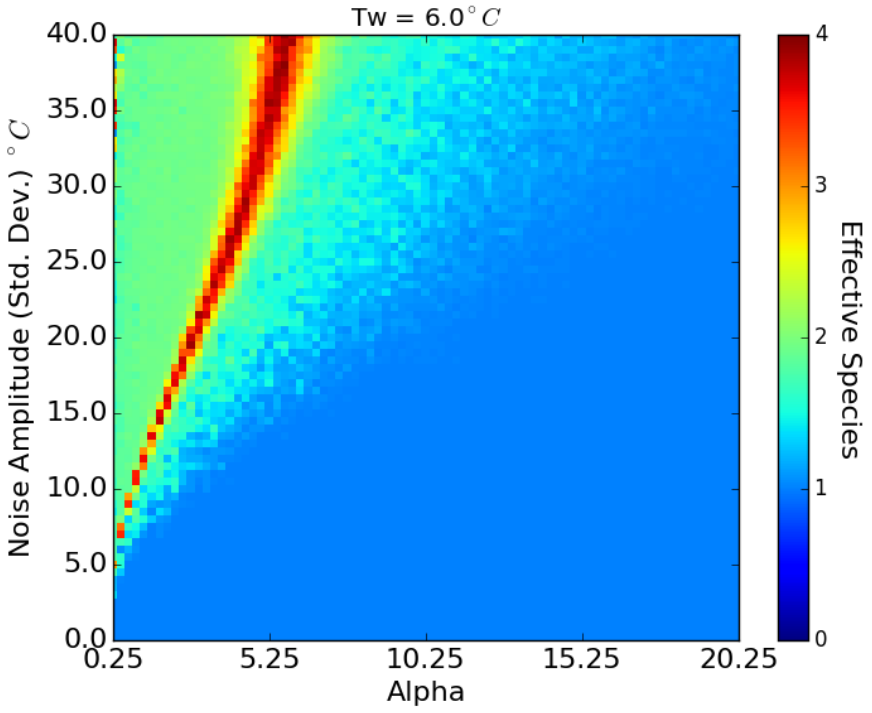
Tw = 6.0°C
Noise Amplitude (Std. Dev.) °C
40.0
35.0
30.0
25.0
20.0
15.0
10.0
5.0
0.0
0.25
5.25
10.25
15.25
20.25
Alpha
Effective Species
4
3
2
1
0

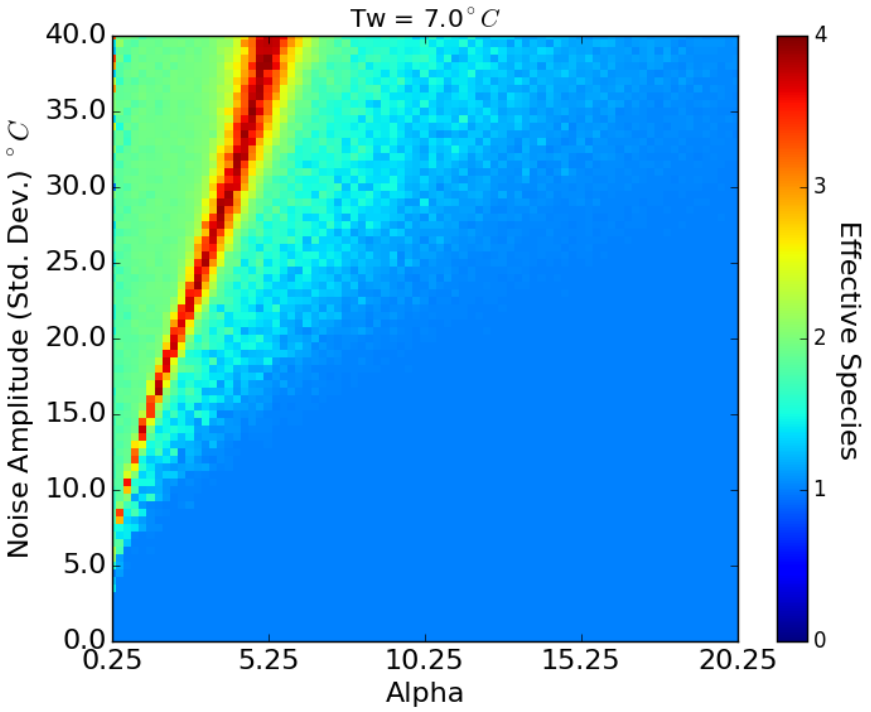
Tw = 7.0°C
Noise Amplitude (Std. Dev.) °C
40.0
35.0
30.0
25.0
20.0
15.0
10.0
5.0
0.0
0.25
5.25
10.25
15.25
20.25
Alpha
Effective Species
4
3
2
1
0

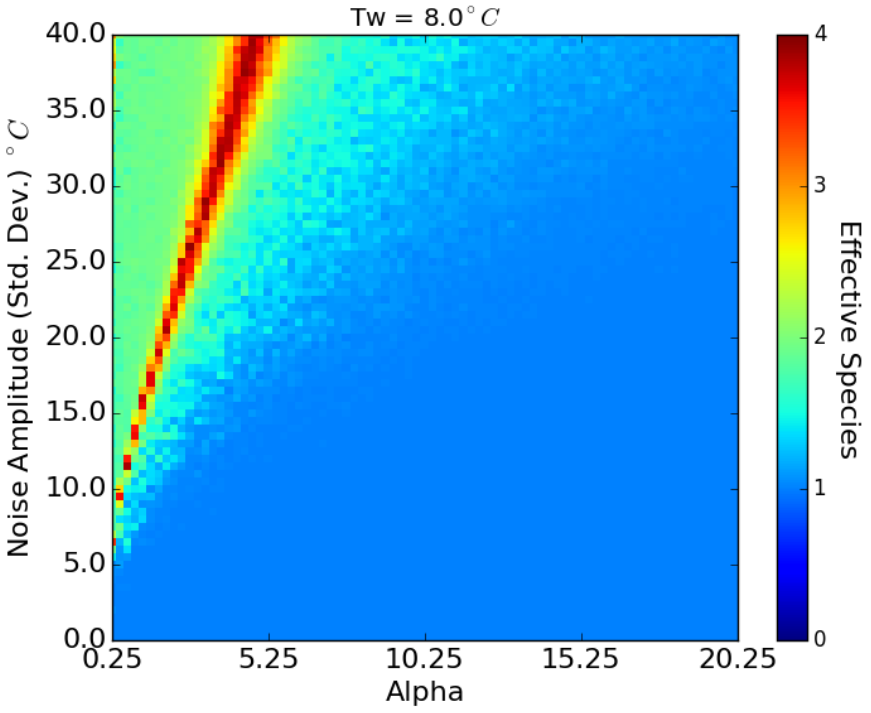
Tw = 8.0°C
Noise Amplitude (Std. Dev.) °C
40.0
35.0
30.0
25.0
20.0
15.0
10.0
5.0
0.0
0.25
5.25
10.25
15.25
20.25
Alpha
Effective Species
4
3
2
1
0

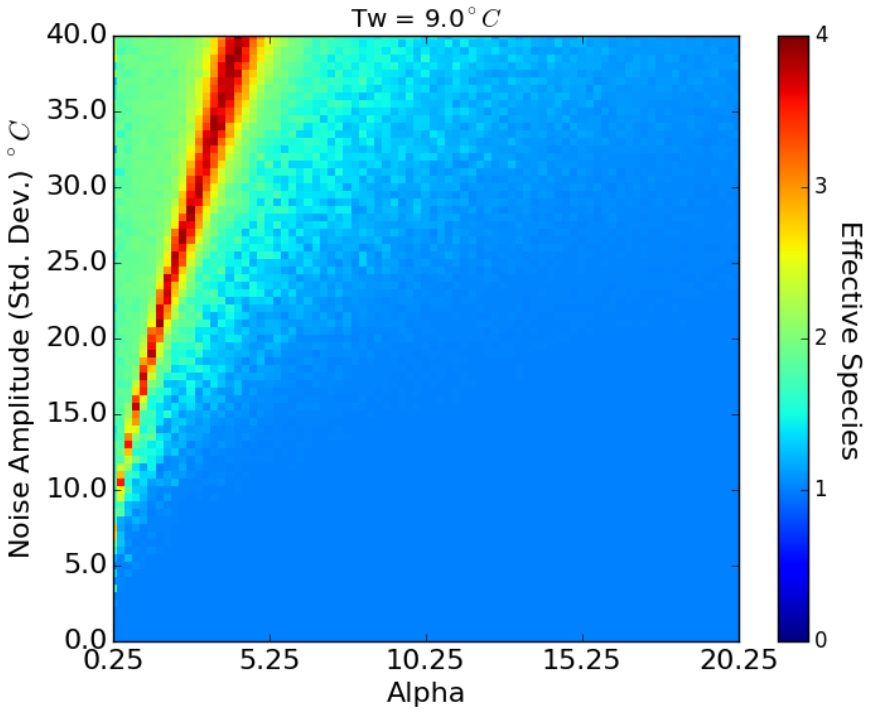
Tw = 9.0 °C
Noise Amplitude (Std. Dev.) °C
40.0
35.0
30.0
25.0
20.0
15.0
10.0
5.0
0.0
0.25
5.25
10.25
15.25
20.25
Alpha
Effective Species
4
3
2
1
0

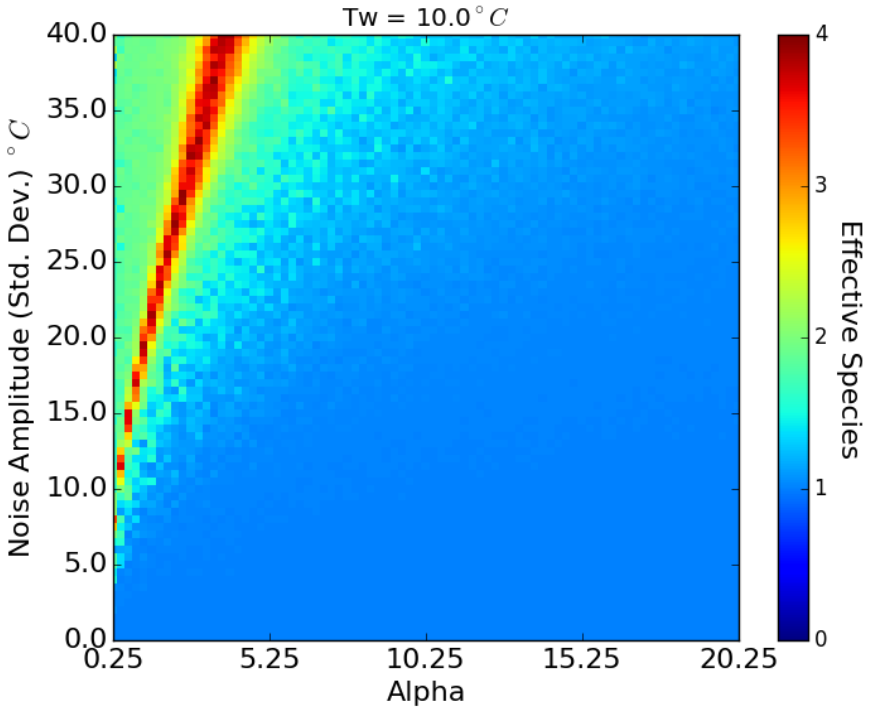
Tw = 10.0 °C
Noise Amplitude (Std. Dev.) °C
40.0
35.0
30.0
25.0
20.0
15.0
10.0
5.0
0.0
0.25
5.25
10.25
15.25
20.25
Alpha
Effective Species
4
3
2
1
0

Appendix D

Change of Size Variable in RED

In the current formulation of RED the size variable is tree carbon mass. In certain circumstances it may be necessary to compare RED to distributions in terms of different size variables (e.g. such as trunk diameter which is more easily and commonly measured than tree mass).

Considering first the continuous (ie not discretized) equation we have: -

$$\frac{\partial n(m,t)}{\partial t} + \frac{\partial}{\partial m}\left(\frac{\partial m(m,t)}{\partial t} n(m,t)\right) = -\gamma n(m,t) \tag{D.0.1}$$

where n(m,t) is the tree density distribution (trees $m^{-2}\ kg^{-1}$) and so the integral of n between two tree massses of m_1 and m_2 will give the number of trees with mass between m_1 and m_2.

$$\int_{m_1}^{m_2} n(m,t)\, dm = \text{no. trees between } m_1 \text{ and } m_2 \tag{D.0.2}$$

If instead we wish to express the continuity equation in terms of height H, first we need a function H = F(m) that maps m to H. In this case the function would be a power law (from allometry).

Defining $H_1 = F(m_1)$ and $H_2 = F(m_2)$ then we know that: -

$$\int_{m_1}^{m_2} n(m,t)\,dm = \int_{H_1}^{H_2} n(H,t)\,dH \tag{D.0.3}$$

So

$$n(m,t) = \frac{d}{dm}\int_{H_1}^{H_2} n(H,t)\,dH = \frac{dH}{dm}\frac{d}{dH}\int_{H_1}^{H_2} n(H,t)\,dH = \frac{dH}{dm}n(H,t) \tag{D.0.4}$$

We can then substitute this result and

$$\frac{\partial m}{\partial t} = \frac{dm}{dH}\frac{\partial m}{\partial t} \tag{D.0.5}$$

into equation D.0.1 to prove that the form of the continuity equation is unchanged if we convert the size variable.

$$\frac{\partial n(H,t)}{\partial t} + \frac{\partial}{\partial H}\left(\frac{\partial H(H,t)}{\partial t}n(H,t)\right) = -\gamma n(H,t) \tag{D.0.6}$$

So to convert the distribution from size variable y to z

$$n(y,t) = \frac{dz}{dy}n(z,t) \tag{D.0.7}$$

Appendix E

Respiration Calculation

In TRIFFID (Cox, 2001) the respiration is defined as

$$R_{pm} = R_d \left(\beta + \left(\frac{N_f + N_s}{N_l} \right) \right) \frac{f_{PAR}}{k} \tag{E.0.1}$$

where β is the moisture stress factor, R_d the dark respiration and N_l, N_s, and N_f are the nitrogen contents of leaf, respiring stem and fine roots and are given by

$$N_l = n_l \, \sigma_l \, L = n_l \, C_l \tag{E.0.2}$$

$$N_f = \mu_{rl} \, n_l \, C_f \tag{E.0.3}$$

$$N_s = a_{ws} \, \mu_{sl} \, n_l \, C_w \tag{E.0.4}$$

where C_f, C_w and C_l are the tree fine root, wood and leaf carbon densities. The respiring stem is taken to be a fixed ratio a_{ws} of the total wood carbon C_w As all above proportional to n_l then we can eliminate n_l from equation for R_{pm} and by also assuming no water stress so $\beta = 1$ we get

$$R_{pm} = R_d \left(1 + \left(\frac{\mu_{rl} m_f + a_{ws} \mu_{sl} m_w}{m_l} \right) \right) \frac{f_{PAR}}{k} \tag{E.0.5}$$

where m_f, m_w and m_l are the tree fine root, stem and leaf carbon masses obtained by multiplying by the tree crown area A by C_f, C_w and C_l.

The dark respiration is defined as

$$R_d = 0.015\, V_{max}\, f_T(q_{10})(365 \cdot 86400 \cdot 0.012) \tag{E.0.6}$$

where V_{max} is the maximum rate of carboxylation of Rubisco and is assumed to be linearly dependent on the leaf nitrogen concentration n_l. For C3 plants this is

$$V_{max} = 0.0008\, n_l \tag{E.0.7}$$

f_T represents the q_{10} temperature dependence

$$f_T(q_{10}) = q_{10}^{0.1(T_c - 25)} \tag{E.0.8}$$

to simplify the model q_{10} is taken to be 3.0 and T_c is assumed to be 25°C so $f_T = 1.0$.

The final term in Equation E.0.6, represents unit conversion from $(mol\, CO_2\, m^{-2}\, s^{-1})$ to $(kg\, C\, m^{-2}\, yr^{-1})$.

Bibliography

Bellassen V, Le Maire G, Dhôte J, Ciais P and Viovy N (2010) Modelling forest management within a global vegetation model–Part 1: Model structure and general behaviour. *Ecological Modelling*, **221**(20): 2458–2474.

Best M, Pryor M, Clark D, Rooney G, Essery R, Ménard C, Edwards J, Hendry M, Porson A, Gedney N, Mercado L, Sitch S, Blyth E, Boucher O, Cox P, Grimmond C and Harding R (2011) The Joint UK Land Environment Simulator (JULES), model description–Part 1: Energy and water fluxes. *Geoscientific Model Development*, **4**(3): 677–699.

Bonan GB (2008a) *Ecological Climatology*. Cambridge University Press, 2nd edition.

Bonan GB (2008b) Forests and climate change: forcings, feedbacks, and the climate benefits of forests. *science*, **320**(5882): 1444–1449.

Bonan GB, Levis S, Sitch S, Vertenstein M and Oleson KW (2003) A dynamic global vegetation model for use with climate models: Concepts and description of simulated vegetation dynamics. *Global Change Biology*, **9**(11): 1543–1566.

Carter R and Prince S (1981) Epidemic models used to explain biogeographical distribution limits. *Nature*, **293**(5834): 644–645.

Chambers JQ, Higuchi N and Schimel JP (1998) Ancient trees in Amazonia. *Nature*, **391**(6663): 135–136.

Chapin III FS, Zavaleta ES, Eviner VT, Naylor RL, Vitousek PM, Reynolds HL, Hooper DU, Lavorel S, Sala OE, Hobbie SE, Mack MC and Diaz S (2000) Consequences of changing biodiversity. *Nature*, **405**(6783): 234–242.

Chave J, Andalo C, Brown S, Cairns M, Chambers J, Eamus D, Fölster H, Fromard F, Higuchi N, Kira T et al. (2005) Tree allometry and improved estimation of carbon stocks and balance in tropical forests. *Oecologia*, **145**(1): 87–99.

Clark D, Mercado L, Sitch S, Jones C, Gedney N, Best M, Pryor M, Rooney G, Essery R, Blyth E, Boucher O, Harding R, Huntingford C and Cox P (2011) The Joint UK Land Environment Simulator (JULES), model description–Part 2: Carbon fluxes and vegetation dynamics. *Geoscientific Model Development*, **4**(3): 701–722.

Coomes DA and Allen RB (2007) Mortality and tree-size distributions in natural mixed-age forests. *Journal of Ecology*, **95**(1): 27–40.

Cox P (2001) Description of the "TRIFFID" dynamic global vegetation model. *Met Office Hadley Centre Technical Note*, **24**.

Cox P, Huntingford C and Harding R (1998) A canopy conductance and photosynthesis model for use in a GCM land surface scheme. *Journal of Hydrology*, **212**: 79–94.

Cox PM, Betts RA, Jones CD, Spall SA and Totterdell IJ (2000) Acceleration of global warming due to carbon-cycle feedbacks in a coupled climate model. *Nature*, **408**(6809): 184–187.

Cramer W, Bondeau A, Woodward FI, Prentice IC, Betts RA, Brovkin V, Cox PM, Fisher V, Foley JA, Friend AD et al. (2001) Global response of terrestrial ecosystem structure and function to CO_2 and climate change: results from six dynamic global vegetation models. *Global change biology*, **7**(4): 357–373.

Dai Y, Dickinson RE and Wang YP (2004) A two-big-leaf model for canopy temperature, photosynthesis, and stomatal conductance. *Journal of Climate*, **17**(12): 2281–2299.

Dakos V, Scheffer M, van Nes E, Brovkin V, Petoukhov V and Held H (2008) Slowing down as an early warning signal for abrupt climate change. *Proceedings of the National Academy of Sciences USA*, **105**(38): 14308.

Dewar RC and Porté A (2008) Statistical mechanics unifies different ecological patterns. *Journal of Theoretical Biology*, **251**(3): 389–403.

Diaz S and Cabido M (2001) Vive la différence: Plant functional diversity matters to ecosystem processes. *Trends in Ecology & Evolution*, **16**(11): 646–655.

Dobson A, Lodge D, Alder J, Cumming GS, Keymer J, McGlade J, Mooney H, Rusak JA, Sala O, Wolters V et al. (2006) Habitat loss, trophic collapse, and the decline of ecosystem services. *Ecology*, **87**(8): 1915–1924.

Dunne J, Williams R and Martinez N (2002) Food-web structure and network theory: The role of connectance and size. *Proceedings of the National Academy of Sciences USA*, **99**(20): 12917–12922.

Elton CS (1958) *Ecology of Invasions by Animals and Plants*. Chapman & Hall.

Enquist BJ, West GB and Brown JH (2009) Extensions and evaluations of a general quantitative theory of forest structure and dynamics. *Proceedings of the National Academy of Sciences*, **106**(17): 7046–7051.

Feldpausch T, Banin L, Phillips O, Baker T, Lewis S, Quesada C, Affum-Baffoe K, Arets E, Berry N and Bird M (2011) Height-diameter allometry of tropical forest trees. *Biogeosciences*, **8**(5): 1081–1106.

Fisher R, McDowell N, Purves D, Moorcroft P, Sitch S, Cox P, Huntingford C, Meir P and Ian Woodward F (2010) Assessing uncertainties in

a second-generation dynamic vegetation model caused by ecological scale limitations. *New Phytologist*, **187**(3): 666–681.

Folke C, Carpenter S, Walker B, Scheffer M, Elmqvist T, Gunderson L and Holling CS (2004) Regime shifts, resilience and biodiversity in ecosystem management. *Annual Review of Ecology, Evolution, and Systematics*, **35**: 557–581.

Friedlingstein P, Cox P, Betts R, Bopp L, Von Bloh W, Brovkin V, Cadule P, Doney S, Eby M, Fung I et al. (2006) Climate-carbon cycle feedback analysis: Results from the C4MIP model intercomparison. *Journal of Climate*, **19**(14): 3337–3353.

Friend A, Schugart H and Running S (1993) A physiology-based gap model of forest dynamics. *Ecology*, **74**(3): 792–797.

Friend A, Stevens A, Knox R and Cannell M (1997) A process-based, terrestrial biosphere model of ecosystem dynamics (Hybrid v3. 0). *Ecological Modelling*, **95**(2): 249–287.

Gienapp P, Teplitsky C, Alho J, Mills J and Merilä J (2008) Climate change and evolution: Disentangling environmental and genetic responses. *Molecular ecology*, **17**(1): 167–178.

Gilbert AJ (2009) Connectance indicates the robustness of food webs when subjected to species loss. *Ecological Indicators*, **9**(1): 72–80.

Grover J (1997) *Resource Competition*. Chapman and Hall.

Hamilton NS, Matthew C and Lemaire G (1995) In defence of the -3/2 boundary rule: A re-evaluation of self-thinning concepts and status. *Annals of Botany*, **76**(6): 569–577.

Hendry A and Kinnison M (2001) An introduction to microevolution: Rate, pattern, process. *Genetica*, **112**(1): 1–8.

Hirose T (2005) Development of the Monsi-Saeki theory on canopy structure and function. *Annals of Botany*, **95**(3): 483–494.

Hoffmann AA and Sgrò CM (2011) Climate change and evolutionary adaptation. *Nature*, **470**(7335): 479–485.

Hubbell S (2001) *The unified theory of biogeography and biodiversity*. Princeton Univ. Press Princeton.

Huntingford C, Booth B, Sitch S, Gedney N, Lowe J, Liddicoat S, Mercado L, Best M, Weedon G, Fisher R et al. (2010) IMOGEN: An intermediate complexity model to evaluate terrestrial impacts of a changing climate. *Geoscientific Model Development*, **3**(2): 679–687.

Huntingford C, Fisher RA, Mercado L, Booth BB, Sitch S, Harris PP, Cox PM, Jones CD, Betts RA, Malhi Y et al. (2008) Towards quantifying uncertainty in predictions of Amazon "Dieback". *Philosophical Transactions of the Royal Society B: Biological Sciences*, **363**(1498): 1857–1864.

IPCC (2013) *Summary for Policymakers. In: Climate Change 2013: The Physical Science Basis. Contribution of Working Group I to the Fifth Assessment Report of the Intergovernmental Panel on Climate Change*. Cambridge University Press, Cambridge, United Kingdom and New York, NY, USA. ISBN 978-1-107-66182-0.

Ives AR and Carpenter SR (2007) Stability and diversity of ecosystems. *Science*, **317**(5834): 58–62.

Jost L (2006) Entropy and diversity. *Oikos*, **113**(2): 363–375.

Kauffman S (1995) *At Home In The Universe*. Penguin.

Kohyama T (1987) Stand dynamics in a primary warm-temperate rain forest analyzed by the diffusion equation. *The botanical magazine= Shokubutsu-gaku-zasshi*, **100**(3): 305–317.

Kohyama T (1991) Simulating stationary size distribution of trees in rain forests. *Annals of Botany*, **68**(2): 173–180.

Kohyama T (1993) Size-structured tree populations in gap-dynamic forest–the forest architecture hypothesis for the stable coexistence of species. *Journal of Ecology*, **81**(1): 131–143.

Kohyama T (2006) The effect of patch demography on the community structure of forest trees. *Ecological Research*, **21**(3): 346–355.

Kosaka Y and Xie SP (2013) Recent global-warming hiatus tied to equatorial pacific surface cooling. *Nature*, **501**(7467): 403–407.

Krebs C (1989) *Ecological Methodology*. Harper & Row.

Krinner G, Viovy N, de Noblet-Ducoudré N, Ogée J, Polcher J, Friedlingstein P, Ciais P, Sitch S and Prentice IC (2005) A dynamic global vegetation model for studies of the coupled atmosphere-biosphere system. *Global Biogeochemical Cycles*, **19**(1).

Lambin EF, Geist HJ and Lepers E (2003) Dynamics of land-use and land-cover change in tropical regions. *Annual review of environment and resources*, **28**(1): 205–241.

Lamlom S and Savidge R (2003) A reassessment of carbon content in wood: variation within and between 41 north american species. *Biomass and Bioenergy*, **25**(4): 381 – 388.

Le Quéré C (2010) Trends in the land and ocean carbon uptake. *Current Opinion in Environmental Sustainability*, **2**(4): 219–224.

Le Quéré C, Raupach MR, Canadell JG, Marland G, Bopp L, Ciais P, Conway TJ, Doney SC, Feely RA, Foster P et al. (2009) Trends in the sources and sinks of carbon dioxide. *Nature Geoscience*, **2**(12): 831–836.

Lehman C and Tilman D (2000) Biodiversity, stability, and productivity in competitive communities. *The American Naturalist*, **156**(5): 534–552.

Lenton TM, Held H, Kriegler E, Hall JW, Lucht W, Rahmstorf S and Schellnhuber HJ (2008) Tipping elements in the earth's climate system. *Proceedings of the National Academy of Sciences*, **105**(6): 1786–1793.

Lonsdale W (1990) The self-thinning rule: dead or alive? *Ecology*, **71**(4): 1373–1388.

Loreau M, Naeem S, Inchausti P, Bengtsson J, Grime JP, Hector A, Hooper DU, Huston MA, Raffaelli D, Schmid B, Tilman D and Wardle DA (2001) Biodiversity and ecosystem functioning: current knowledge and future challenges. *Science*, **294**(5543): 804–808.

MacArthur R (1965) Patterns of species diversity. *Biological Reviews*, **40**: 510–533.

MacArthur RH (1955) Fluctuation of animal populations and a measure of community stability. *Ecology*, **36**(3): 533–536.

Malhi Y, Doughty C and Galbraith D (2011) The allocation of ecosystem net primary productivity in tropical forests. *Philosophical Transactions of the Royal Society B: Biological Sciences*, **366**(1582): 3225–3245.

Martin TG and Watson JE (2016) Intact ecosystems provide best defence against climate change. *Nature Climate Change*, **6**(2): 122–124.

May R and McLean A (2007) *Theoretical ecology: Principles and applications*. Oxford University Press, USA.

May RM (1974) *Stability and Complexity in Model Ecosystems*. Princeton Univ. Press, 2nd edition.

McCann KS (2000) The diversity-stability debate. *Nature*, **405**(6783): 228–233.

Mercado LM, Huntingford C, Gash JH, Cox PM and Jogireddy V (2007) Improving the representation of radiation interception and photosynthesis for climate model applications. *Tellus B*, **59**(3): 553–565.

Monsi M and Saeki T (1953) Über den lichtfaktor in den pflanzengesellschaften und seine bedeutung für die stoffproduktion. *Japanese Journal of Botany*, **14**(1): 22–52.

Montoya JM, Pimm SL and Solé RV (2006) Ecological networks and their fragility. *Nature*, **442**(7100): 259–264.

Mooney H, Larigauderie A, Cesario M, Elmquist T, Hoegh-Guldberg O, Lavorel S, Mace GM, Palmer M, Scholes R and Yahara T (2009) Biodiversity, climate change, and ecosystem services. *Current Opinion in Environmental Sustainability*, **1**(1): 46–54.

Moorcroft P, Hurtt G and Pacala SW (2001) A method for scaling vegetation dynamics: the ecosystem demography model (ED). *Ecological monographs*, **71**(4): 557–586.

Naeem S (2002) Biodiversity equals instability? *Nature*, **416**(6876): 23–24.

Nicotra AB, Atkin OK, Bonser SP, Davidson AM, Finnegan E, Mathesius U, Poot P, Purugganan MD, Richards C, Valladares F et al. (2010) Plant phenotypic plasticity in a changing climate. *Trends in plant science*, **15**(12): 684–692.

Niklas KJ and Spatz HC (2004) Growth and hydraulic (not mechanical) constraints govern the scaling of tree height and mass. *Proceedings of the National Academy of Sciences of the United States of America*, **101**(44): 15661–15663.

Odum EP (1953) *Fundamentals of Ecology*. Saunders.

Onalan O (2009) Financial modelling with ornstein–uhlenbeck processes driven by lévy process. In *Proceedings of the World Congress on Engineering*, volume 2, (pp. 1–3).

Pascual M and Guichard F (2005) Criticality and disturbance in spatial ecological systems. *Trends in Ecology & Evolution*, **20**(2): 88–95.

Pitman AJ (2003) The evolution of, and revolution in, land surface schemes designed for climate models. *International Journal of Climatology*, **23**: 479–510.

Poorter L, Bongers L and Bongers F (2006) Architecture of 54 moist-forest tree species: traits, trade-offs, and functional groups. *Ecology*, **87**(5): 1289–1301.

Purvis A and Hector A (2000) Getting the measure of biodiversity. *Nature*, **405**(6783): 212–219.

Rabosky DL (2013) Diversity-dependence, ecological speciation, and the role of competition in macroevolution. *Annual Review of Ecology, Evolution, and Systematics*, **44**: 481–502.

Rietkerk M, Dekker SC, de Ruiter PC and van de Koppel J (2004) Self-organized patchiness and catastrophic shifts in ecosystems. *Science*, **305**(5692): 1926–1929.

Rockström J, Steffen W, Noone K, Persson Å, Chapin FS, Lambin EF, Lenton TM, Scheffer M, Folke C, Schellnhuber HJ et al. (2009) A safe operating space for humanity. *Nature*, **461**(7263): 472–475.

Rubin BD, Manion PD and Faber-Langendoen D (2006) Diameter distributions and structural sustainability in forests. *Forest Ecology and Management*, **222**(1): 427–438.

Sato H, Itoh A and Kohyama T (2007) SEIB–DGVM: A new Dynamic Global Vegetation Model using a spatially explicit individual-based approach. *Ecological Modelling*, **200**(3): 279–307.

Scheffer M, Bascompte J, Brock WA, Brovkin V, Carpenter SR, Dakos V, Held H, Van Nes EH, Rietkerk M and Sugihara G (2009) Early-warning signals for critical transitions. *Nature*, **461**(7260): 53–59.

Scheffer M, Carpenter S, Foley J, Folke C and Walker B (2001) Catastrophic shifts in ecosystems. *Nature*, **413**(6856): 591–596.

Scheiter S, Langan L and Higgins SI (2013) Next-generation dynamic global vegetation models: learning from community ecology. *New Phytologist*, **198**(3): 957–969.

Sellers P, Berry J, Collatz G, Field C and Hall F (1992) Canopy reflectance, photosynthesis, and transpiration. iii. a reanalysis using improved leaf models and a new canopy integration scheme. *Remote sensing of environment*, **42**(3): 187–216.

Sellers P, Dickinson R, Randall D, Betts A, Hall F, Berry J, Collatz G, Denning A, Mooney H, Nobre C et al. (1997) Modeling the exchanges of energy, water, and carbon between continents and the atmosphere. *Science*, **275**(5299): 502–509.

Shannon C (1948) A mathematical theory of communication. *Bell System Technical Journal*, **27**: 379–423.

Shinozaki K, Yoda K, Hozumi K and Kira T (1964a) A quantitative analysis of plant form-the pipe model theory: I. Basic analyses. *Japanese Journal of Ecology*, **14**(3): 97–105.

Shinozaki K, Yoda K, Hozumi K and Kira T (1964b) A quantitative analysis of plant form-the pipe model theory: Ii. Further evidence of the theory and its application in forest ecology. *Japanese Journal of Ecology*, **14**(4): 133–139.

Silvertown J (1987) *Introduction to Plant Population Ecology*. Longman, 2nd edition.

Sitch S, Friedlingstein P, Gruber N, Jones SD, Murray-Tortarolo G, Ahlström A, Doney SC, Graven H, Heinze C, Huntingford C, Levis S, Levy PE, Lomas M, Poulter B, Viovy N, Zaehle S, Zeng N, Arneth A, Bonan G, Bopp L, Canadell JG, Chevallier F, Ciais P, Ellis R, Gloor M, Peylin P, Piao SL, Le Quéré C, Smith B, Zhu Z and Myneni R (2015) Recent trends and drivers of regional sources and sinks of carbon dioxide. *Biogeosciences*, **12**(3): 653–679.

Sitch S, Huntingford C, Gedney N, Levy P, Lomas M, Piao S, Betts R, Ciais P, Cox P, Friedlingstein P et al. (2008) Evaluation of the terrestrial carbon cycle, future plant geography and climate-carbon cycle feedbacks using five Dynamic Global Vegetation Models (DGVMs). *Global Change Biology*, **14**(9): 2015–2039.

Sitch S, Smith B, Prentice IC, Arneth A, Bondeau A, Cramer W, Kaplan J, Levis S, Lucht W, Sykes M et al. (2003) Evaluation of ecosystem dynamics, plant geography and terrestrial carbon cycling in the LPJ dynamic global vegetation model. *Global Change Biology*, **9**(2): 161–185.

Solé RV, Alonso D and McKane A (2002) Self-organized instability in complex ecosystems. *Philosophical Transactions of the Royal Society B: Biological Sciences*, **357**(1421): 667–671.

Staaland H, Holand Ø, Nellemann C and Smith M (1998) Time scale for forest regrowth: Abandoned grazing and agricultural areas in southern norway. *Ambio*, **27**(6): 456–460.

Stephenson NL, Das A, Condit R, Russo S, Baker P, Beckman N, Coomes D, Lines E, Morris W, Rüger N et al. (2014) Rate of tree carbon accumulation increases continuously with tree size. *Nature*, **507**(7490): 90–93.

Sura P and Gille ST (2003) Interpreting wind-driven southern ocean variability in a stochastic framework. *Journal of marine research*, **61**(3): 313–334.

Tilman D (1982) *Resource competition and community structure*. Princeton University Press.

Tilman D (2000) Causes, consequences and ethics of biodiversity. *Nature*, **405**(6783): 208–211.

Tilman D (2004) Niche tradeoffs, neutrality, and community structure: a stochastic theory of resource competition, invasion, and community assembly. *Proceedings of the National Academy of Sciences*, **101**(30): 10854–10861.

Uhlenbeck GE and Ornstein LS (1930) On the theory of the Brownian motion. *Physical Review*, **36**(5): 823–841.

Wang X, Wang C, Zhang Q and Quan X (2010) Heartwood and sapwood allometry of seven Chinese temperate tree species. *Annals of Forest Science*, **67**(4): 410.

Watson A and Lovelock J (1983) Biological homeostasis of the global environment: the parable of daisyworld. *Tellus. Series B. Chemical and physical meteorology*, **35**(4): 284–289.

West GB, Enquist BJ and Brown JH (2009) A general quantitative theory of forest structure and dynamics. *Proceedings of the National Academy of Sciences*, **106**(17): 7040–7045.

Westoby M (1984) The self-thinning rule. *Advances in ecological research*, **14**: 167–226.

Whitfield J (2002) Ecology: Neutrality versus the niche. *Nature*, **417**(6888): 480–481.

Wood AJ, Ackland GJ, Dyke JG, Williams HTP and Lenton TM (2008) Daisyworld: A review. *Reviews of Geophysics*, **46**(1).

Woodward F and Lomas M (2004) Vegetation dynamics–simulating responses to climatic change. *Biological reviews*, **79**(03): 643–670.

Worm B and Duffy JE (2003) Biodiversity, productivity and stability in real food webs. *Trends in Ecology & Evolution*, **18**(12): 628–632.

Yodzis P (1981) The stability of real ecosystems. *Nature*, **298**: 674–676.

Zaehle S, Sitch S, Prentice IC, Liski J, Cramer W, Erhard M, Hickler T and Smith B (2006) The importance of age-related decline in forest NPP for modeling regional carbon balances. *Ecological Applications*, **16**(4): 1555–1574.

Zenner EK (2005) Development of tree size distributions in douglas-fir forests under differing disturbance regimes. *Ecological applications*, **15**(2): 701–714.